Dynamic Equivalence Conditions and Controller Scaling Laws for Robotic Manipulators

by

Milind Ghanekar

A thesis
presented to the University of Waterloo
in fulfilment of the
thesis requirement for the degree of
Doctor of Philosophy
in
Electrical Engineering

Waterloo, Ontario, Canada, 1997

The University of Waterloo requires the signatures of all persons using or photocopying this thesis. Please sign below, and give address and date.

Dynamic Equivalence Conditions and Controller Scaling Laws for Robotic Manipulators

In many engineering disciplines, it is standard practice to construct prototype models of the actual system, for the purposes of testing and analysis. Traditional examples of this practice are the shipbuilding and the aeronautics industries. A prototype gives the engineer physical insight about the system, and allows the engineer to determine dynamic effects not contained in the theoretical model of the system. In addition, by constructing a smaller prototype, a cost savings can be achieved since a smaller quantity of material is required.

As the twenty-first century approaches, the use of large robotic manipulators is increasing. Long flexible manipulators are being used to clean out underground tanks containing hazardous materials. Large robots are being used in mining, and in forestry to prune and harvest trees. In space, the Canadarm is already being used on the space shuttle, and soon more manipulators will be used on the international space station. Looking into the future, robots that will be designed and tested on Earth, will be sent to the Moon, and even to Mars, which have different gravitational environments than the Earth.

In order to quantitatively *scale* the results obtained on the prototype model to the actual large manipulator, the dynamic equivalence conditions for robotic manipulator systems must be determined. With such a *dynamically equivalent* prototype, the dynamic behaviour of the prototype can be directly scaled to predict the behaviour of the actual system.

In this dissertation, the scaling conditions for rigid and flexible robotic manipulators are determined. The robots examined are of the broad class of manipulators

with n links, p actuators, any link topology, and having unconstrained motion. The dynamic equivalence conditions are defined by *nondimensional groups*, which can be found by applying dimensional analysis to the manipulator dynamics. Robot motion is achieved by implementing controllers on the joint actuators. Scaling laws are required for the controllers, so that a control scheme designed on the prototype can be scaled and implemented on another dynamically equivalent robot. In this thesis, scaling laws for linear and nonlinear controllers are developed and presented.

The theoretical scaling laws are illustrated by application to several sample manipulator systems. The examples include rigid and flexible manipulators, linear and nonlinear control strategies, and friction effects.

The thesis concludes with a summary of the main results. The major contributions of this work are identified, and avenues for future research are proposed.

Acknowledgements

I would like to thank my co-supervisors Dr. David Wang and Dr. Glenn Heppler for their unending support, guidance, and motivation throughout the duration of this research. Their experience and insight into dynamics and controls was an invaluable asset to which I was fortunate enough to have access. I am also forever indebted to them for funding my travels abroad, allowing me to broaden my horizons on the international robotics and controls stage. Most of all, I am thankful for the friendship that the three of us have formed. It was a pleasure and an honour to have worked with them.

Finally, I would like to thank the Tick. His profound, and humorous, words of inspiration were always a constant source of encouragement.

> *"You've got to ride that wave, you've got to suck that lozenge, 'cause if you don't, who will?"*

This thesis is dedicated to Krista, Aai, Baba, and Anand.

Contents

List of Figures

List of Tables

Chapter 1

Introduction

In many engineering disciplines, it is standard practice to construct prototype models of the actual system, for the purposes of testing and analysis. Traditional examples of this practice are the shipbuilding and the aeronautics industries. In ship building, engineers construct small-scale ship hulls in order to establish the dynamics of the ship-water interaction. In the construction of airplanes, wind tunnels are used to determine the aerodynamic properties of small-scale airplane models.

The advantages of constructing prototype models are numerous, so only a few will be listed. The first advantage is cost; small prototypes are typically less costly than the actual system because a smaller quantity of material is required. Secondly, a prototype gives the engineer physical insight about the system; it allows the engineer to validate the theoretical model of the system, and perhaps improve upon it by including previously unmodelled dynamic effects. Another advantage is safety; by constructing prototype models for intensive testing, safety issues can be identified and corrected.

Because of the nature of robotics, it is not always necessary to construct prototype robots. Typically, the manipulators are not large in size, and the actual system can be studied within a conventional research lab. However, as the twenty-first century approaches, the use of large robotic manipulators is increasing. Manipulators

such as the Canadarm are already being used on the space shuttle, and soon more will be used on the international space station. Long flexible robot arms are being used to clean out large underground tanks containing toxic waste. The forestry industry is beginning to make use of large manipulators to prune and harvest trees. In the future, robots built on Earth may be used on missions to the moon or to Mars, inaccessible environments with different gravitational accelerations than Earth (1.62 $\mathrm{m\,s^{-2}}$ for the Moon, 3.74 $\mathrm{m\,s^{-2}}$ for Mars[1]).

A question arises as to how large robots can be designed and tested efficiently. Because of their size, it is necessary that *smaller* prototypes be constructed to fit into conventional research labs. With robots destined for outer space, the question also arises as to how to compensate for the difference in gravitational acceleration. Common approaches would be to use air cushions or water buoyancy to compensate for Earth's gravity.

There is one answer to both questions: *scale model* prototypes. As is done in the aeronautics industry, the prototype airplanes are dynamic scale models of the actual systems they are modelling. In this way, the dynamic behaviour of the prototype can be used to quantitatively predict the behaviour of the actual system. Dynamic scale model prototypes scale all dynamic aspects of the system, including gravitational effects. Such a prototype is termed a *dynamically equivalent* model, because the dynamic behaviour of the prototype can be *directly scaled* to predict the behaviour of the actual manipulator.

The topic of this dissertation is to determine the dynamic equivalence conditions for robotic manipulator systems. A manipulator system is essentially composed of four parts: the manipulator links and joints, the actuators, the control laws, and any friction effects. The scaling conditions will allow prototype manipulators to not only be constructed of a smaller size, but also out of different materials, and in different gravitational environments.

Robot motion is achieved by implementing controllers on the joint actuators. Once scaling conditions for the manipulator dynamics have been developed, it is necessary to determine scaling laws for the controllers operating on these manipulators. The advantage of this is that once a controller has been tuned to give

the prototype manipulator some desired performance, the controller parameters can be scaled to produce the same, albeit scaled, performance on the actual larger manipulator.

The tool used to achieve these results is *dimensional analysis*. Given the parameters of a physical system, dimensional analysis can be used to determine the conditions which characterize the system behaviour. With this technique, the *nondimensional groups* or *dimensionless groups* for robotic manipulators can be determined. These nondimensional groups precisely define the dynamic equivalence conditions that are sought.

1.1 Thesis Outline

The backbone of the research developed in this thesis is from the field of dimensional analysis. In Chapter 2, the concepts and ideas behind dimensional analysis are presented. Nondimensional variables and nondimensional groups as a method of characterizing system behaviour are also discussed. The best known dimensional analysis technique is the Buckingham Pi method. This method provides a systematic way of determining the nondimensional groups which characterize the dynamic behaviour of a system.

With the background of dimensional analysis in place, Chapter 3 applies the ideas to robotic manipulators, the systems of interest here. The nondimensional groups characterizing the dynamics of rigid and flexible manipulators are determined using two methods: directly from the nondimensional equations of motion, and also by directly applying the Buckingham Pi method to the manipulator dynamics. From the Pi groups obtained for these systems, a general theorem is stated regarding the form of the nondimensional Pi group for *any* parameter of the manipulator system. A theorem stating the equivalence of the rigid and flexible Pi groups is also presented and proved. In addition, manipulators composed of both rigid and flexible links are examined. Examples are given for all the manipulator types presented. A design methodology is also provided to illustrate the method in

which the nondimensional Pi groups can be used to create dynamically equivalent manipulators out of different materials, or in different gravitational environments.

Chapter 4 is the first of three chapters which examine the overall manipulator system as a whole. In addition to the mechanism, the other components of the system include the actuator dynamics, the controller, and any friction effects. This chapter presents a general form for the actuator dynamics, and determines the nondimensional Pi groups which define the scaling conditions for arbitrary actuator parameters.

The scaling conditions for general control laws are derived and presented in Chapter 5. Here, a general structure for all possible control schemes is proposed, and the parameters characterizing an arbitrary control law are collected into a set. The nondimensional Pi groups determined for the controller parameters define the scaling conditions for the controller. Examples presented include PID control and sliding mode control.

Friction effects are the topic of Chapter 6. Effects such as Coulomb friction and the Stribeck effect are presented, and scaling conditions for the friction parameters are determined using dimensional analysis.

Theoretically, different manipulators are dynamically equivalent *if and only if* the values for *all* the Pi groups are identical. Practically, this is impossible to achieve because of manufacturing imprecision. Chapter 7 discusses a method of measuring the sensitivity of the dynamic equations to variations in the values of the nondimensional Pi groups. If the sensitivity to a particular Pi group is within an acceptable tolerance, then the manipulators in question could be considered to be dynamically equivalent for all intents and purposes. Finally, for rigid link manipulators, a nonlinear feedback compensation technique is proposed which allows the manipulator dynamics to *appear* dynamically equivalent. The cost of this technique is the additional control effort required to maintain the illusion.

To illustrate all the theoretical results, Chapter 8 presents simulation results of five different manipulator-controller systems. All the simulations are performed using MATLAB™.

Finally, in Chapter 9, the body of research presented in this thesis is summarized, and the contributions of the work are stated. In addition, the extension of this work into future research areas is discussed. A table of the nomenclature used throughout the thesis is presented in Appendix A.

1.2 Contributions

Although the field of dimensional analysis is more than one hundred years old, its application to different engineering disciplines continues unabated. The novel contribution of this thesis is to apply dimensional analysis to robotic manipulator systems. Specifically,

- dynamic equivalence conditions are determined and verified for general rigid link, flexible link, and composite link manipulators,
- the equivalence of the rigid and flexible Pi groups is proved,
- a general form for manipulator actuators is presented and the Pi groups for these actuators are determined,
- the characteristic parameters of a general controller are identified, and scaling laws for arbitrary control laws are presented,
- the Pi groups for general friction effects are determined,
- a nonlinear feedback technique is proposed to compensate for errors between the desired and actual dynamic behaviour of a manipulator.

In the context of this thesis, *general* robotic manipulator refers to the broad class of manipulators with n links, p actuators, any link topology, and having unconstrained motion. In addition, the terms *general actuator* and *general controller* are used to indicate that no predefined structure is assumed for the form of the actuator and controller equations.

Chapter 2

Dimensional Analysis

Dimensional analysis is a technique used to reduce the complexity of variables describing a certain physical phenomenon. There is an abundance of literature about dimensional analysis[2]-[9], which will be surveyed in this chapter. The first section gives an overview of dimensional analysis, and discusses: units, dimensions, dimensionless numbers, dimensional analysis techniques, the theory of similitude, and the construction of scale models. Some of the areas of application of dimensional analysis are also reviewed. In the second section, the Buckingham Pi Method is described.

2.1 Overview of Dimensional Analysis

2.1.1 Units, Dimensions, and Dimensionless Numbers

Units are used to identify the standard measure to which the physical quantity of interest is referenced. There are many *units* for distances: kilometres, feet, centimetres, inches, etc. Similarly, areas are measured in units of acres, square metres, etc. The number expressing the magnitude of a quantity with respect to a

particular unit is termed the *measure* of the quantity in those units[2]. Throughout this thesis, the standard *Système Internationale* units, or SI units, will be used. These are listed in Table 2.1.

Unit	Symbol	Quantity	Dimension
kilogram	kg	mass	$[M]$
metre	m	length	$[L]$
second	s	time	$[T]$
ampere	A	current	$[A]$
kelvin	K	temperature	$[\Theta]$
candela	cd	luminous intensity	$[cd]$
mole	mol	amount of substance	$[mol]$

Table 2.1: Table of Système Internationale (SI) Units

The meaning of the word *dimension*, on the other hand, is different from *units*. Every unit that measures distance, from cubits to kilometres, has the dimension of length. Every unit that measures area has dimensions of length squared. A square bracket notation is used to denote the dimension of a quantity, and hence distance has dimension $[L]$, and area has dimension $[L]^2$. Furthermore, when discussing dimensions, only the nature of the quantity is of interest, not its measure in any particular measurement units[2]. Fundamental dimensions are independent dimensions which form the basis of a system of measurement. All physical quantities can be characterized using seven fundamental dimensions[10, 11], which are: mass $[M]$, length $[L]$, time $[T]$, electric current $[A]$, temperature $[\Theta]$, amount of substance $[mol]$, and luminous intensity$[cd]$[1]. A common measurement system used in *mechanics* is based only on the three fundamental dimensions: mass, length, and time,

[1]Instead of current, electric charge is sometimes used as a fundamental dimension. The relationship is $[Q] \equiv [A][T]$.

and is referred to as an **MLT** system. However, all seven of the fundamental dimensions pertain directly to robotics. The dimensions of current $[A]$ and temperature $[\Theta]$ are necessary when considering electrical actuators. When considering sensors, such as chemical sensors and photovoltaic sensors, the dimensions of amount of substance $[mol]$, and luminous intensity $[cd]$ also become important. Once a set of fundamental dimensions is established, the dimensions of all other variables may be expressed in terms of the fundamental dimensions.

Consider a variable v measuring the speed of an object. The variable v has dimensions $[L][T]^{-1}$. Now suppose that it is desired to measure the speed of this object relative to some reference speed v_0. By the definition of speed, v_0 must also have dimensions $[L][T]^{-1}$. A new variable, $\hat{v}$, is defined such that,

$$\hat{v} \triangleq \frac{v}{v_0} \quad \Rightarrow \quad \hat{v} \equiv \frac{[L][T]^{-1}}{[L][T]^{-1}} \equiv [L]^0[T]^0.$$

Notice that exponents of the length and time dimensions are zero. Hence, although the variable $\hat{v}$ gives a measure of the speed of the object, it is a *dimensionless*, or *nondimensional*, variable. The above equation also introduces the notation ($\equiv$), which indicates that the dimensions of a variable are being presented. For example, in the MLT system, the dimensions of a variable of force would be expressed by $F \equiv [M]^1[L]^1[T]^{-2}$.

2.1.2 Nondimensional Groups and System Behaviour

A *nondimensional group* is a combination of variables which produces a dimensionless quantity. For example, the Reynolds number(R_e), generally accepted as the most important parameter in fluid mechanics[3], is a nondimensional group which characterizes the force on a body of length L, which is immersed in a stream of fluid with velocity U, density ρ, and viscosity, μ. In terms of fundamental dimensions,

$$R_e = \frac{\rho U L}{\mu} \equiv \frac{([M][L]^{-3})([L][T]^{-1})([L])}{[M][L]^{-1}[T]^{-1}} \equiv [M]^0[L]^0[T]^0.$$

Example: Flexible Beam

As an example of how nondimensional groups can be used to succinctly describe system behaviour, consider a flexible beam of length L, stiffness EI, and linear mass density ρ. The beam deflection, $\mathrm{w}(x,t)$, is described by the partial differential equation[12]

$$\rho\frac{\partial^2 \mathrm{w}(x,t)}{\partial t^2} + EI\frac{\partial^4 \mathrm{w}(x,t)}{\partial x^4} = 0, \quad 0 \le x \le L. \tag{2.1}$$

To make this equation independent of the specific beam parameters, the variables can be nondimensionalized. A natural length scale is the beam length, L. So, the position x along the beam can be equivalently represented by the nondimensional variable ξ, where

$$\xi \triangleq \frac{x}{L}.$$

A natural time scale is defined by the frequency of the motion, ω. So, define the nondimensional time variable, τ,

$$\tau \triangleq \omega t.$$

The beam deflection, which has dimensions of length, can also be nondimensionalized by the beam length,

$$\hat{\mathrm{w}}(\xi,\tau) \triangleq \frac{\mathrm{w}(x,t)}{L}.$$

Substituting into (2.1) and simplifying gives,

$$\rho L\omega^2\frac{\partial^2 \hat{\mathrm{w}}(\xi,\tau)}{\partial \tau^2} + \frac{EI}{L^3}\frac{\partial^4 \hat{\mathrm{w}}(\xi,\tau)}{\partial \xi^4} = 0, \quad 0 \le \xi \le 1,$$

which upon rearrangement gives,

$$\frac{\partial^2 \hat{\mathrm{w}}}{\partial \tau^2} + \left(\frac{EI}{\rho L^4\omega^2}\right)\frac{\partial^4 \hat{\mathrm{w}}}{\partial \xi^4} = 0.$$

Now, the first term in the equation is dimensionless, because $\hat{\mathrm{w}}$ and τ are both nondimensional by definition. An equation describing a physical system must be dimensionally homogeneous[3, 4], which means that the second term is also nondimensional. In the second term, $\hat{\mathrm{w}}$ and ξ are dimensionless, which means that the

coefficient of the second term must be nondimensional. This can also be verified by directly examining the fundamental dimensions of EI, ρ, L, and ω. Denoting the nondimensional coefficient by Π,

$$\Pi \triangleq \frac{EI}{\rho L^4 \omega^2} \equiv \frac{[M][L]^3[T]^{-2}}{([M][L]^{-1})([L]^4)([T]^{-2})} \equiv [M]^0[L]^0[T]^0.$$

So the *nondimensional* equation describing the deflection of a flexible beam can be written as

$$\frac{\partial^2 \hat{w}}{\partial \tau^2} + \Pi \frac{\partial^4 \hat{w}}{\partial \xi^4} = 0, \quad 0 \leq \xi \leq 1.$$

This has several implications. Firstly, to observe the effect of beam parameters on deflection, the number of parameters has been *reduced* from four to one. Secondly, and most importantly, the deflection behaviour of *all* flexible beams, whose parameters combine to produce the same value of Π, are characterized by the above nondimensional equation.

In general, several systems whose variables combine to produce the same value for a nondimensional group will exhibit similar behaviour. Hence, nondimensional groups can be used to characterize the dynamics of a *class* of systems.

In the flexible beam example, the dynamic equations were nondimensionalized directly in order to obtain the nondimensional Π group. Alternatively, the same Π group could have been obtained by applying dimensional analysis to the system.

2.1.3 Dimensional Analysis Techniques

There are several methods which can be used to determine the nondimensional groups which characterize the dynamics of a system. In 1822, Fourier outlined the *principle of dimensional homogeneity*[3, 4]:

> *"If an equation truly expresses a proper relationship among variables in a physical process it will be dimensionally homogeneous; i.e. each of its additive terms will have the same dimensions."*

Dimensional analysis techniques make use of this principle in order to reduce the number of variables describing a physical phenomenon.

There are two approaches to dimensional analysis. One approach requires knowledge of the variables which affect the system behaviour. Based on these variables, a nondimensional functional relation which characterizes the system is determined. Some examples of this approach are the method of dimensions, proposed by Lord Rayleigh in 1877[2, 4], the indicial method[2], and the Buckingham Pi method[5] proposed by Buckingham in 1914. The Buckingham Pi method is perhaps the best known of the dimensional analysis techniques. It provides a systematic method of determining the minimum number of nondimensional groups for a system. This method was extensively examined by Bridgman[6].

The second approach involves deriving the nondimensional system dynamics. By using *characteristic parameters* of the system, the system variables are made nondimensional[2, 7]. The dynamic equations and system boundary conditions are then written in dimensionless form, and the nondimensional groups characterizing the behaviour will appear in these nondimensional equations. This approach was taken in the flexible beam example of section 2.1.2.

The first approach has the advantage that it is easy to apply to any system. However, it is not possible to know if *all* of the variables describing the system have been considered, and hence some of the nondimensional groups characterizing the system behaviour may not be included in the system description. By the nature of the second approach, all the variables involved in the system dynamics are considered, and the nondimensional groups present in these equations completely describe the system behaviour. However, for complicated systems it can be very tedious to derive the dynamic equations.

In this research, dimensional analysis will be used to verify the nondimensional groups obtained by directly nondimensionalizing the dynamics of general robotic manipulators. With these results, the first approach mentioned above can be used with confidence that the nondimensional groups obtained completely describe the system behaviour.

2.1.4 Similitude and Scale Models

Before constructing a large engineering system, it is often advantageous to build a *small prototype*. To ensure that the behaviour of the scaled prototype and the actual system is similar, the theory of *similitude* must be considered[8, 9].

The conditions for similarity between the prototype and the actual system come from the results of dimensional analysis. In order for the dynamics of the two systems to be similar, the nondimensional dynamics must be identical. In other words, the two systems must have the same values for all of the nondimensional groups. Let the prototype and actual system be denoted by p and a respectively, and let Π_i denote the nondimensional groups for the system, then the similarity condition is,

$$\{\Pi_1, \Pi_2, \ldots, \Pi_n\}_p = \{\Pi_1, \Pi_2, \ldots, \Pi_n\}_a .$$

By satisfying the above equation, the correct geometric and material properties of the smaller prototype can be determined so that it is similar to the actual system. By ensuring that the actual system and prototype are similar, results obtained on the prototype can be *directly* scaled to apply to the full-size system.

There are different types of similarity: geometric similarity, kinematic similarity, and dynamic similarity[3, 9]. In geometric similarity, there is a *homologous* (point to point) relationship between the points on the prototype and points on the actual system. That is, points on the scale-model are related to points on the actual system by some *constant* scale factor. Kinematic similarity introduces the notion of homologous time. That is, the time scales of the prototype and actual system are related by a constant time scale factor. Dynamic similarity means that homologous parts of the prototype and actual system experience similar forces [9]. However, dynamic similarity does not imply kinematic or geometric similarity. Finally, if *all* the nondimensional variables have the same values for the prototype and the actual system, then the two are *completely similar*[9].

2.1.5 Areas of Application

Almost every article on dimensional analysis makes reference to its extensive use in the fields of fluid dynamics[3] and thermodynamics[2]. However, it has also been applied to aerodynamics[9], structural dynamics[2, 9, 13], and electromagnetics[2, 4, 7, 8, 9]. Other applications of dimensional analysis can be found in such fields as theoretical physics[6], acoustics[8], illumination[8], economics[14], and astrophysics[15].

The ideas of dimensional analysis are applied to robotic manipulators in [16]. In it, nondimensional variables for time, for the three dimensional Cartesian coordinates, for velocity, and for mass are defined. With these variables, the dimensionless equations of motion for a rigid robot manipulator are determined. These nondimensional equations formulate the dynamics of a class of similar manipulators with various physical properties. For a specific manipulator class, the insignificant terms in the equations are identified by their numerical order, and removed to simplify the nondimensional dynamic equations.

Although similar to the work in [16], this thesis has several significant differences. This thesis directly addresses the issue of dynamic equivalence, and applies dimensional analysis to the robot manipulator in order to determine the nondimensional groups which define the dynamic equivalence conditions. Rigid *and* flexible manipulators will be analyzed, and the results will be used in the development of scaling laws for linear and nonlinear controllers of robot manipulators.

2.2 Buckingham Pi Method

One particular dimensional analysis tool is the Buckingham Pi method[6]. This method provides a systematic method of determining the minimum number of variables which characterize the dynamics of a system. By the nature of the method, these variables will be *nondimensional* in their fundamental dimensions.

Theorem 2.1 *Buckingham Pi Theorem[6]*
Let $\phi(v_1, v_2, \ldots, v_n) = 0$ be a set of equations in n parameters and m fundamental dimensions. Then ϕ can be equivalently written as a set of equations, $\mathbf{F}$, in $n - m$ parameters which are dimensionless in the fundamental dimensions; i.e. as $\mathbf{F}(\Pi_1, \Pi_2, \ldots, \Pi_{n-m}) = 0$, where the Π_i are the nondimensional groups which characterize the system behaviour.

A proof of the Buckingham Pi theorem can be found in Bridgman[6] or Ghanekar[17].

The Π groups themselves are found by solving a set of linear algebraic equations. The method can be explained quite easily. The dimensions of each variable v_i can be expressed in terms of powers, p_j^i, of the m fundamental dimensions, u_j, $j \in [1, m]$. That is,

$$v_i \equiv [u_1]^{p_1^i}[u_2]^{p_2^i} \cdots [u_m]^{p_m^i}, \quad i \in [1, n].$$

Each Π group is composed of a product of all the system variables raised to various exponents. For a particular Π group, let e_i be the exponent of the variable v_i in the Π group. The problem, now, is to solve for e_i such that the Π group is nondimensional. A typical Π group is defined as,

$$\Pi = v_1^{e_1} v_2^{e_2} \cdots v_n^{e_n}.$$

Because the Π group is nondimensional, it has the following dimensions in terms of the fundamental dimensions,

$$\Pi \equiv [u_1]^0[u_2]^0 \cdots [u_m]^0.$$

That is, the exponent of each fundamental unit is zero. Therefore, writing v_i in terms of its fundamental dimensions, and collecting common fundamental dimensions, results in the following equation,

$$\Pi \equiv [u_1]^{e_1 p_1^1 + e_2 p_1^2 + \cdots + e_n p_1^n} \cdots [u_m]^{e_1 p_m^1 + e_2 p_m^2 + \cdots + e_n p_m^n} = [u_1]^0 \cdots [u_m]^0.$$

One equation results for each fundamental dimension, and hence a system of m equations in the n unknowns $e_1, e_2, \ldots, e_n$, is obtained.

$$\begin{aligned} u_1 : &\quad e_1 p_1^1 + e_2 p_1^2 + \cdots + e_n p_1^n = 0 \\ u_2 : &\quad e_1 p_2^1 + e_2 p_2^2 + \cdots + e_n p_2^n = 0 \\ &\vdots \\ u_m : &\quad e_1 p_m^1 + e_2 p_m^2 + \cdots + e_n p_m^n = 0. \end{aligned}$$

Typically, m is less than n, which means that there are at most m independent solutions[2]. Therefore $n - m$ of the unknowns are "free", and can be set arbitrarily. Every arbitrary choice of these $n - m$ unknowns will result in a different set of $n - m$ nondimensional Π groups. However, a matrix transformation relates all these different sets of Π groups[17, 18]. Hence, regardless of the particular choice of the value for the $n - m$ unknowns, every set of Π groups obtained *equivalently* describes the system behaviour.

The Buckingham Pi method will be illustrated in the next chapter when determining the nondimensional Pi groups for robotic manipulators.

[2]If $n - m \leq 0$, this means that there are not enough parameters to form a Pi group.

Chapter 3

Dynamic Equivalence Conditions

Now that the ideas behind dimensional analysis have been presented, the technique will be used to determine the dynamic equivalence conditions for general robotic manipulators. As an initial step, the manipulators will be examined independently of actuator effects, friction, and controllers. In this chapter, the manipulators will be modelled as an interconnection of links and joints. At this stage, *actuated* joints will be modelled simply as rigid bodies with mass and inertia. It will be assumed that the mass and inertia of *unactuated* joints, such as a pin-joint between two links, are negligible. Rigid and flexible links will both be considered in this analysis. The scaling conditions for actuators, friction, and controllers will be determined in subsequent chapters.

3.1 Chapter Overview

Excluding this overview, this chapter is composed of six main sections. The first two sections examine general n-link rigid manipulators, and general n-link flexible manipulators respectively. Once again, the term *general* refers to the class of manipulators with n links, p actuators, any link topology, and having unconstrained motion. In both sections, the nondimensional groups are determined by

direct nondimensionalization, and also by applying the Buckingham Pi method. In the third section, nondimensionalization theorems regarding the nondimensional groups for the rigid and flexible manipulators are presented and proved.

A method for determining the nondimensional groups for manipulators that are composed of both rigid *and* flexible links is presented in the fourth section. A summary and interpretation of the rigid and flexible manipulator Pi groups is given in the fifth section. In the final section, a design methodology is presented, which illustrates the way in which the nondimensional Pi groups can be used to construct dynamically equivalent manipulators.

3.1.1 Basic Approach

The basic approach taken in determining and validating the nondimensional groups for the rigid and flexible manipulators will be outlined here. Recall from section 2.1.3 that the nondimensional groups characterizing a system can be determined in two different ways. The first uses dimensional analysis, and the second examines the nondimensional equations of motion. Here, the nondimensional equations of motion will be examined first, and then dimensional analysis will be used to validate the findings.

Lagrange's method can be used to determine the system equations of motion. For the i^{th} generalized coordinate q_i, the equation of motion can be expressed in terms of the Lagrangian, $L = T - V$, as:

$$\frac{d}{dt}\left(\frac{\partial L}{\partial \dot{q}_i}\right) - \frac{\partial L}{\partial q_i} = Q_i, \quad i \in [1, p], \tag{3.1}$$

where T and V represent the system kinetic energy and system potential energy respectively, and Q_i denotes the net generalized non-conservative force acting on the link.

Now, for complicated systems it can be very tedious to derive the equations of motion. However, it is clear that the equations of motion are dependent on the kinetic and potential energies of the system. Furthermore, the nondimensional

groups being sought are functions of the system parameters and are *not* dependent on the generalized coordinate q_i. Therefore, for the purposes of finding the nondimensional groups in the nondimensional equations of motion, it is sufficient to derive the nondimensional kinetic and potential energy expressions in terms of q_i.

To verify these nondimensional groups, the Buckingham Pi method is applied to the manipulator dynamics. The results obtained are reconciled with those from the direct nondimensionalization approach.

3.2 General n-Link Rigid Manipulators

In this thesis, the term, *general n-link rigid manipulator* refers to the class of manipulators with n rigid links, p actuators (actuated joints), any link topology, and having unconstrained motion. Because there are p actuators, the manipulator has at least p degrees of freedom.

This section will begin with the development of the *nondimensional* kinetic and potential energy expressions. However, it will be assumed that the masses and inertias of the *unactuated* joints are insignificant, and make negligible contributions to the energy expressions. Therefore, only the n rigid links, and p actuated joints will be examined in this and subsequent development. In addition, throughout the remainder of this chapter, references to the term *joint* refer to actuated joints only.

3.2.1 Nondimensional Dynamics

The variables defining the system dynamics can be determined by considering the i^{th} link and the j^{th} actuated joint in an inertial reference frame ($\mathcal{F}_0$). Furthermore, define frame c_i ($\mathcal{F}_{c_i}$) to be a principal body-fixed frame[19] at the centre of mass of link i (Figure 3.1). In the following derivation, the ranges for i and j are $i \in [1, n]$ and $j \in [1, p]$. Define the following variables (boldface variables indicate 3×1

vectors or 3×3 matrices in $\mathcal{F}_0$ coordinates) as:

$$
\begin{aligned}
\boldsymbol{d}_0^{c_i}(t) &\triangleq \text{distance to centre of mass of link } i \text{ from } O_0 \\
\boldsymbol{\omega}_0^{c_i}(t) &\triangleq \text{angular velocity of } \mathcal{F}_{c_i} \text{ with respect to } \mathcal{F}_0 \\
\boldsymbol{R}_0^{c_i}(t) &\triangleq \text{rotation matrix from } \mathcal{F}_{c_i} \text{ to } \mathcal{F}_0 \\
\boldsymbol{J}_{c_i} &\triangleq diag\{J_i^{xx}, J_i^{yy}, J_i^{zz}\} \triangleq \text{inertia matrix in } \mathcal{F}_{c_i} \\
\boldsymbol{d}_0^{j}(t) &\triangleq \text{distance to joint } j \text{ from } O_0 \\
\boldsymbol{\omega}_0^{j}(t) &\triangleq \text{angular velocity of joint } j \text{ with respect to } \mathcal{F}_0 \\
I_j^h &\triangleq \text{moment of inertia of joint } j \text{ about the actuating axis.}
\end{aligned}
$$

The joint model assumes that for a revolute joint, the most significant inertial term is that about the actuating axis, and that the inertia about the other axes is negligible. For a prismatic joint $I_j^h = 0$.

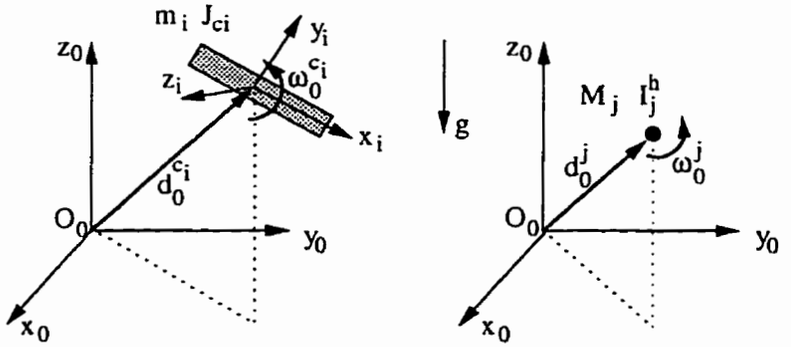

Figure 3.1: Inertial Frame with i^{th} Link and j^{th} Joint

Nondimensional Kinetic Energy

The total kinetic energy of the system T is equal to the sum of the kinetic energies of all the links and joints,

$$T(t) = \sum_{i=1}^{n} T_i^{\text{link}}(t) + \sum_{j=1}^{p} T_j^{\text{joint}}(t).$$

Furthermore, the total kinetic energy of a body is composed of translational and rotational kinetic energy. Therefore, by definition[20],

$$T_i^{\text{link}}(t) = \frac{1}{2} m_i \frac{d\boldsymbol{d}_0^{c_i}}{dt}^T \frac{d\boldsymbol{d}_0^{c_i}}{dt} + \frac{1}{2} \boldsymbol{\omega}_0^{c_i T} \boldsymbol{R}_0^{c_i} \boldsymbol{J}_{c_i} \boldsymbol{R}_0^{c_i T} \boldsymbol{\omega}_0^{c_i} \tag{3.2}$$

$$T_j^{\text{joint}}(t) = \frac{1}{2} M_j \frac{d\boldsymbol{d}_0^{j}}{dt}^T \frac{d\boldsymbol{d}_0^{j}}{dt} + \frac{1}{2} I_j^h \boldsymbol{\omega}_0^{j T} \boldsymbol{\omega}_0^{j}. \tag{3.3}$$

In order to obtain a nondimensional expression for the link kinetic energy, all the manipulator-dependent variables in (3.2) must be nondimensionalized (section 2.1.1). In (3.2), the following variables must be nondimensionalized:

$$t,\ m_i,\ \boldsymbol{d}_0^{c_i}(t),\ \boldsymbol{J}_{c_i},\ \boldsymbol{\omega}_0^{c_i}(t),\ \boldsymbol{R}_0^{c_i}(t).$$

Time

Nondimensionalizing the time variable will provide a common time frame in which the history of the motion of different manipulators can be compared. A suitable reference value for time may be a characteristic time constant, say T_0, of the system or equivalently a characteristic system frequency, Ω. Equivalently, define the nondimensional time variable, τ,

$$\tau \triangleq \frac{t}{T_0} = \Omega t.$$

In this thesis, the latter option will be chosen. Although for rigid manipulators, the notion of a "characteristic frequency" is meaningless, the use of Ω as a reference value will be apparent when flexible manipulators are examined in future sections.

To illustrate the purpose of nondimensionalizing time, consider two manipulators. Let t_1 and t_2 be the time variables for each manipulator respectively, and let the values for the reference values be Ω_1 and Ω_2. Converting to the common nondimensional time base reveals:

$$\tau = \Omega_1 t_1 = \Omega_2 t_2 \quad \Rightarrow \quad t_2 = \frac{\Omega_1}{\Omega_2} t_1.$$

Hence the ratio of the reference value for each system gives a measure of the relative "speed" between the systems.

Mass and Inertia

It is natural to represent all the link masses, m_i, as a fraction of the mass of the first link, m_1. Now, consider the mass moments of inertia of link 1 about its principal axes. Define J_1 be one of J_1^{xx}, J_1^{yy}, or J_1^{zz}. Then, select J_1 to be the reference value for all inertia quantities. In other words, define the nondimensional mass variables and inertia variables as

$$\hat{m}_i \triangleq \frac{m_i}{m_1}. \quad \hat{J}_{c_i} \triangleq \frac{1}{J_1} J_{c_i} = diag\left\{\frac{J_i^{xx}}{J_1}, \frac{J_i^{yy}}{J_1}, \frac{J_i^{zz}}{J_1}\right\}.$$

Length

Given the inertial properties of a rigid link, and a desired link shape, the physical dimensions of the link can be computed. Hence, by using the link mass and link mass moments of inertia, the link can be described independently of its physical dimensions. In particular, this means that the link length is not available as an explicit link parameter to be used for length scaling. Instead, an appropriate characteristic length for a link is its *radius of gyration* about one of the principal axes. Let J_i be one of the principal mass moments of inertia, and consider the axis about which J_i is computed. Recall that the radius of gyration of the link about this axis is denoted by k_i, and is defined[19] as

$$k_i \triangleq \sqrt{\frac{J_i}{m_i}}. \tag{3.4}$$

The radius of gyration is the distance from this axis that the total link mass m_i must be concentrated in order to have an inertia equal to J_i. As a reference value, the radius of gyration of link 1, k_1, corresponding to the inertia J_1 and mass m_1, can be used to nondimensionalize length variables. For the *time dependent* variable $d_0^{c_i}(t)$, define the nondimensional variable, $\hat{d}_0^{c_i}(\tau)$, such that:

$$\hat{d}_0^{c_i}(\tau) \triangleq \frac{d_0^{c_i}\left(\frac{\tau}{\Omega}\right)}{k_1}.$$

Rotational Terms

The angular velocity, $\boldsymbol{\omega}_0^{c_i}$, of the i^{th} link has units of frequency, and can therefore be represented with respect to the already defined reference frequency, Ω. The rotation matrix, $\boldsymbol{R}_0^{c_i}$, is nondimensional by definition. However, both these quantities are time dependent, and hence must be nondimensionalized in time. Define the following nondimensional variables:

$$\hat{\boldsymbol{\omega}}_0^{c_i}(\tau) \triangleq \frac{\boldsymbol{\omega}_0^{c_i}\left(\frac{\tau}{\Omega}\right)}{\Omega}, \quad \hat{\boldsymbol{R}}_0^{c_i}(\tau) \triangleq \boldsymbol{R}_0^{c_i}\left(\frac{\tau}{\Omega}\right).$$

Returning to the link kinetic energy (3.2), substitute the nondimensional variables defined above and simplify to give

$$T_i^{\text{link}}\left(\frac{\tau}{\Omega}\right) = \frac{1}{2} m_1 k_1^2 \Omega^2 \hat{m}_i \frac{d\hat{\boldsymbol{d}}_0^{c_i\,T}}{d\tau} \frac{d\hat{\boldsymbol{d}}_0^{c_i}}{d\tau} + \frac{1}{2} J_1 \Omega^2\, \hat{\boldsymbol{\omega}}_0^{c_i\,T} \hat{\boldsymbol{R}}_0^{c_i} \hat{\boldsymbol{J}}_{c_i} \hat{\boldsymbol{R}}_0^{c_i\,T} \hat{\boldsymbol{\omega}}_0^{c_i}. \tag{3.5}$$

Realizing that $J_1 = m_1 k_1^2$, and dividing through by the reference values, gives:

$$\frac{1}{m_1 k_1^2 \Omega^2} T_i^{\text{link}}\left(\frac{\tau}{\Omega}\right) = \frac{1}{2} \hat{m}_i \frac{d\hat{\boldsymbol{d}}_0^{c_i\,T}}{d\tau} \frac{d\hat{\boldsymbol{d}}_0^{c_i}}{d\tau} + \frac{1}{2}\, \hat{\boldsymbol{\omega}}_0^{c_i\,T} \hat{\boldsymbol{R}}_0^{c_i} \hat{\boldsymbol{J}}_{c_i} \hat{\boldsymbol{R}}_0^{c_i\,T} \hat{\boldsymbol{\omega}}_0^{c_i}. \tag{3.6}$$

Define the nondimensional link kinetic energy to be

$$\hat{T}_i^{\text{link}}(\tau) \triangleq \frac{1}{m_1 k_1^2 \Omega^2} T_i^{\text{link}}\left(\frac{\tau}{\Omega}\right),$$

and substitute this definition into (3.6) to obtain the nondimensional link kinetic energy,

$$\hat{T}_i^{\text{link}}(\tau) = \frac{1}{2} \hat{m}_i \frac{d\hat{\boldsymbol{d}}_0^{c_i\,T}}{d\tau} \frac{d\hat{\boldsymbol{d}}_0^{c_i}}{d\tau} + \frac{1}{2}\, \hat{\boldsymbol{\omega}}_0^{c_i\,T} \hat{\boldsymbol{R}}_0^{c_i} \hat{\boldsymbol{J}}_{c_i} \hat{\boldsymbol{R}}_0^{c_i\,T} \hat{\boldsymbol{\omega}}_0^{c_i}. \tag{3.7}$$

For consistency, the same reference values used for the link kinetic energy are used for the joint kinetic energy. Define the following nondimensional variables:

$$\hat{M}_j \triangleq \frac{M_j}{m_1}$$

$$\hat{I}_j^h \triangleq \frac{I_j^h}{J_1}$$

$$\hat{\boldsymbol{d}}_0^j(\tau) \triangleq \frac{\boldsymbol{d}_0^j\left(\frac{\tau}{\Omega}\right)}{k_1}$$

$$\hat{\boldsymbol{\omega}}_0^j(\tau) \triangleq \frac{\boldsymbol{\omega}_0^j\left(\frac{\tau}{\Omega}\right)}{\Omega}.$$

With these substitutions, the joint kinetic energy expression (3.3) becomes

$$\frac{1}{m_1 k_1^2 \Omega^2} T_j^{\text{joint}}(t) = \frac{1}{2} \hat{M}_j \frac{d\hat{\boldsymbol{d}}_0^j}{d\tau}^T \frac{d\hat{\boldsymbol{d}}_0^j}{d\tau} + \frac{1}{2} \hat{I}_j^h \, \hat{\boldsymbol{\omega}}_0^{j\,T} \hat{\boldsymbol{\omega}}_0^j.$$

To be consistent with the definition of the Lagrangian ($L = T - V$), *all* the energy expressions (link and joint kinetic and potential energies), must be nondimensionalized by the same variables, in this case, the product $m_1 k_1^2 \Omega^2$. In this manner, the nondimensional Lagrangian can be correctly assembled as $\hat{L} = \hat{T} - \hat{V}$. From (3.1), this leads to a valid set of nondimensional equations of motion. Define

$$\hat{T}_j^{\text{joint}}(\tau) \triangleq \frac{1}{m_1 k_1^2 \Omega^2} T_j^{\text{joint}}(t),$$

so that the nondimensional joint kinetic energy becomes

$$\hat{T}_j^{\text{joint}}(\tau) = \frac{1}{2} \hat{M}_j \frac{d\hat{\boldsymbol{d}}_0^j}{d\tau}^T \frac{d\hat{\boldsymbol{d}}_0^j}{d\tau} + \frac{1}{2} \hat{I}_j^h \, \hat{\boldsymbol{\omega}}_0^{j\,T} \hat{\boldsymbol{\omega}}_0^j. \tag{3.8}$$

Therefore, the total nondimensional kinetic energy is given by

$$\hat{T}(\tau) = \sum_{i=1}^{n} \hat{T}_i^{\text{link}}(\tau) + \sum_{j=1}^{p} \hat{T}_j^{\text{joint}}(\tau),$$

and contains the following set of nondimensional groups

$$\left\{ \hat{m}_i, \ \hat{\boldsymbol{J}}_{c_i}, \ \hat{M}_j, \ \hat{I}_j^h \right\}.$$

Nondimensional Potential Energy

For this manipulator, all the potential energy occurs as stored gravitational potential energy in the links and joints. Therefore,

$$V(t) = \sum_{i=1}^{n} V_i^{\text{link}}(t) + \sum_{j=1}^{p} V_j^{\text{joint}}(t).$$

Let $\boldsymbol{g}$ be the gravity vector with $|\boldsymbol{g}| = g$, and define $\boldsymbol{s}$ to be the unit gravity vector

$$\boldsymbol{s} \triangleq \frac{\boldsymbol{g}}{|\boldsymbol{g}|} = \frac{\boldsymbol{g}}{g}. \tag{3.9}$$

Then, the potential energies of the i^{th} link and the j^{th} joint can be expressed as,

$$V_i^{\text{link}}(t) = -m_i(\boldsymbol{g}\cdot\boldsymbol{d}_0^{c_i}) = -m_i g(\boldsymbol{s}\cdot\boldsymbol{d}_0^{c_i}) \tag{3.10}$$

$$V_j^{\text{joint}}(t) = -M_j\left(\boldsymbol{g}\cdot\boldsymbol{d}_0^{j}\right) = -M_j g\left(\boldsymbol{s}\cdot\boldsymbol{d}_0^{j}\right). \tag{3.11}$$

As with the kinetic energy, the nondimensional potential energy expressions are found by nondimensionalizing the system dependent variables in (3.10) and (3.11). The following variables must be nondimensionalized:

$$t,\ m_i,\ M_j,\ \boldsymbol{d}_0^{c_i},\ \boldsymbol{d}_0^{j},\ g.$$

Except for g, reference values for all of these variables have been presented in the kinetic energy section.

Gravitational Acceleration

A natural reference value for the acceleration due to gravity is the value of the gravitational acceleration on Earth. Denote this gravitational acceleration by g_0, then define the nondimensional acceleration due to gravity by

$$\hat{g} \triangleq \frac{g}{g_0}.$$

In addition, as with the kinetic energy, define

$$\hat{V}_i^{\text{link}}(\tau) \triangleq \frac{1}{m_1 k_1^2 \Omega^2} V_i^{\text{link}}(t)$$

$$\hat{V}_i^{\text{joint}}(\tau) \triangleq \frac{1}{m_1 k_1^2 \Omega^2} V_i^{\text{joint}}(t),$$

where, equivalently, $m_1 k_1^2 = J_1$.

Then, the nondimensional link and joint potential energy expressions are

$$\hat{V}_i^{\text{link}}(t) = -\hat{m}_i \hat{g} \frac{g_0}{k_1\Omega^2}\left(\boldsymbol{s}\cdot\hat{\boldsymbol{d}}_0^{c_i}\right) \tag{3.12}$$

$$\hat{V}_j^{\text{joint}}(t) = -\hat{M}_j \hat{g} \frac{g_0}{k_1\Omega^2}\left(\boldsymbol{s}\cdot\hat{\boldsymbol{d}}_0^{j}\right). \tag{3.13}$$

Hence, the total nondimensional potential energy for the manipulator is given by

$$\hat{V}(\tau) = \sum_{i=1}^{n} \hat{V}_i^{\text{link}}(\tau) + \sum_{j=1}^{p} \hat{V}_j^{\text{joint}}(\tau), \tag{3.14}$$

and contains the following set of nondimensional groups

$$\left\{\hat{m}_i,\ \hat{M}_j,\ \hat{g},\ \frac{g_0}{k_1\Omega^2}\right\}.$$

Together, the nondimensional kinetic and potential energy expressions contain the following set of nondimensional groups

$$\left\{\hat{m}_i,\ \hat{J}_{c_i},\ \hat{M}_j,\ \hat{I}_j^h,\ \hat{g},\ \frac{g_0}{k_1\Omega^2}\right\}.$$

Because these groups are time independent, their presence in the energy expressions confirms their presence in the actual nondimensional equations of motion. In the next subsection, dimensional analysis will be applied to the manipulator to verify the nondimensional groups defined here.

3.2.2 Dimensional Analysis

In section 2.2, the Buckingham Pi method was described. This method will be illustrated by using it to determine the nondimensional Pi groups for the n-link rigid manipulator. In order to perform dimensional analysis on the system, the variables characterizing the system dynamics must be identified. The dynamic behaviour is a function of the link parameters, the joint parameters, gravity, and time. By including gravity as an independent parameter, the dimensional analysis will characterize the manipulator dynamics in different gravitational environments such as on the Moon, or in Earth orbit.

The dynamics of the i^{th} link are characterized by its mass m_i and the mass moments of inertia about each of its three principal axes, J_i^{xx}, J_i^{yy}, and J_i^{zz}. Intrinsic to the moments of inertia are the physical dimensions of the link. However, by characterizing the link by the moments of inertia instead of its physical dimensions, the link can be described *independently* of its shape. For example, the same values for the principal moments of inertia can describe both a cylinder and rectangular prism of different physical dimensions.

The j^{th} actuated joint is assumed to be a rigid body with mass M_j, and rotational inertia I_j^h about the actuating axis (revolute actuators only). The inertias

about the other joint axes are assumed negligible. The acceleration due to gravity is denoted by g, and time will be measured relative to a *time scaling frequency*, Ω. The fundamental dimensions associated with these variables are:

$$\begin{aligned} i^{th} \text{ link}: &\quad m_i \equiv [M],\ J_i^{xx} \equiv [M][L]^2,\ J_i^{yy} \equiv [M][L]^2,\ J_i^{zz} \equiv [M][L]^2, \\ j^{th} \text{ joint}: &\quad M_j \equiv [M],\ I_j^h \equiv [M][L]^2, \\ \text{gravity}: &\quad g \equiv [L][T]^{-2}, \\ \text{time scaling}: &\quad \Omega \equiv [T]^{-1}. \end{aligned}$$

Therefore, $4n + 2p + 2$ variables describe the system, and the equation of motion can be written as:

$$\phi(m_i, J_i^{xx}, J_i^{yy}, J_i^{zz}, M_j, I_j^h, g, \Omega) = 0, \quad i \in [1, n],\ j \in [1, p].$$

The measurement system being used has three fundamental dimensions (mass, length, time), and therefore, according to the Buckingham Pi theorem, the expected number of nondimensional Pi groups is:

$$N_\Pi = (4n + 2p + 2) - 3 = 4n + 2p - 1. \tag{3.15}$$

By definition, each nondimensional Pi group is a product of all the system variables raised to real exponents. For the k^{th} Pi group, define the real-valued exponents:

$$\alpha^k,\ \beta^k,\ \gamma_i^k,\ \delta_i^k,\ \kappa_i^k,\ \theta_i^k,\ \sigma_j^k,\ \rho_j^k, \quad i \in [1, n],\ j \in [1, p],$$

where the superscript k denotes the associated Pi group. Then the form of each Pi group is

$$\Pi_k = \Omega^{\alpha^k} g^{\beta^k} \prod_{i=1}^{n} (m_i)^{\gamma_i^k} (J_i^{xx})^{\delta_i^k} (J_i^{yy})^{\kappa_i^k} (J_i^{zz})^{\theta_i^k} \prod_{j=1}^{p} (M_j)^{\sigma_j^k} (I_j^h)^{\rho_j^k}, \quad k \in [1, N_\Pi]. \tag{3.16}$$

In terms of the fundamental dimensions, each Pi group can be expressed as

$$\Pi_k \equiv [T^{-1}]^{\alpha^k} [LT^{-2}]^{\beta^k} \prod_{i=1}^{n} [M]^{\gamma_i^k} [ML^2]^{\delta_i^k} [ML^2]^{\kappa_i^k} [ML^2]^{\theta_i^k} \prod_{j=1}^{p} [M]^{\sigma_j^k} [ML^2]^{\rho_j^k}.$$

In order to find the nondimensional Pi groups, values for the individual exponents must be found, so that the total exponent for each fundamental dimension is zero. Collecting the exponents associated with each fundamental dimension gives way to three equations in $4n + 2p + 2$ unknowns:

$$\begin{aligned}
[M]: &\quad \sum_{i=1}^{n}\left(\gamma_i^k + \delta_i^k + \kappa_i^k + \theta_i^k\right) + \sum_{j=1}^{p}\left(\sigma_j^k + \rho_j^k\right) = 0 \\
[L]: &\quad \beta^k + \sum_{i=1}^{n}\left(2\delta_i^k + 2\kappa_i^k + 2\theta_i^k\right) + \sum_{j=1}^{p} 2\rho_j^k = 0 \\
[T]: &\quad -\alpha^k - 2\beta^k = 0.
\end{aligned} \tag{3.17}$$

From this set of equations the values of $4n+2p-1$ variables can be set arbitrarily, and the values for the three remaining variables can be solved for. To rewrite the system of equations in terms of three variables, the following selections of three variables are possible: either α^k or β^k, but not both; only one from δ_i^k, κ_i^k, θ_i^k or ρ_j^k; only one from γ_i^k or σ_j^k. The first group corresponds to the variables Ω and g, whose fundamental dimensions include time $[T]$. The second group corresponds to the inertia variables($[M][L]^2$), and the third to mass variables($[M]$). By choosing the three variables in this manner, regardless of the three selected, these three variables will represent parameters whose dimensions are $[T]$, $[M][L]^2$, and $[M]$. Hence, the parameters are *independent of each other in their fundamental dimensions.*

Introducing the following notation

$$\Gamma_{a\to b} \triangleq \{\Gamma_a,\ \Gamma_{a+1},\ \ldots,\ \Gamma_b\},$$

allows the definition of the vector

$$\boldsymbol{x}^k \triangleq \left[\beta^k,\ \gamma_{2\to n}^k,\ \sigma_{1\to p}^k,\ \delta_{2\to n}^k,\ \kappa_{1\to n}^k,\ \theta_{1\to n}^k,\ \rho_{1\to p}^k\right]^T,$$

where $\boldsymbol{x}^k$ has dimensions $(4n + 2p - 1) \times 1$.

Then, from (3.17), choosing to solve for α^k, γ_1^k, and δ_1^k in terms of the arbitrarily valued exponents in $\boldsymbol{x}^k$ gives the following matrix relationship

$$\begin{bmatrix} \alpha^k \\ \gamma_1^k \\ \delta_1^k \end{bmatrix} = \begin{bmatrix} -2 & 0_{2\to n} & 0_{1\to p} & 0_{2\to n} & 0_{1\to n} & 0_{1\to n} & 0_{1\to p} \\ \frac{1}{2} & -1_{2\to n} & -1_{1\to p} & 0_{2\to n} & 0_{1\to n} & 0_{1\to n} & 0_{1\to p} \\ -\frac{1}{2} & 0_{2\to n} & 0_{1\to p} & -1_{2\to n} & -1_{1\to n} & -1_{1\to n} & -1_{1\to p} \end{bmatrix} \boldsymbol{x}^k,$$

or equivalently,

$$\boldsymbol{a}^k = \Lambda \boldsymbol{x}^k \quad k \in [1, N_\Pi],$$

where the vector $\boldsymbol{a}^k$ has dimensions 3×1, and the dimensions of matrix Λ are $3 \times (4n + 2p - 1)$. For the zeros and ones in the matrix, the subscripts have no meaning, and hence the notation $0_{a \to b}$ and $1_{a \to b}$ simply represent a list of $b - a + 1$ values.

This equation corresponds to the k^{th} Pi group. By allowing k to vary from 1 to N_Π, a matrix equation for all the Pi groups can be obtained. Namely,

$$\left[\boldsymbol{a}^1 \cdots \boldsymbol{a}^{N_\Pi}\right] = \Lambda \left[\boldsymbol{x}^1 \cdots \boldsymbol{x}^{N_\Pi}\right],$$

or

$$A = \Lambda X.$$

The matrix A has dimension $3 \times N_\Pi$, and the matrix X has dimension $(4n + 2p - 1) \times N_\Pi$. In fact, by the definition of N_Π in (3.15), it is clear that X is a square matrix of dimension $N_\Pi \times N_\Pi$.

Define V to be the matrix obtained by stacking X over A. Then by the definitions of X and A, each column of V contains the exponents for one of the Pi groups. That is,

$$V \triangleq \begin{bmatrix} X \\ A \end{bmatrix} = \begin{bmatrix} I \\ \Lambda \end{bmatrix} X, \tag{3.18}$$

with V a $(4n + 2p + 2) \times N_\Pi$ matrix.

The linear independence of all the Pi groups is a function of the matrix V. Since each column of V contains the exponents for one of the Pi groups, linear independence of the Pi groups is guaranteed if no column of V can be represented as a linear combination of the other columns. In other words, independent Pi groups require that V have full rank. Furthermore, from (3.18),

$$\text{rank}(V) = \min\left(\text{rank}\begin{bmatrix} I \\ \Lambda \end{bmatrix}, \text{rank}(X)\right) = \min(N_\Pi, \text{rank}(X)).$$

Hence, in order for V to have full rank (N_Π), the matrix X must also have rank N_Π, which implies that X must be nonsingular. Recall that X contains the

arbitrary valued exponents. Every different nonsingular X will result in a different set of $4n + 2p - 1$ nondimensional Pi groups for the manipulator. However, every such set is not unique in that it can be converted via a matrix transformation to another independent set of Pi groups. Let X_1 and X_2 be two different non-singular matrices, with corresponding V_1 and V_2. Then,

$$V_1 = \Lambda X_1, \quad V_2 = \Lambda X_2 \quad \Rightarrow \quad \Lambda = V_1(X_1)^{-1} = V_2(X_2)^{-1} \quad \Rightarrow \quad V_2 = V_1(X_1)^{-1}X_2.$$

The number of variables in each Pi group can be minimized by selecting X to be the identity matrix of appropriate dimension. The exponents for each Pi group are obtained by substituting $X = I$ into (3.18) to give $V = [I \quad \Lambda]^T$. Then, substituting the values from each column of V into (3.16) reveals the following $N_\Pi = 4n + 2p - 1$ nondimensional Pi groups:

$$\begin{aligned}
\Pi_G &= \frac{g m_1^{\frac{1}{2}}}{\Omega^2 (J_1^{xx})^{\frac{1}{2}}} \\
\Pi_{m_i} &= \frac{m_i}{m_1}, \quad i \in [2, n] \\
\Pi_{M_j} &= \frac{M_j}{m_1}, \quad j \in [1, p] \\
\Pi_{J_i^{xx}} &= \frac{J_i^{xx}}{J_1^{xx}}, \quad i \in [2, n] \\
\Pi_{J_i^{yy}} &= \frac{J_i^{yy}}{J_1^{xx}}, \quad i \in [1, n] \\
\Pi_{J_i^{zz}} &= \frac{J_i^{zz}}{J_1^{xx}}, \quad i \in [1, n] \\
\Pi_{I_j^h} &= \frac{I_j^h}{J_1^{xx}}, \quad j \in [1, p].
\end{aligned}$$

Using the expression for the radius of gyration from (3.4), Π_G can be rewritten as

$$\Pi_G = \frac{g}{k_1 \Omega^2}.$$

These Pi groups can now be compared to the nondimensional groups that were found in the nondimensional energy expressions. By defining $J_1 = J_1^{xx}$, the following

relationships exist:

$$\begin{aligned}
\Pi_{m_i} &= \frac{m_i}{m_1} = \hat{m}_i \\
\Pi_{M_j} &= \frac{M_j}{m_1} = \hat{M}_j \\
\Pi_{J_{c_i}} &= diag\{\Pi_{J_i^{xx}}, \Pi_{J_i^{yy}}, \Pi_{J_i^{zz}}\} = \hat{J}_{c_i} \\
\Pi_{I_j^h} &= \frac{I_j^h}{J_1} = \hat{I}_j^h \\
\Pi_G &= \frac{g}{k_1\Omega^2} = \frac{g}{g_0}\frac{g_0}{k_1\Omega^2} = \hat{g}\frac{g_0}{k_1\Omega^2}.
\end{aligned}$$

Notice how the single Pi group Π_G combines the effect of the two nondimensional groups, $\hat{g}$ and $\frac{g_0}{k_1\Omega^2}$, found in the nondimensional energy expressions. This indicates that the group involving solely the reference values g_0, k_1, and Ω is redundant. Instead the Buckingham Pi theorem gives the result that acceleration due to gravity can be scaled by the product $k_1\Omega^2$, and hence the reference variable g_0 need not be introduced.

Therefore, the dynamics of a general n-link rigid manipulator are characterized by the following set of nondimensional Pi groups

$$\left\{\Pi_{m_i} = \frac{m_i}{m_1},\ \Pi_{J_{c_i}} = \frac{1}{J_1}J_{c_i},\ \Pi_{M_j} = \frac{M_j}{m_1},\ \Pi_{I_j^h} = \frac{I_j^h}{J_1},\ \Pi_G = \frac{g}{k_1\Omega^2}\right\}. \quad (3.19)$$

Hence, the dimensional dynamic equations for general n-link rigid manipulators have been reduced to the nondimensional equations as per:

$$\underbrace{\phi\left(m_i, J_i^{xx}, J_i^{yy}, J_i^{zz}, M_j, I_j^h, g, \Omega\right)}_{4n+2p+2 \text{ parameters}} = \underbrace{F\left(\Pi_{m_i}, \Pi_{J_i^{xx}}, \Pi_{J_i^{yy}}, \Pi_{J_i^{zz}}, \Pi_{M_j}, \Pi_{I_j^h}, \Pi_G\right)}_{4n+2p-1 \text{ parameters}}.$$

Length Scaling

It still remains to be determined how an arbitrary length parameter, $\mathcal{L}$, scales in the manipulator system. Prime examples of such length parameters would be the physical dimensions of each link. In fact, as may be expected, all length parameters of the system scale via the parameter k_1, as shown in the following lemma.

Lemma 3.1 (Length Scaling: Rigid Manipulators)
Given a length parameter, $\mathcal{L}$, of a rigid manipulator system, and the rigid Pi groups

$$\Pi_{m_i},\ \Pi_{J_i^{xx}},\ \Pi_{J_i^{yy}},\ \Pi_{J_i^{zz}},$$

a nondimensional Pi group for $\mathcal{L}$ is

$$\Pi_{\mathcal{L}} = \frac{\mathcal{L}}{k_1}.$$

Proof
By definition,

$$\begin{aligned} J_i^{xx} &= \int_{m_i} y_i^2 + z_i^2 dm_i, \\ J_i^{yy} &= \int_{m_i} x_i^2 + z_i^2 dm_i, \\ J_i^{zz} &= \int_{m_i} x_i^2 + y_i^2 dm_i. \end{aligned}$$

Without loss of generality, consider J_i^{xx}. By definition of $\Pi_{J_i^{xx}}$,

$$\begin{aligned} \Pi_{J_i^{xx}} &= \frac{J_i^{xx}}{J_1} \\ &= \frac{1}{m_1 k_1^2} \int_{m_i} y_i^2 + z_i^2 dm_i \\ &= \int_{\frac{m_i}{m_1}} \left(\frac{y_i}{k_1}\right)^2 + \left(\frac{z_i}{k_1}\right)^2 d\frac{m_i}{m_1} \\ &= \int_{\Pi_{m_i}} \left(\frac{y_i}{k_1}\right)^2 + \left(\frac{z_i}{k_1}\right)^2 d\Pi_{m_i}. \end{aligned}$$

Similarly, it is straightforward to show

$$\begin{aligned} \Pi_{J_i^{yy}} &= \int_{\Pi_{m_i}} \left(\frac{x_i}{k_1}\right)^2 + \left(\frac{z_i}{k_1}\right)^2 d\Pi_{m_i}, \\ \Pi_{J_i^{zz}} &= \int_{\Pi_{m_i}} \left(\frac{x_i}{k_1}\right)^2 + \left(\frac{x_i}{k_1}\right)^2 d\Pi_{m_i}. \end{aligned}$$

By adding and subtracting these equations, the following can be achieved

$$\begin{aligned}
\int_{\Pi_{m_i}} \left(\frac{x_i}{k_1}\right)^2 d\Pi_{m_i} &= \frac{1}{2}\left(-\Pi_{J_i^{xx}} + \Pi_{J_i^{yy}} + \Pi_{J_i^{zz}}\right), \\
\int_{\Pi_{m_i}} \left(\frac{y_i}{k_1}\right)^2 d\Pi_{m_i} &= \frac{1}{2}\left(\Pi_{J_i^{xx}} - \Pi_{J_i^{yy}} + \Pi_{J_i^{zz}}\right), \\
\int_{\Pi_{m_i}} \left(\frac{z_i}{k_1}\right)^2 d\Pi_{m_i} &= \frac{1}{2}\left(\Pi_{J_i^{xx}} + \Pi_{J_i^{yy}} - \Pi_{J_i^{zz}}\right).
\end{aligned}$$

These equations indicate that if the manipulator is scaled with respect to the Pi groups $\Pi_{J_i^{xx}}$, $\Pi_{J_i^{yy}}$, $\Pi_{J_i^{zz}}$, and Π_{m_i}, then each coordinate axis, x_i, y_i, and z_i is scaled by the factor k_1. If the coordinate axes are scaled, then any length parameter, $\mathcal{L}$, of the manipulator system must be scaled according to the nondimensional group

$$\Pi_{\mathcal{L}} = \frac{\mathcal{L}}{k_1}.$$

■

This lemma shows that length scaling is accomplished automatically by satisfying the scaling conditions specified by Π_{m_i}, $\Pi_{J_i^{xx}}$, $\Pi_{J_i^{yy}}$, and $\Pi_{J_i^{zz}}$. This property will be useful when examining the sample systems in section 3.2.4.

3.2.3 Comments

In this section, three comments regarding the modelling of the rigid links are presented. The first two comments justify that the principal moments of inertia are sufficient to characterize the inertial properties of the rigid link, even in the case when the body-fixed frame is not at the centre of mass. The final comment addresses the issue of characterizing the link using its *mass density* instead of its mass.

Principal Axes & Products of Inertia

The situation where the body-fixed frame for the i^{th} link is *not* selected to be at the centre of mass can also be handled by the methodology. In the general case, the inertia matrix is no longer diagonal, as the products of inertia are not necessarily zero. The inertia matrix has the following form[19]:

$$J = \int_m \begin{bmatrix} y^2+z^2 & -xy & -xz \\ -xy & x^2+z^2 & -yz \\ -xz & -yz & x^2+y^2 \end{bmatrix} dm \triangleq \begin{bmatrix} J_i^{xx} & J_i^{xy} & J_i^{xz} \\ J_i^{xy} & J_i^{yy} & J_i^{yz} \\ J_i^{xz} & J_i^{yz} & J_i^{zz} \end{bmatrix}.$$

Let J be an inertia matrix with respect to a body-fixed frame $\mathcal{F}$. A rotation matrix can be found such that the inertia matrix with respect to the rotated frame is *diagonal*. The rotated frame, $\mathcal{F}_p$, forms a set of *principal axes* for the body[19]. Let R denote the rotation matrix, which is nondimensional, and J_p the inertia matrix with respect to $\mathcal{F}_p$. Then the following relationship exists

$$J = RJ_pR^T, \quad J_p = diag\left\{J_p^{xx}, J_p^{yy}, J_p^{zz}\right\}.$$

Therefore, the moments of inertia $(J_i^{xx}, J_i^{yy}, J_i^{zz})$, and the products of inertia $(J_i^{xy}, J_i^{yz}, J_i^{xz})$, in J, can all be expressed in terms of the three principal moments of inertia in J_p. In particular, this means that the inertial Pi groups in J can be expressed in terms of the three inertial Pi groups in J_p.

Parallel-Axis Theorem

By using the parallel-axis theorem, the inertial properties at any point in the body can be expressed in terms of the principal moments of inertia at the centre of mass. Let J_{c_i} be the inertia matrix containing the principal moments of inertia at the centre of the i^{th} link (frame $\mathcal{F}_{ci}$), and let J be the inertia matrix about a coordinate frame $\mathcal{F}$ parallel to $\mathcal{F}_{ci}$. Let the distance vector between the origins of $\mathcal{F}_{ci}$ and $\mathcal{F}$ be $[s_x\ s_y\ s_z]^T$. Then, because $\mathcal{F}_{ci}$ is at the centre of mass, the parallel-axis theorem

states[19],

$$\begin{aligned} J^{xx} &= J_{ci}^{xx} + m_i(s_y^2 + s_z^2) \\ J^{yy} &= J_{ci}^{yy} + m_i(s_x^2 + s_z^2) \\ J^{zz} &= J_{ci}^{zz} + m_i(s_x^2 + s_y^2) \\ J^{xy} &= m_i s_x s_y \\ J^{xz} &= m_i s_x s_z \\ J^{yz} &= m_i s_y s_z. \end{aligned}$$

Let $s = [s_x \ s_y \ s_z]^T$, then it is algebraic to show

$$J = J_{c_i} + m_i \left[s^T s I - s s^T \right].$$

Nondimensionalizing these equations by $J_1 = m_1 k_1^2$ gives,

$$\frac{1}{J_1} J = \Pi_{J_{ci}} + \Pi_{m_i} \left[\Pi_S^T \Pi_S I - \Pi_S \Pi_S^T \right],$$

where $\Pi_S = \frac{s}{k_1}$.

From Lemma 3.1, it is known that scaling Π_{m_i} and $\Pi_{J_{ci}}$ automatically defines a length scaling, and hence, the distance s will scale according to Π_S. Therefore, even for an inertia matrix about any body-fixed frame, only the Pi groups for the mass and the principal moments of inertia about the centre of mass are required to characterize the i^{th} link.

Mass versus Mass Density

In characterizing the link dynamics, instead of using the link mass, m_i, it may be more practical to use the volume mass density of the link material, ρ_i^v. The advantage of this link description is that it facilitates the specification of different link materials in designing dynamically equivalent robots. Although mathematically equivalent to the Pi groups in (3.19), the Pi groups obtained using ρ_1^v in place of m_1 appear more complicated. With the base parameters as m_1 and J_1, a natural

length measure is the radius of gyration, $k_1 = \sqrt{J_1 m_1^{-1}}$. Instead, with the base parameters ρ_1^v, and J_1, neither such a length measure nor a mass measure can be found, complicating the form of the Pi groups.

Regardless, for completeness, the Pi groups obtained from the Buckingham Pi theorem with the base parameters ρ_1^v, J_1 and Ω are as follows:

$$\left\{ \Pi_{\rho_i^v} = \frac{\rho_i^v}{\rho_1^v}, \quad \Pi_{\boldsymbol{J}_{c_i}} = \frac{1}{J_1}\boldsymbol{J}_{c_i}, \quad \Pi_{M_j} = \frac{M_j}{(\rho_1^v)^{\frac{2}{5}} J_1^{\frac{3}{5}}}, \quad \Pi_{I_j^h} = \frac{I_j^h}{J_1}, \quad \Pi_G = \left(\frac{\rho_1^v}{J_1}\right)^{\frac{1}{5}} \frac{g}{\Omega^2} \right\}. \tag{3.20}$$

3.2.4 Examples

To illustrate the application of the theory, a two-link rigid elbow manipulator, and a five-bar-linkage robot are examined in this section. For each robot, the parameters characterizing the manipulator dynamics are identified, and then (3.19) is used to determine the corresponding nondimensional Pi groups. In order to verify that the Pi groups do indeed characterize the system dynamics, the nondimensional equations of motion for each manipulator are presented.

Two-Link Rigid Manipulator

The dynamics of a two-link rigid elbow manipulator (Figure 3.2) are characterized by the following 14 parameters:

link 1: m_1, J_1^{xx}, J_1^{yy}, J_1^{zz}
link 2: m_2, J_2^{xx}, J_2^{yy}, J_2^{zz}
joint 1: M_1, I_1^h
joint 2: M_2, I_2^h
gravitational accel.: g
time scaling: Ω.

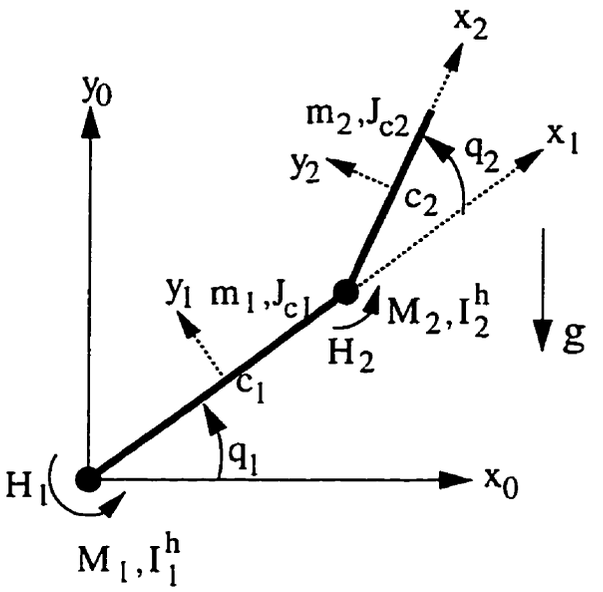

Figure 3.2: Two-Link Rigid Manipulator

The generalized coordinates associated with the two actuated joints are denoted by q_1 and q_2 in the figure. Furthermore, the actuation torques are described by H_1 and H_2.

Choosing $m_1, J_1 = J_1^{xx}$, and Ω as the base variables, and defining the radius of gyration k_1, the 11 Pi groups for this manipulator can be found, using (3.19), to be:

$$\text{link 1: } \Pi_{J_1^{yy}} = \frac{J_1^{yy}}{J_1}, \quad \Pi_{J_1^{zz}} = \frac{J_1^{zz}}{J_1}$$

$$\text{link 2: } \Pi_{m_2} = \frac{m_2}{m_1}, \quad \Pi_{J_2^{xx}} = \frac{J_2^{xx}}{J_1}, \quad \Pi_{J_2^{yy}} = \frac{J_2^{yy}}{J_1}, \quad \Pi_{J_2^{zz}} = \frac{J_2^{zz}}{J_1}$$

$$\text{joint 1: } \Pi_{M_1} = \frac{M_1}{m_1}, \quad \Pi_{I_1^h} = \frac{I_1^h}{J_1}$$

$$\text{joint 2: } \Pi_{M_2} = \frac{M_2}{m_1}, \quad \Pi_{I_2^h} = \frac{I_2^h}{J_1}$$

$$\text{gravitational accel.: } \Pi_G = \frac{g}{k_1 \Omega^2}.$$

The nondimensional equations of motions for this manipulator were derived

with $m_1, J_1 = J_1^{xx}$, and Ω as base parameters. In deriving the equations, the links were assumed to be uniform rectangular prisms, and their dimensions were computed from the given inertial properties. In particular, the link lengths l_i, and distances to the link centres of mass l_{ci}, were used in the derivation, and hence the nondimensional equations contain the Pi groups Π_{l_i} and $\Pi_{l_{ci}}$. However, from Lemma (3.1), it is known that these length Pi groups are actually functions of the mass and inertia Pi groups for each link. In terms of the Pi groups, the two nondimensional equations of motion for the rigid elbow manipulator are:

$$\begin{aligned}
&\left(\Pi_{I_1^h} + \Pi_{I_2^h} + \Pi_{M_2}\Pi_{l_1}^2 + \Pi_{l_{c1}}^2 + \Pi_{J_1^{zz}} + \Pi_{m_2}\Pi_{l_1}^2 + \Pi_{m_2}\Pi_{l_{c2}}^2 + \Pi_{J_2^{zz}}\right.\\
&\qquad \left. +2\Pi_{m_2}\Pi_{l_1}\Pi_{l_{c2}}\cos(\hat{q}_2)\right)\ddot{\hat{q}}_1\\
&\qquad + \left(\Pi_{I_2^h} + \Pi_{m_2}\Pi_{l_{c2}}^2 + \Pi_{J_2^{zz}} + \Pi_{m_2}\Pi_{l_1}\Pi_{l_{c2}}\cos(\hat{q}_2)\right)\ddot{\hat{q}}_2\\
&\qquad -2\Pi_{m_2}\Pi_{l_1}\Pi_{l_{c2}}\sin(\hat{q}_2)\dot{\hat{q}}_1\dot{\hat{q}}_2 - \Pi_{m_2}\Pi_{l_1}\Pi_{l_{c2}}\sin(\hat{q}_2)\dot{\hat{q}}_2^2\\
&\qquad +\Pi_G\left(\Pi_{M_2}\Pi_{l_1} + \Pi_{l_{c1}} + \Pi_{m_2}\Pi_{l_1}\right)\cos(\hat{q}_1)\\
&\qquad +\Pi_G\Pi_{m_2}\Pi_{l_{c2}}\cos(\hat{q}_1 + \hat{q}_2) = \hat{H}_1(\tau)
\end{aligned}$$

$$\begin{aligned}
&\left(\Pi_{I_2^h} + \Pi_{m_2}\Pi_{l_{c2}}^2 + \Pi_{J_2^{zz}} + \Pi_{m_2}\Pi_{l_1}\Pi_{l_{c2}}\cos(\hat{q}_2)\right)\ddot{\hat{q}}_1\\
&\qquad + \left(\Pi_{I_2^h} + \Pi_{m_2}\Pi_{l_{c2}}^2 + \Pi_{J_2^{zz}}\right)\ddot{\hat{q}}_2\\
&\qquad +\Pi_{l_1}\Pi_{l_{c2}}\sin(\hat{q}_2)\dot{\hat{q}}_1^2 + \Pi_G\Pi_{m_2}\Pi_{l_{c2}}\cos(\hat{q}_1 + \hat{q}_2) = \hat{H}_2(\tau).
\end{aligned}$$

The nondimensional joint torques are given by $\hat{H}_1$ and $\hat{H}_2$.

Since the first joint does not translate, the joint mass M_1 does not affect the dynamics. Also, because the motion of the manipulator is restricted to a plane, the moments of inertia J_i^{xx} and J_i^{yy} do not have a role in the equations of motion. Correspondingly, the nondimensional equations of motion do *not* contain Pi groups for M_1, J_i^{xx}, and J_i^{yy}. This means that these three Pi groups are not required to define the dynamic equivalence conditions for this manipulator. Simulation results using the two-link rigid manipulator are presented in Chapter 8.

Five-bar-Linkage Manipulator

The five-bar-linkage manipulator is a robot with four rigid links in a parallelogram configuration (Figure 3.3). The "fifth" link is the ground. There are three actuated joints: a base joint, and two planar joints. There are also three unactuated pin-joints between links 2 and 3, links 3 and 4, and between links 1 and 4. The manipulator dynamics are characterized by the following 23 parameters

link 1: m_1, J_1^{xx}, J_1^{yy}, J_1^{zz}
link 2: m_2, J_2^{xx}, J_2^{yy}, J_2^{zz}
link 3: m_3, J_3^{xx}, J_3^{yy}, J_3^{zz}
link 4: m_4, J_4^{xx}, J_4^{yy}, J_4^{zz}
joint 1: I_1^h
joint 2: M_2, I_2^h
joint 2: M_3, I_3^h
gravitational accel.: g
time scaling: Ω.

The base joint does not translate, so its joint mass M_1 does not affect the dynamics. The generalized coordinates and actuation torques associated with the three actuated joints are denoted by q_1, q_2, q_3 and H_1, H_2, H_3 in the figure.

Choosing $m_1, J_1 = J_1^{xx}$, and Ω as the base variables, and defining the radius of gyration k_1, the 20 Pi groups for this manipulator can be found using (3.19):

link 1: $\Pi_{J_1^{yy}} = \dfrac{J_1^{yy}}{J_1}$, $\Pi_{J_1^{zz}} = \dfrac{J_1^{zz}}{J_1}$

link 2: $\Pi_{m_2} = \dfrac{m_2}{m_1}$, $\Pi_{J_2^{xx}} = \dfrac{J_2^{xx}}{J_1}$, $\Pi_{J_2^{yy}} = \dfrac{J_2^{yy}}{J_1}$, $\Pi_{J_2^{zz}} = \dfrac{J_2^{zz}}{J_1}$

link 3: $\Pi_{m_3} = \dfrac{m_3}{m_1}$, $\Pi_{J_3^{xx}} = \dfrac{J_3^{xx}}{J_1}$, $\Pi_{J_3^{yy}} = \dfrac{J_3^{yy}}{J_1}$, $\Pi_{J_3^{zz}} = \dfrac{J_3^{zz}}{J_1}$

link 4: $\Pi_{m_4} = \dfrac{m_4}{m_1}$, $\Pi_{J_4^{xx}} = \dfrac{J_4^{xx}}{J_1}$, $\Pi_{J_4^{yy}} = \dfrac{J_4^{yy}}{J_1}$, $\Pi_{J_4^{zz}} = \dfrac{J_4^{zz}}{J_1}$

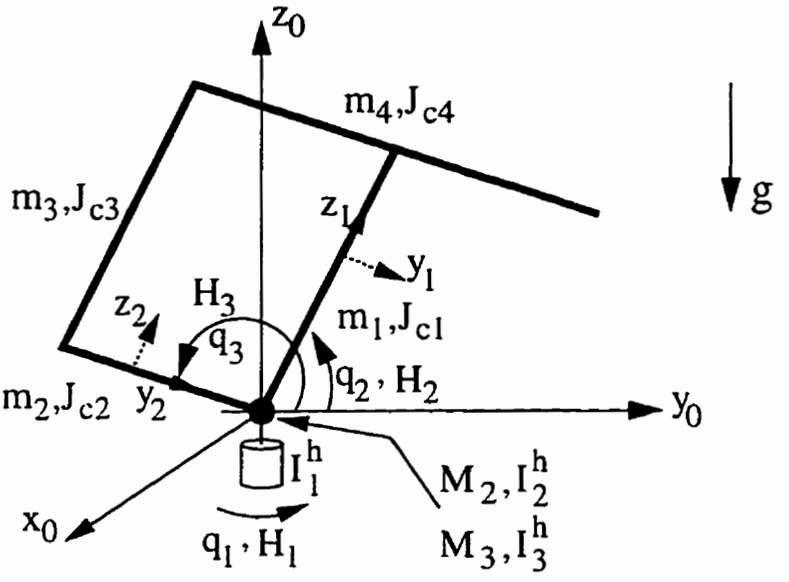

Figure 3.3: Five-Link Rigid Manipulator

joint 1: $\Pi_{I_1^h} = \dfrac{I_1^h}{J_1}$

joint 2: $\Pi_{M_2} = \dfrac{M_2}{m_1}, \quad \Pi_{I_2^h} = \dfrac{I_2^h}{J_1}$

joint 3: $\Pi_{M_3} = \dfrac{M_3}{m_1}, \quad \Pi_{I_3^h} = \dfrac{I_3^h}{J_1}$

gravitational accel.: $\Pi_G = \dfrac{g}{k_1 \Omega^2}.$

Appropriate selection of link lengths and masses allows the planar motion to become decoupled. The dynamic equations for this manipulator were derived in [21]. In the derivation, the local co-ordinate axes for links 1 and 3 are parallel, as are the axes for links 2 and 4. Let r_2 and r_3 be the distances of the joint masses M_2 and M_3 from the q_1 axis of rotation (z_0). Then, in terms of the rigid Pi groups (3.19),

the nondimensional form of these equations (with m_1, J_1^{xx}, Ω as base parameters) is

$$\left(\hat{M}_{11} + \Pi_{M_2}\Pi_{r_2}^2 + \Pi_{M_3}\Pi_{r_3}^2 + \Pi_{I_1^h}\right)\ddot{\hat{q}}_1 + \frac{\partial \hat{M}_{11}}{\partial \hat{q}_2}\dot{\hat{q}}_1\dot{\hat{q}}_2 + \frac{\partial \hat{M}_{11}}{\partial \hat{q}_3}\dot{\hat{q}}_1\dot{\hat{q}}_3 = \hat{H}_1(\tau)$$

$$\left(\hat{M}_{22} + \Pi_{I_2^h}\right)\ddot{\hat{q}}_2 - \frac{1}{2}\frac{\partial \hat{M}_{11}}{\partial \hat{q}_2}\dot{\hat{q}}_1^2 + \Pi_G\left(\Pi_{l_{c1}} + \Pi_{m_3}\Pi_{l_{c3}} + \Pi_{m_4}\Pi_{l_1}\right)\cos(\hat{q}_2) = \hat{H}_2(\tau)$$

$$\left(\hat{M}_{33} + \Pi_{I_3^h}\right)\ddot{\hat{q}}_3 - \frac{1}{2}\frac{\partial \hat{M}_{11}}{\partial \hat{q}_3}\dot{\hat{q}}_1^2 + \Pi_G\left(\Pi_{m_2}\Pi_{l_{c2}} + \Pi_{m_3}\Pi_{l_2} - \Pi_{m_4}\Pi_{l_{c4}}\right)\cos(\hat{q}_3) = \hat{H}_3(\tau),$$

where

$$\begin{aligned}\hat{M}_{11} = &\left(\Pi_{l_{c1}}^2 + \Pi_{m_3}\Pi_{l_{c3}}^2 + \Pi_{m_4}\Pi_{l_1}^2 + \Pi_{J_1^{yy}} + \Pi_{J_3^{yy}}\right)\cos(\hat{q}_2)^2 \\ &+\left(\Pi_{J_1^{zz}} + \Pi_{J_3^{zz}}\right)\sin(\hat{q}_2)^2 \\ &+\left(\Pi_{m_3}\Pi_{l_2}^2 + \Pi_{m_4}\Pi_{l_{c4}}^2 + \Pi_{m_2}\Pi_{l_{c2}}^2 + \Pi_{J_2^{zz}} + \Pi_{J_4^{zz}}\right)\cos(\hat{q}_3)^2 \\ &+\left(\Pi_{J_2^{yy}} + \Pi_{J_4^{yy}}\right)\sin(\hat{q}_3)^2\end{aligned}$$

$$\hat{M}_{22} = \Pi_{l_{c1}}^2 + \Pi_{m_3}\Pi_{l_{c3}}^2 + \Pi_{m_4}\Pi_{l_1}^2 + 1 + \Pi_{J_3^{zz}}$$

$$\hat{M}_{33} = \Pi_{m_3}\Pi_{l_2}^2 + \Pi_{m_4}\Pi_{l_{c4}}^2 + \Pi_{m_2}\Pi_{l_{c2}}^2 + \Pi_{J_2^{zz}} + \Pi_{J_4^{zz}}.$$

The nondimensional actuation torques are given by $\hat{H}_1$, $\hat{H}_2$, and $\hat{H}_3$.

As with the two-link manipulator, these dynamic equations were also derived in terms of link lengths, and hence the nondimensional groups,

$$\Pi_{l_i} = \frac{l_i}{k_1}, \quad \text{and} \quad \Pi_{l_{ci}} = \frac{l_{ci}}{k_1},$$

appear within the nondimensional equations. Recall from Lemma 3.1 that these Pi groups can be written in terms of the mass and inertia Pi groups.

3.3 General n-Link Flexible Manipulators

The term *general n-link flexible manipulator* refers to the class of manipulators with n flexible links, p actuators, any link topology, and having unconstrained motion.

Each link is assumed to have a uniform cross-section, bending in two directions, and high axial rigidity (i.e. torsional and axial vibrations are not modelled). The purpose of this section is to determine the dynamic equivalence conditions for this class of manipulators. The structure of the development will be the same as that used for the rigid manipulators. As with the previous section, references to the term *joint* will be used to indicate actuated joints only.

In this derivation, the flexible links are assumed to be long and slender, and are modelled using an Euler-Bernoulli beam model[22]. Nondimensional groups associated with extensions to this flexible link model, such as damping, and torsional vibration, will be addressed in section 3.3.4.

3.3.1 Nondimensional Dynamics

In Figure (3.4), the i^{th} flexible link is depicted in an inertial reference frame ($\mathcal{F}_0$). In addition, attach frame i ($\mathcal{F}_i$) to one end of the link with the z_i-axis parallel to the undeflected link. Define the following variables (boldface variables indicate 3×1 vectors or 3×3 matrices expressed in $\mathcal{F}_0$ coordinates):

- $\mathrm{w}_{x_i}(z,t)$ - deflection of link parallel to x_i axis
- $\mathrm{w}_{y_i}(z,t)$ - deflection of link parallel to y_i axis
- $\boldsymbol{d}_0^i(t)$ - distance from O_0 to O_i in $\mathcal{F}_0$ coordinates
- $\boldsymbol{r}_i(t) = [\mathrm{w}_{x_i}\ \mathrm{w}_{y_i}\ z_i]^T$ - position of link element dm_i in $\mathcal{F}_i$ coordinates
- $\boldsymbol{p}_i(t)$ - position of link element dm_i in $\mathcal{F}_0$ coordinates
- $\boldsymbol{R}_0^i(t)$ - rotation matrix from $\mathcal{F}_i$ to $\mathcal{F}_0$.

The variables for the joint parameters are the same as in Figure 3.1, namely:

$$I_j^h,\ M_j,\ \boldsymbol{d}_0^j(t),\ \boldsymbol{\omega}_0^j(t).$$

Again, it is assumed that the inertia about the other joint axes is negligible.

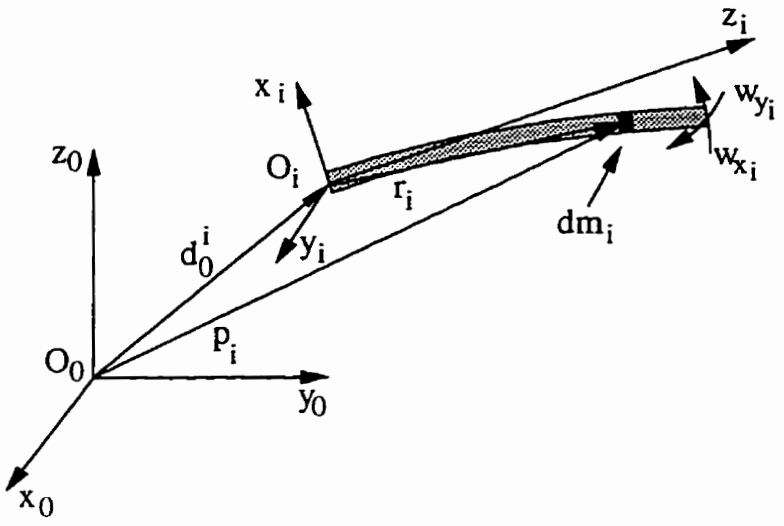

Figure 3.4: i^{th} Flexible Link in Inertial Frame

Nondimensional Kinetic Energy

The total kinetic energy of the system, T, is equal to the sum of the kinetic energies of all the links and joints. That is,

$$T(t) = \sum_{i=1}^{n} T_i^{\text{link}}(t) + \sum_{j=1}^{p} T_j^{\text{joint}}(t).$$

Because the flexible link is a distributed parameter system, the kinetic energy is computed as an integration over the length of the link. In representing the dynamics of flexible link systems with uniform links, the link mass m_i, is frequently represented by the equivalent, $\rho_i l_i$, where ρ_i is the linear mass density of the link, and l_i is the length of the link. The joint is treated as a rigid body. Therefore,

$$T_i^{\text{link}}(t) = \frac{1}{2}\rho_i \int_0^{l_i} \left(\frac{d\boldsymbol{p}_i}{dt}\right)^T \frac{d\boldsymbol{p}_i}{dt}\, dz_i \tag{3.21}$$

$$T_j^{\text{joint}}(t) = \frac{1}{2} M_j \left(\frac{d\boldsymbol{d}_0^j}{dt}\right)^T \frac{d\boldsymbol{d}_0^j}{dt} + \frac{1}{2} I_j^h\, \boldsymbol{\omega}_0^{j\,T}\, \boldsymbol{\omega}_0^j. \tag{3.22}$$

To obtain the expression for the nondimensional kinetic energy, the following

variables in (3.21) and (3.22) must be nondimensionalized:

$$t,\ \rho_i,\ l_i,\ dz_i,\ \boldsymbol{p}_i(t),\ M_j,\ \boldsymbol{d}_0^j(t),\ I_j^h,\ \boldsymbol{\omega}_0^j(t).$$

The reference values for time will again be selected to be the reference frequency Ω. The reference value for ρ_i will be the linear mass density of the first link, ρ_1. The reference value for inertia will be hub inertia of the first joint, I_1^h. Finally, the length of the first link, l_1, can be taken as an intuitive reference value for length variables. The values ρ_1 and l_1 naturally define a reference value for mass, namely the mass of the first link $m_1 = \rho_1 l_1$. Hence, define the following nondimensional variables:

$$\begin{aligned}
\tau &\triangleq \Omega t \\
\hat{\rho}_i &\triangleq \frac{\rho_i}{\rho_1} \\
\hat{\boldsymbol{p}}_i(\tau) &\triangleq \frac{\boldsymbol{p}_i\left(\frac{\tau}{\Omega}\right)}{l_1} \\
\hat{\boldsymbol{d}}_0^j(\tau) &\triangleq \frac{\boldsymbol{d}_0^j\left(\frac{\tau}{\Omega}\right)}{l_1} \\
d\hat{z}_i &\triangleq \frac{1}{l_1} dz_i \\
\hat{l}_i &\triangleq \frac{l_i}{l_1} \\
\hat{M}_j &\triangleq \frac{M_j}{m_1} \\
\hat{I}_j^h &\triangleq \frac{I_j^h}{I_1^h} \\
\hat{\boldsymbol{\omega}}_0^j(\tau) &\triangleq \frac{\boldsymbol{\omega}_0^j\left(\frac{\tau}{\Omega}\right)}{\Omega}.
\end{aligned}$$

Substitution of these nondimensional variables into (3.21) and (3.22) gives

$$\begin{aligned}
T_i^{\text{link}}\left(\frac{\tau}{\Omega}\right) &= \frac{1}{2}\rho_1 l_1^3 \Omega^2 \hat{\rho}_i \int_0^{\hat{l}_i} \left(\frac{d\hat{\boldsymbol{p}}_i}{d\tau}\right)^T \frac{d\hat{\boldsymbol{p}}_i}{d\tau}\, d\hat{z}_i \\
T_j^{\text{joint}}\left(\frac{\tau}{\Omega}\right) &= \frac{1}{2} m_1 l_1^2 \Omega^2 \hat{M}_j \left(\frac{d\hat{\boldsymbol{d}}_0^j}{d\tau}\right)^T \frac{d\hat{\boldsymbol{d}}_0^j}{d\tau} + \frac{1}{2} I_1^h \Omega^2 \hat{I}_j^h\, \hat{\boldsymbol{\omega}}_0^{j\,T}\, \hat{\boldsymbol{\omega}}_0^j.
\end{aligned}$$

Using the identity $m_1 = \rho_1 l_1$, divide through both equations by $m_1 l_1^2 \Omega^2$ to obtain

$$\begin{aligned}
\frac{1}{m_1 l_1^2 \Omega^2} T_i^{\text{link}}\left(\frac{\tau}{\Omega}\right) &= \frac{1}{2}\hat{\rho}_i \int_{\hat{l}_i} \left(\frac{d\hat{\boldsymbol{p}}_i}{d\tau}\right)^T \frac{d\hat{\boldsymbol{p}}_i}{d\tau}\, d\hat{z}_i \\
\frac{1}{m_1 l_1^2 \Omega^2} T_j^{\text{joint}}\left(\frac{\tau}{\Omega}\right) &= \frac{1}{2}\hat{M}_j \left(\frac{d\hat{\boldsymbol{d}}_0^j}{d\tau}\right)^T \frac{d\hat{\boldsymbol{d}}_0^j}{d\tau} + \frac{1}{2}\frac{I_1^h}{m_1 l_1^2}\hat{I}_j^h\, \hat{\boldsymbol{\omega}}_0^{j\,T}\, \hat{\boldsymbol{\omega}}_0^j.
\end{aligned}$$

Again, the same term $m_1 l_1^2 \Omega^2$ must be used to nondimensionalize all the energy expressions for the flexible manipulator. This is required for dimensional consistency of the Lagrangian in the general equation of motion (3.1).

Define the nondimensional kinetic energies

$$\hat{T}_i^{\text{link}}(\tau) \triangleq \frac{1}{m_1 l_1^2 \Omega^2} T_i^{\text{link}}\left(\frac{\tau}{\Omega}\right), \quad \hat{T}_i^{\text{joint}}(\tau) \triangleq \frac{1}{m_1 l_1^2 \Omega^2} T_i^{\text{joint}}\left(\frac{\tau}{\Omega}\right),$$

and then the nondimensional link and joint kinetic energy can be written as

$$\hat{T}_i^{\text{link}}(\tau) = \frac{1}{2}\hat{\rho}_i \int_0^{\hat{l}_i} \left(\frac{d\hat{\boldsymbol{p}}_i}{d\tau}\right)^T \frac{d\hat{\boldsymbol{p}}_i}{d\tau}\, d\hat{z}_i \tag{3.23}$$

$$\hat{T}_i^{\text{joint}}(\tau) = \frac{1}{2}\hat{M}_j \left(\frac{d\hat{\boldsymbol{d}}_0^j}{d\tau}\right)^T \frac{d\hat{\boldsymbol{d}}_0^j}{d\tau} + \frac{1}{2}\frac{I_1^h}{m_1 l_1^2}\hat{I}_j^h\, \hat{\boldsymbol{\omega}}_0^{j\,T}\, \hat{\boldsymbol{\omega}}_0^j. \tag{3.24}$$

Notice the presence of the nondimensional group composed of the reference variables: m_1, l_1, I_1^h. It will become evident in the subsequent section that this is a redundant group. In fact, the product $m_1 l_1^2$ can be used as a reference value for inertia quantities instead of I_1^h.

The total nondimensional kinetic energy is given by

$$\hat{T}(\tau) = \sum_{i=1}^{n} \hat{T}_i^{\text{link}}(\tau) + \sum_{j=1}^{p} \hat{T}_j^{\text{joint}}(\tau),$$

and contains the following nondimensional groups:

$$\left\{\hat{\rho}_i,\ \hat{l}_i,\ \hat{M}_j,\ \hat{I}_j^h,\ \frac{I_1^h}{m_1 l_1^2}\right\}.$$

Nondimensional Potential Energy

The total potential energy is equal to the stored gravitational potential energy in the links and joints, plus the strain energy stored in the flexible links. The strain energy in the i^{th} link is a function of the stiffness and deflection in each direction of vibration. By definition of the link frame $\mathcal{F}_i$ (Figure 3.4), the link cross-section will be in the $x_i - y_i$ plane. Denote the area moment of inertias about the x_i and y_i axis by I_{x_i} and I_{y_i} respectively. By assumption, the link is composed of a uniform material of elastic modulus E_i.

With this notation, the strain energy can be expressed as[22],

$$V_i^{\text{strain}}(t) = \frac{1}{2} E_i I_{x_i} \int_0^{l_i} \left(\frac{\partial^2 \mathrm{w}_{x_i}}{\partial {z_i}^2} \right)^2 \, dz_i + \frac{1}{2} E_i I_{y_i} \int_0^{l_i} \left(\frac{\partial^2 \mathrm{w}_{y_i}}{\partial {z_i}^2} \right)^2 \, dz_i. \tag{3.25}$$

The gravitational potential energy is a function of the 'height' of the i^{th} link and j^{th} joint. Using the s vector defined in (3.9), the stored gravitational energy can be expressed as,

$$V^{\text{grav}}(t) = \sum_{i=1}^{n} \rho_i g \int_0^{l_i} (s \cdot p_i) \; dz_i + \sum_{j=1}^{p} M_j g \left(s \cdot d_0^j \right). \tag{3.26}$$

As with the kinetic energy, the nondimensional potential energy expressions are found by nondimensionalizing the variables in (3.25) and (3.26). The following variables must be nondimensionalized:

$$t,\ l_i,\ z_i,\ E_i,\ I_{x_i},\ I_{y_i},\ \mathrm{w}_{x_i}(z_i,t),\ \mathrm{w}_{y_i}(z_i,t),\ \rho_i,\ M_j,\ p_i(t),\ d_0^j(t),\ g.$$

Some of these variables have already been nondimensionalized in the section on kinetic energy. Introduce E_1 and I_{x_1} as the reference values for elastic modulus and area moment of inertia respectively, and define the following nondimensional variables:

$$\hat{E}_i \triangleq \frac{E_i}{E_1}$$
$$\hat{I}_{xi} \triangleq \frac{I_{x_i}}{I_{x_1}}$$

$$\hat{I}_{y_i} \triangleq \frac{I_{y_i}}{I_{x_1}}$$

$$\hat{\mathrm{w}}_{x_i}(\hat{z}_i, \tau) \triangleq \frac{\mathrm{w}_{x_i}\left(l_1\hat{z}_i, \left(\frac{\tau}{\Omega}\right)\right)}{l_1}$$

$$\hat{\mathrm{w}}_{y_i}(\hat{z}_i, \tau) \triangleq \frac{\mathrm{w}_{y_i}\left(l_1\hat{z}_i, \left(\frac{\tau}{\Omega}\right)\right)}{l_1}.$$

In addition, consistent with the nondimensional kinetic energies, define the nondimensional potential energies

$$\hat{V}_i^{\text{link}}(\tau) \triangleq \frac{1}{m_1 l_1^2 \Omega^2} V_i^{\text{link}}\left(\frac{\tau}{\Omega}\right)$$

$$\hat{V}_i^{\text{joint}}(\tau) \triangleq \frac{1}{m_1 l_1^2 \Omega^2} V_i^{\text{joint}}\left(\frac{\tau}{\Omega}\right).$$

Substituting these into (3.25) and (3.26) gives the nondimensional potential energy expressions

$$\hat{V}_i^{\text{strain}}(\tau) = \frac{1}{2}\frac{E_1 I_{x_1}}{m_1 l_1^3 \Omega^2}\hat{E}_i I_{x_i}\int_0^{\hat{l}_i}\left(\frac{\partial^2 \hat{\mathrm{w}}_{x_i}}{\partial \hat{z}_i^2}\right)^2 d\hat{z}_i + \frac{1}{2}\frac{E_1 I_{x_1}}{m_1 l_1^3 \Omega^2}\hat{E}_i \hat{I}_{y_i}\int_0^{\hat{l}_i}\left(\frac{\partial^2 \hat{\mathrm{w}}_{y_i}}{\partial \hat{z}_i^2}\right)^2 d\hat{z}_i$$

$$\hat{V}^{\text{grav}}(\tau) = \sum_{i=1}^{n}\hat{\rho}_i\hat{g}\frac{g_0}{l_1\Omega^2}\int_0^{\hat{l}_i}(s\cdot\hat{\boldsymbol{p}}_i)\, d\hat{z}_i + \sum_{j=1}^{p}\hat{M}_j\hat{g}\frac{g_0}{l_1\Omega^2}\left(s\cdot\hat{\boldsymbol{d}}_0^j\right). \tag{3.27}$$

Notice the presence of the nondimensional groups,

$$\frac{E_1 I_{x_1}}{m_1 l_1^3 \Omega^2} = \frac{E_1}{m_1 l_1^{-1}\Omega^2}\frac{I_{x_1}}{l_1^4}, \quad \frac{g_0}{l_1\Omega^2}.$$

These groups are a function of reference variables only, and hence are redundant nondimensional groups, as will be shown. In fact, the product $m_1 l_1^{-1}\Omega^2$ can be used to nondimensionalize the elastic modulus (instead of E_1), and l_1^4 can be used to nondimensionalize area moment of inertia (instead of I_{x_1}).

The total nondimensional potential energy is

$$\hat{V}(\tau) = \sum_{i=1}^{n}\hat{V}_i^{\text{strain}}(\tau) + \hat{V}^{\text{grav}}(\tau),$$

and contains the set of nondimensional groups

$$\left\{\hat{l}_i,\ \hat{E}_i,\ \hat{I}_{x_i},\ \hat{I}_{y_i},\ \hat{\rho}_i,\ \hat{M}_j,\ \hat{g},\ \frac{g_0}{l_1\Omega^2},\ \frac{E_1}{m_1 l_1^{-1}\Omega^2},\ \frac{I_{x_1}}{l_1^4}\right\}.$$

Together, the nondimensional kinetic and potential energy expressions contain the nondimensional groups

$$\left\{\hat{\rho}_i,\ \hat{M}_j,\ \hat{l}_i,\ \hat{I}_j^h,\ \hat{E}_i,\ \hat{I}_{x_i},\ \hat{I}_{y_i},\ \hat{g},\ \frac{g}{l_1\Omega^2},\ \frac{I_1^h}{m_1 l_1^2},\ \frac{E_1}{m_1 l_1^{-1}\Omega^2},\ \frac{I_{x_1}}{l_1^4}\right\}.$$

Because these groups are time independent, their presence in the energy expressions confirms their presence in the actual nondimensional equations of motion. In the next subsection, dimensional analysis will be applied to the manipulator to verify the nondimensional groups defined here. Interestingly, it will be shown that four of these groups are redundant, and are not required to characterize the dynamics of a general n-link flexible manipulator.

3.3.2 Dimensional Analysis

For the i^{th} link, the body-fixed link coordinate frame has its origin O_i at the base of the link, with the z_i axis running along the undeflected link. The x_i and y_i axes are the principal axes of the cross-section, and are placed to form a dextrous coordinate system. The variables characterizing the uniform i^{th} link are length l_i, linear mass density ρ_i, elastic modulus E_i, and the cross-sectional area moments of inertia I_{x_i} and I_{y_i}. The area moments of inertia are used, instead of the physical dimensions of the cross-section, in order to be able to describe the link *independently* of the cross-sectional shape.

As with the rigid manipulator, the j^{th} joint is assumed to be a rigid body with mass M_j. For revolute joints, the moment of inertia about the rotation axis will be denoted I_j^h. Gravitational acceleration is denoted by g, and time will be measured relative to the time scaling frequency Ω. The fundamental dimensions associated

with these variables are given below:

$$
\begin{aligned}
i^{th} \text{ link}: &\quad l_i \equiv [L],\ \rho_i \equiv [M][L],\ E_i \equiv [M][L]^{-1}[T]^{-2},\ I_{x_i} \equiv [L]^4,\ I_{y_i} \equiv [L]^4 \\
j^{th} \text{ joint}: &\quad M_j \equiv [M],\ I_j^h \equiv [M][L]^2, \\
\text{gravity}: &\quad g \equiv [L][T]^{-2} \\
\text{time scaling}: &\quad \Omega \equiv [T]^{-1}.
\end{aligned}
$$

The flexible manipulator system is described by $5n + 2p + 2$ variables. Applying the Buckingham Pi theorem with the variables ρ_1 , l_1, and Ω (which are independent in fundamental dimensions) results in the following Pi groups:

$$
\begin{aligned}
\Pi_{\rho_i} &= \frac{\rho_i}{\rho_1}, \quad i \in [2, n] \\
\Pi_{l_i} &= \frac{l_i}{l_1}, \quad i \in [2, n] \\
\Pi_{E_i} &= \frac{E_i}{\rho_1 \Omega^2} = \frac{E_i}{m_1 l_1^{-1} \Omega^2}, \quad i \in [1, n] \\
\Pi_{I_{x_i}} &= \frac{I_{x_i}}{l_1^4}, \quad i \in [1, n] \\
\Pi_{I_{y_i}} &= \frac{I_{y_i}}{l_1^4}, \quad i \in [1, n] \\
\Pi_{M_j} &= \frac{M_j}{\rho_1 l_1} = \frac{M_j}{m_1}, \quad j \in [1, p] \\
\Pi_{I_j^h} &= \frac{I_j^h}{\rho_1 l_1^3} = \frac{I_j^h}{m_1 l_1^2}, \quad j \in [1, p] \\
\Pi_G &= \frac{g}{l_1 \Omega^2},
\end{aligned}
$$

where the relationship $m_1 = \rho_1 l_1$ is used to simplify Π_{E_i}, Π_{M_j}, and $\Pi_{I_j^h}$.

These Pi groups can now be compared to the nondimensional groups that were found in the nondimensional energy expressions. Recall that four "extra" nondimensional groups which were composed entirely of reference values were found, namely,

$$
\frac{I_1^h}{m_1 l_1^2}, \quad \frac{E_1}{m_1 l_1^{-1} \Omega^2}, \quad \frac{I_{x_1}}{l_1^4}, \quad \text{and} \quad \frac{g_0}{l_1 \Omega^2}.
$$

The following relationships exist:

$$\begin{aligned}
\Pi_{\rho_i} &= \frac{\rho_i}{\rho_1} = \hat{\rho}_i \\
\Pi_{l_i} &= \frac{l_i}{l_1} = \hat{l}_i \\
\Pi_{E_i} &= \frac{E_i}{m_1 l_1^{-1}\Omega^2} = \frac{E_i}{E_1}\frac{E_1}{m_1 l_1^{-1}\Omega^2} = \hat{E}_i \frac{E_1}{m_1 l_1^{-1}\Omega^2} \\
\Pi_{I_{x_i}} &= \frac{I_{x_i}}{l_1^4} = \frac{I_{x_i}}{I_{x_1}}\frac{I_{x_1}}{l_1^4} = \hat{I}_{x_i}\frac{I_{x_1}}{l_1^4} \\
\Pi_{I_{y_i}} &= \frac{I_{y_i}}{l_1^4} = \frac{I_{y_i}}{I_{x_1}}\frac{I_{x_1}}{l_1^4} = \hat{I}_{y_i}\frac{I_{x_1}}{l_1^4} \\
\Pi_{M_j} &= \frac{M_j}{m_1} = \hat{M}_j \\
\Pi_{I_j^h} &= \frac{I_j^h}{m_1 l_1^2} = \frac{I_j^h}{I_1^h}\frac{I_1^h}{m_1 l_1^2} = \hat{I}_j^h \frac{I_1^h}{m_1 l_1^2} \\
\Pi_G &= \frac{g}{l_1\Omega^2} = \frac{g}{g_0}\frac{g_0}{l_1\Omega^2} = \hat{g}\frac{g_0}{l_1\Omega^2}.
\end{aligned}$$

Notice how the single Pi groups $\Pi_{E_i}, \Pi_{I_{x_i}}, \Pi_{I_{y_i}}$ and $\Pi_{I_j^h}$ each respectively combine the effects of *two* nondimensional groups. This indicates that the "extra" nondimensional groups can be equivalently replaced by the Pi group generated from the dimensional analysis. Furthermore, the Buckingham Pi theorem provides the results that inertial quantities can be nondimensionalized by $m_1 l_1^2$, and elastic modulus by $m_1 l_1^{-1}\Omega^2$. The result for Π_G is the same as for the general n-link rigid manipulator, but with the length reference value as l_1 instead of k_1. Therefore, the reference values I_1^h, E_1, I_{x_1}, and g_0 are not required to define the dynamic equivalence conditions.

Hence, the dynamics of a general n-link flexible manipulator are characterized by the following set of nondimensional Pi groups

$$\left\{\Pi_{\rho_i} = \frac{\rho_i}{\rho_1},\ \Pi_{l_i} = \frac{l_i}{l_1},\ \Pi_{I_{x_i}} = \frac{I_{x_i}}{l_1^4},\ \Pi_{I_{y_i}} = \frac{I_{y_i}}{l_1^4},\right.$$
$$\left.\Pi_{E_i} = \frac{E_i}{m_1 l_1^{-1}\Omega^2},\ \Pi_{M_j} = \frac{M_j}{m_1},\ \Pi_{I_j^h} = \frac{I_j^h}{m_1 l_1^2},\ \Pi_G = \frac{g}{l_1\Omega^2}\right\}. \quad (3.28)$$

The total number of Pi groups is $5n + 2p - 1$, as expected. Therefore, the dimensional dynamic equations ϕ, have been reduced to the nondimensional equations $\boldsymbol{F}$, according to

$$\underbrace{\phi\left(\rho_i, l_i, E_i, I_{x_i}, I_{y_i}, M_j, I_j^h, g, \Omega\right)}_{5n+2p+2 \text{ parameters}} = \underbrace{\boldsymbol{F}\left(\Pi_{\rho_i}, \Pi_{l_i}, \Pi_{E_i}, \Pi_{I_{x_i}}, \Pi_{I_{y_i}}, \Pi_{M_j}, \Pi_{I_j^h}, \Pi_G\right)}_{5n+2p-1 \text{ parameters}}.$$

Length Scaling

As was done for the rigid manipulators, a scaling condition for arbitrary length parameters, $\mathcal{L}$, of the flexible manipulator system needs to be determined.

Lemma 3.2 (Length Scaling: Flexible Manipulators)
Given a length parameter $\mathcal{L}$, of a flexible manipulator system, and the flexible Pi groups

$$\Pi_{l_i},\ \Pi_{I_{x_i}},\ \Pi_{I_{y_i}}$$

a nondimensional Pi group for $\mathcal{L}$ is

$$\Pi_{\mathcal{L}} = \frac{\mathcal{L}}{l_1}.$$

Proof
By definition,

$$\begin{aligned} I_{x_i} &= \int_{A_i} y_i^2 dA_i \\ I_{y_i} &= \int_{A_i} x_i^2 dA_i. \end{aligned}$$

Without loss of generality, consider I_{x_i}. By definition of $\Pi_{I_{x_i}}$,

$$\begin{aligned}
\Pi_{I_{x_i}} &= \frac{I_{x_i}}{l_1^4} \\
&= \frac{1}{l_1^4}\int_{A_i} y_i^2 dA_i \\
&= \int_{\frac{A_i}{l_1^2}} \left(\frac{y_i}{l_1}\right)^2 d\frac{A_i}{l_1^2} \\
&= \int_{\left(\frac{y_i}{l_1}\right)} \int_{\left(\frac{z_i}{l_1}\right)} \left(\frac{y_i}{l_1}\right)^2 d\left(\frac{x_i}{l_1}\right) d\left(\frac{y_i}{l_1}\right).
\end{aligned}$$

Similarly, it is straightforward to show

$$\Pi_{I_{y_i}} = \int_{\left(\frac{y_i}{l_1}\right)} \int_{\left(\frac{z_i}{l_1}\right)} \left(\frac{x_i}{l_1}\right)^2 d\left(\frac{x_i}{l_1}\right) d\left(\frac{y_i}{l_1}\right).$$

Also, by the definition of Π_{l_i},

$$\begin{aligned}
\Pi_{l_i} &= \frac{l_i}{l_1} \\
&= \frac{1}{l}\int_0^{l_i} dz_i \\
&= \int_0^{\left(\frac{l_i}{l}\right)} d\left(\frac{z_i}{l_1}\right) \\
&= \int_0^{\Pi_{l_i}} d\left(\frac{z_i}{l_1}\right).
\end{aligned}$$

The equations indicate that if the manipulator is scaled with respect to $\Pi_{I_{x_i}}$, $\Pi_{I_{y_i}}$, and Π_{l_i}, then each coordinate axis, x_i , y_i, and z_i gets scaled by the factor l_1. Scaling the coordinate axes implies that any length parameter, $\mathcal{L}$ will also get scaled according to the Pi group

$$\Pi_{\mathcal{L}} = \frac{\mathcal{L}}{l_1}.$$

■

3.3.3 Scaling of Natural Frequencies and Mode Shapes

Natural Frequencies

From the flexible link Pi groups (3.28), the scaling condition for the natural frequencies is easily determined. Without loss of generality, only horizontal vibrations will be considered, with the final result being the same for vertical vibrations. Consider the i^{th} flexible manipulator link, and denote the natural frequency of the k^{th} mode by ω_k. The dimensions of ω_k are $[T]^{-1}$, and hence, ω_k can be nondimensionalized by the time scaling frequency Ω, which has the same fundamental dimensions. That is,

$$\omega_k \equiv [T]^{-1} \quad \Rightarrow \quad \hat{\omega}_k \triangleq \frac{\omega_k}{\Omega},$$

where $\hat{\omega}_k$ is the nondimensional natural frequency.

This nondimensional frequency results naturally from the flexible link Pi groups defined in (3.28). This can be shown using the relationship (for the i^{th} link)[12]

$$\omega_k = \sqrt{\frac{E_i I_{x_i}}{\rho_i l_i^4}}\beta_k, \quad k \in [1, \infty], \; i \in [1, n],$$

where β_k is the k^{th} solution of the exact transcendental equation

$$(1 + \cos(\beta_k)\cosh(\beta_k)) + \frac{\rho_i l_i^3}{I_i^h \beta_k^3}(\cosh(\beta_k)\sin(\beta_k) - \sinh(\beta_k)\cos(\beta_k)) = 0,$$

proposed by Bellezza et al.[36].

Therefore,

$$\begin{aligned}
\hat{\omega}_k &= \frac{\omega_k}{\Omega} \\
&= \sqrt{\frac{E_i I_{x_i}}{\rho_i l_i^4 \Omega^2}}\beta_k \\
&= \sqrt{\frac{E_i}{\rho_i \Omega^2}\frac{I_{x_i}}{l_i^4}}\beta_k \\
&= \sqrt{\frac{E_i}{m_1 l_1^{-1}\Omega^2}\frac{m_1 l_1^{-1}}{\rho_i}\frac{I_{x_i}}{l_1^4}\frac{l_1^4}{l_i^4}}\beta_k \\
&= \sqrt{\frac{\Pi_{E_i}}{\Pi_{\rho_i}}\frac{\Pi_{I_{x_i}}}{\Pi_{l_i}^4}}\beta_k.
\end{aligned}$$

Hence, scaling the manipulator using the Pi groups Π_{E_i}, Π_{ρ_i}, $\Pi_{I_{x_i}}$, and Π_{l_i} guarantees that the natural frequencies will scale by Ω.

Mode Shapes

The horizontal deflection of the i^{th} link is denoted by $\mathrm{w}_{x_i}(z_i, t)$. Assuming that w_{x_i} can be separated into its spatial and temporal components[23] results in

$$\mathrm{w}_{x_i}(z_i, t) = \sum_{k=1}^{\infty} \phi_{x_k}(z_i) q_k(t), \tag{3.29}$$

where ϕ_{x_k} is the horizontal mode shape, and q_k is the k^{th} modal coordinate. Now, since w_{x_i} has dimensions of length, it can be nondimensionalized by l_1 as follows

$$\hat{\mathrm{w}}_{x_i}(z_i, t) = \frac{\mathrm{w}_{x_i}}{l_1} = \frac{1}{l_1} \sum_{k=1}^{\infty} \phi_{x_k}(z_i) q_k(t).$$

Since the modal coordinate q_k is nondimensional by definition (it is a weighting on the mode shape), then for dimensional consistency in (3.29), this implies that ϕ_{x_i} must have dimensions of length. Hence

$$\hat{\mathrm{w}}_{x_i}(z_i, t) = \sum_{k=1}^{\infty} \frac{\phi_{x_k}(z_i)}{l_1} q_k(t).$$

Therefore, the nondimensional group for the mode shapes is

$$\Pi_{\phi_{x_k}} = \frac{\phi_{x_k}}{l_1},$$

which is consistent with the length scaling result of Lemma 3.2.

3.3.4 Extensions to Flexible Link Model

Many extensions can be made to the flexible link model described in the preceding section. In the following subsections, the Buckingham Pi method will be used to determined the nondimensional groups associated with damping effects, and torsional vibrations. In addition, the situation where *volume* mass density is used, instead of linear mass density, will be addressed.

Damping

Scaling conditions for the damping effects in flexible structures can also be determined. In previous research[17], the damping mechanisms for a single flexible link manipulator were modelled. The damping effects can be combined into two groups: inertia damping and stiffness damping. The damping coefficients for each type are denoted by d^I and d^S respectively, and have the following fundamental dimensions.

$$d^I \equiv [T]^{-1}, \quad d^S \equiv [T].$$

These damping coefficients are physical material properties of the flexible link, and can be determined experimentally. Often, the damping effects are expressed in terms of modal damping ratios ξ_k, associated with the k^{th} mode of vibration. For a Rayleigh, or proportional, damping model, the damping ratio for the k^{th} mode can be expressed in terms of the k^{th} modal frequency ω_k[18],

$$\xi_k = \left(\frac{d^I}{\omega_k} + d^S \omega_k \right). \tag{3.30}$$

Practically, it is easier to measure the modal properties ξ_k and ω_k than the proportionality constants d^I and d^S. So, given values for ξ_k and ω_k for the first *two* modes, (3.30) can be used to compute corresponding values for d^I and d^S[23].

If these damping constants are included in the physical parameters for the i^{th} flexible link of the manipulator, the corresponding nondimensional Pi groups resulting from dimensional analysis are

$$\Pi_{d_i^I} = \frac{d_i^I}{\Omega}, \quad \Pi_{d_i^S} = d_i^S \Omega. \tag{3.31}$$

Torsional Vibration

If torsion is included in the flexible link model, then it will contribute to the potential energy expression. Defining G to be the shear modulus and J the polar moment of inertia, the term added to the potential energy will be of the form GJ

(akin to EI for elastic modulus and area moment of inertia). Two new nondimensional groups will result, one for the shear modulus, and one for the polar moment of inertia,

$$\Pi_{G_{shear}} = \frac{G}{m_1 l_1^{-1} \Omega^2}, \quad \Pi_{J_{polar}} = \frac{J}{l_1^4}.$$

Linear Mass Density versus Volume Mass Density

If the material density of the i^{th} link is specified in terms of *volume* mass density ρ_i^v, instead of linear mass density ρ_i, then a slight modification must be made to the flexible link Pi groups. The mass of the link is

$$m_i = \rho_i^v V_i, \quad \rho_i \equiv [M][L]^{-3},$$

where V_i is the link volume.

The Pi groups are of the same form and quantity as (3.28), and are found by making the following substitution into (3.28)

$$\rho_1 \quad \Rightarrow \quad \rho_1^v l_1^2.$$

This in no way implies that ρ_1 is *equal* to $\rho_1^v l_1^2$, which is obviously false. With this substitution, the Pi groups that would result with ρ_1^v used as a base parameter in the Buckingham Pi method are obtained. The resulting Pi groups are,

$$\left\{ \Pi_{\rho_i} = \frac{\rho_i^v}{\rho_1^v}, \quad \Pi_{l_i} = \frac{l_i}{l_1}, \quad \Pi_{I_{x_i}} = \frac{I_{x_i}}{l_1^4}, \quad \Pi_{I_{y_i}} = \frac{I_{y_i}}{l_1^4}, \right.$$
$$\left. \Pi_{E_i} = \frac{E_i}{\rho_1^v l_1^2 \Omega^2}, \quad \Pi_{M_j} = \frac{M_j}{\rho_1^v l_1^3}, \quad \Pi_{I_j^h} = \frac{I_j^h}{\rho_1^v l_1^5}, \quad \Pi_G = \frac{g}{l_1 \Omega^2} \right\}. \quad (3.32)$$

3.3.5 Examples

To illustrate the general scaling conditions determined for flexible manipulators, several flexible link manipulators are examined. In the first example, the general results of this section are reconciled with the initial manipulator scaling results

obtained by Ghanekar[17, 18] for a single flexible link manipulator. In the final two examples, a flexible link with two degrees of vibration, and a two-link flexible manipulator are examined. In both examples, dimensional analysis is used to determine the Pi groups for the system. The Pi groups obtained are then verified by examining the nondimensional equations of motion.

Single Flexible Link Manipulator

Consider a single flexible link (SFL) manipulator with only horizontal vibrations, and with gravity and damping neglected. The dynamics are characterized by the following parameters.

link: $\rho_1,\ l_1,\ I_1^x,\ E_1$
joint: I_1^h
time scaling: Ω.

The mass of the link is given by $m_1 = \rho_1 l_1$. According to (3.28), the following three Pi groups characterize this SFL.

$$\Pi_{I_1^h} = \frac{I_1^h}{m_1 l_1^2},\quad \Pi_{E_1} = \frac{E_1}{m_1 l_1^{-1}\Omega^2},\quad \Pi_{I_1^x} = \frac{I_1^x}{l_1^4}. \tag{3.33}$$

The dynamic equivalence conditions for this manipulator were examined by Ghanekar et al. in [18] and found to be,

$$\Pi_{I_1^h} = \frac{I_1^h}{\rho_1^v A_1 l_1^3},\quad \Pi_{E_1 I_1^x} = \frac{E_1 I_1^x}{\rho_1^v A_1 l_1^4 \Omega^2},$$

where ρ_1^v and A_1 are the volume mass density and link cross-sectional area respectively. In [18], the stiffness of the link $E_1 I_1^x$ was modelled as a single parameter. The Pi group $\Pi_{E_1 I_1^x}$ can be divided into the product of two Pi groups,

$$\Pi_{E_1 I_1^x} = \frac{E_1 I_1^x}{\rho_1^v A_1 l_1^4 \Omega^2} = \frac{E_1}{\rho_1^v A_1 \Omega^2}\frac{I_1^x}{l_1^4}.$$

Clearly, since the mass of the link is equal to $m_1 = \rho_1^v A_1 l_1$, then the results obtained in this section verify those from [18].

Flexible Link with Two Degrees of Vibration

A uniform flexible link with horizontal and vertical vibration is considered (Figure 3.5). There are two joints at the base of the link which excite horizontal and vertical oscillations. The link is characterized by the following 9 parameters:

$$\begin{aligned}
&\text{link: } \rho_1,\ l_1,\ I_1^x,\ I_1^y,\ E_1\\
&\text{joint 1: } I_1^h\\
&\text{joint 2: } I_2^h\\
&\text{gravitational accel.: } g\\
&\text{time scaling: } \Omega.
\end{aligned}$$

The mass of the link is $m_1 = \rho_1 l_1$. Also, because the joints do not translate, the joint masses M_1 and M_2 do not affect the dynamic equations. According to (3.28), the 6 nondimensional Pi groups for this manipulator are:

$$\begin{aligned}
&\text{link: } \Pi_{I_1^x} = \frac{I_1^x}{l_1^4},\ \Pi_{I_1^y} = \frac{I_1^y}{l_1^4},\ \Pi_{E_1} = \frac{E_1}{m_1 l_1^{-1}\Omega^2}\\
&\text{joint 1: } \Pi_{I_1^h} = \frac{I_1^h}{m_1 l_1^2}\\
&\text{joint 2: } \Pi_{I_2^h} = \frac{I_2^h}{m_1 l_1^2}\\
&\text{gravitational accel.: } \Pi_G = \frac{g}{l_1\Omega^2}.
\end{aligned}$$

These Pi groups can be verified by deriving and examining the nondimensional equations of motion. In this example, without loss of generality, only one mode of vibration will be examined. First some preliminary definitions are needed. The horizontal deflections, $\mathrm{w}_h(z,t)$, and the vertical deflections, $\mathrm{w}_v(z,t)$ are represented by,

$$\mathrm{w}_h(z,t) = \sum_{i=1}^{\infty} \phi_{hi}(z) h_i(t),\quad \mathrm{w}_v(z,t) = \sum_{i=1}^{\infty} \phi_{vi}(z) v_i(t),$$

where ϕ_{hi} and ϕ_{vi} are the mode shapes, and $h_i(t)$ and $v_i(t)$ are the generalized coordinates. Also,

$$\mathrm{w}_h \equiv [L] \quad \Rightarrow \quad \phi_{hi} \equiv [L],\quad h_i \equiv [L]^0,$$

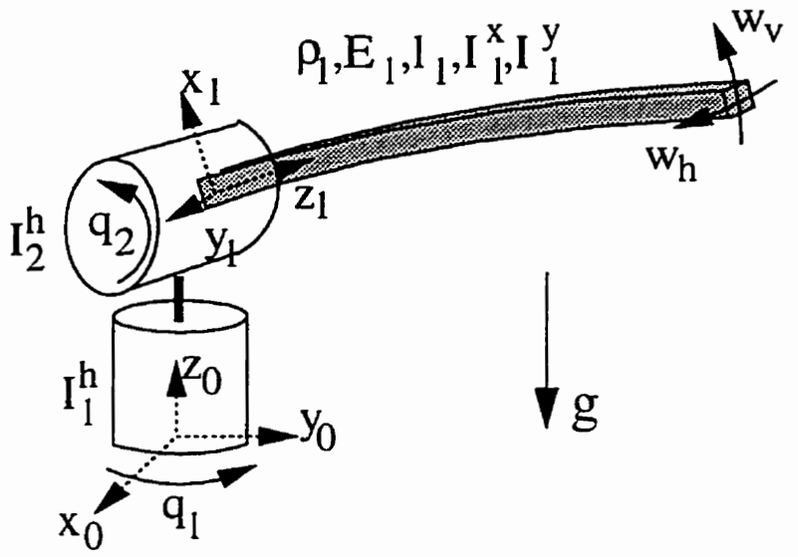

Figure 3.5: Flexible Link with Two Degrees of Vibration

and similarly for w_v, ϕ_{vi} and v_i.

In this example, the link is assumed to have a square cross-section. Therefore,

$$\phi_{hi}(z) = \phi_{vi}(z) \triangleq \phi_i(z).$$

Define the following mode shape dependent constants:

$$\begin{aligned} a_i &\triangleq \int_0^{l_1} \phi_i(z)dz \equiv [L]^2 \\ b_i &\triangleq \int_0^{l_1} \phi_i''(z)^2dz \equiv [L]^{-1} \\ c_i &\triangleq \int_0^{l_1} \phi_i(z)^2dz \equiv [L]^3 \\ \mu_i &\triangleq \int_0^{l_1} z\phi_i(z)dz \equiv [L]^3. \end{aligned}$$

Hence, in addition to the Pi groups in (3.28), define the Pi groups

$$\Pi_a \triangleq \frac{a}{l_1^2},\ \Pi_b \triangleq bl_1,\ \Pi_c \triangleq \frac{c}{l_1^3},\ \Pi_\mu \triangleq \frac{\mu}{l_1^3}.$$

As the constants a_i, b_i, c_i, and μ_i are all length measures, the Pi groups defined are consistent with Lemma 3.2 regarding length scaling.

If the $\phi_i(z)$ are *vibrational* mode shapes, then it should be noted that the parameters defining the manipulator system (e.g. ρ_1, l_1, I_1^h etc.) are sufficient to determine the mode shape. For example, if a clamped-free link model is assumed, only l_1 is required to determine $\phi_i(z)$. For a pinned-free link model, l_1 and I_1^h are required.

In this example, only the first mode of vibration will be examined. Therefore, for all modal dependent parameters (e.g. ϕ_1, c_1), the subscript 1 will be dropped for clarity. Let the variables $\hat{q}_1$ and $\hat{q}_2$ be the nondimensional joint angular position. The nondimensional generalized coordinates for the link deflection will be denoted $\hat{h}$ and $\hat{v}$ for the horizontal and vertical deflections respectively. Then, in terms of the Pi groups, the nondimensional equations of motion are derived, using the Euler-Lagrange equations, to be,

$$
\begin{aligned}
&A\ddot{\hat{q}}_1 + B\ddot{\hat{q}}_2 + C\ddot{\hat{h}} + D\ddot{\hat{v}} + E = \hat{H}_1(\tau) \\
&B\ddot{\hat{q}}_1 + F\ddot{\hat{q}}_2 + \Pi_\mu\ddot{\hat{v}} + G = \hat{H}_2(\tau) \\
&C\ddot{\hat{q}}_1 + \Pi_c\ddot{\hat{h}} + H = 0 \\
&D\ddot{\hat{q}}_1 + \Pi_\mu\ddot{\hat{q}}_2 + \Pi_c\ddot{\hat{v}} + K = 0,
\end{aligned}
$$

where

$$
\begin{aligned}
A &= \Pi_{I_1^h} + \frac{1}{3}\cos(\hat{q}_2)^2 + \Pi_c\hat{h}^2 + \Pi_c\sin(\hat{q}_2)^2\hat{v}^2 - \Pi_\mu\sin(2\hat{q}_2)\hat{v} \\
B &= -\Pi_c\cos(\hat{q}_2)\hat{h}\hat{v} + \Pi_\mu\sin(\hat{q}_2)\hat{h} \\
C &= \Pi_c\sin(\hat{q}_2)\hat{v} - \Pi_\mu\cos(\hat{q}_2) \\
D &= -\Pi_c\sin(\hat{q}_2)\hat{h}
\end{aligned}
$$

$$
\begin{aligned}
E &= \left(\Pi_c \sin(2\hat{q}_2)\hat{v}^2 - \frac{1}{3}\sin(2\hat{q}_2) - 2\Pi_\mu \cos(2\hat{q}_2)\hat{v}\right)\dot{\hat{q}}_1\dot{\hat{q}}_2 \\
&\quad +2\Pi_c\hat{h}\dot{\hat{q}}_1\dot{\hat{h}} + \left(2\Pi_c \sin(\hat{q}_2)^2\hat{v}\dot{\hat{v}} - \Pi_\mu \sin(2\hat{q}_2)\dot{\hat{v}}\right)\dot{\hat{q}}_1 \\
&\quad + \left(\Pi_c \sin(\hat{q}_2)\hat{h}\hat{v} + \Pi_\mu \cos(\hat{q}_2)\hat{h}\right)\dot{\hat{q}}_2^2 \\
&\quad + \left(\Pi_c(\sin(\hat{q}_2) - \cos(\hat{q}_2))\hat{v}\dot{\hat{h}} + 2\Pi_\mu \sin(\hat{q}_2)\dot{\hat{h}}\right)\dot{\hat{q}}_2 \\
&\quad -2\Pi_c \cos(\hat{q}_2)\hat{h}\dot{\hat{v}}\dot{\hat{q}}_2 \\
F &= \Pi_{I_2^h} + \frac{1}{3} + \Pi_c\hat{v}^2 \\
G &= -\left(\frac{1}{2}\Pi_c \sin(2\hat{q}_2)\hat{v}^2 - \frac{1}{2}\sin(2\hat{q}_2) - \Pi_\mu \cos(2\hat{q}_2)\hat{v}\right)\dot{\hat{q}}_1^2 \\
&\quad -2\Pi_c \cos(\hat{q}_2)\dot{\hat{h}}\hat{v}\dot{\hat{q}}_1 + 2\Pi_c\hat{v}\dot{\hat{v}}\dot{\hat{q}}_2 \\
&\quad +\frac{1}{2}\Pi_G \cos(\hat{q}_2) - \Pi_G\Pi_a \sin(\hat{q}_2)\hat{v} \\
H &= -\Pi_c\hat{h}\dot{\hat{q}}_1^2 + 2\Pi_c \cos(\hat{q}_2)\hat{v}\dot{\hat{q}}_1\dot{\hat{q}}_2 + 2\Pi_c \sin(\hat{q}_2)\dot{\hat{v}}\dot{\hat{q}}_1 + \Pi_E\Pi_{I^*}\Pi_b\hat{h} \\
K &= -\left(\Pi_c \sin(\hat{q}_2)^2\hat{v} - \frac{1}{2}\Pi_\mu \sin(2\hat{q}_2)\right)\dot{\hat{q}}_1^2 - \Pi_c\hat{v}\dot{\hat{q}}_2^2 - 2\Pi_c \sin(\hat{q}_2)\dot{\hat{q}}_1\dot{\hat{h}} \\
&\quad +\Pi_E\Pi_{I^y}\Pi_b\hat{v} + \Pi_G\Pi_a \cos(\hat{q}_2).
\end{aligned}
$$

The nondimensional actuation torques are denoted by $\hat{H}_1$ and $\hat{H}_2$. These equations verify that the Pi groups predicted by dimensional analysis do indeed characterize the system dynamics. Simulation results with this manipulator are presented in Chapter 8.

Two-Link Flexible Manipulator

The dynamic equations of a planar two-link flexible elbow manipulator are examined by Ding et al.[24]. The configuration of the manipulator is the same as the rigid manipulator of Figure 3.2, except the links are flexible. Only vertical deflections are permitted, and hence the area moment of inertia in the horizontal direction (I_{y_i}) is neglected for both links. Also, joint effects are not modelled in [24]. Therefore, the

manipulator is a function of the following 10 parameters:

$$\begin{aligned}
&\text{link 1: } \rho_1,\ l_1,\ I_1^x,\ E_1\\
&\text{link 2: } \rho_2,\ l_2,\ I_2^x,\ E_2\\
&\text{gravitational accel.: } g\\
&\text{time scaling: } \Omega.
\end{aligned}$$

From (3.28), the 7 nondimensional Pi groups for this manipulator are:

$$\begin{aligned}
&\text{link 1: } \Pi_{I_{x_1}} = \frac{I_{x_1}}{l_1^4},\ \Pi_{E_1} = \frac{E_1}{m_1 l_1^{-1}\Omega^2}\\
&\text{link 2: } \Pi_{\rho_2} = \frac{\rho_2}{\rho_1},\ \Pi_{l_2} = \frac{l_2}{l_1},\ \Pi_{I_{x_2}} = \frac{I_{x_2}}{l_1^4},\ \Pi_{E_2} = \frac{E_2}{m_1 l_1^{-1}\Omega^2}\\
&\text{gravitational accel.: } \Pi_G = \frac{g}{l_1\Omega^2}.
\end{aligned}$$

The equations of motion for this manipulator are derived in [24]. Using the flexible link terminology of section 3.3.1 and Figure 3.4, the nondimensional dynamic equations, in terms of the flexible Pi groups, are

$$\begin{aligned}
&\sum_{i=1}^{2}\left\{\int_{-\Pi_{l_i}}^{0}\left(\frac{\partial\hat{\boldsymbol{p}}_i}{\partial\hat{q}_1}\right)^T\ddot{\hat{\boldsymbol{p}}}_i\Pi_{\rho_i}d\hat{z}_i - [0\ 0\ \Pi_G]\frac{\partial\bar{\hat{\boldsymbol{p}}}_i}{\partial\hat{q}_i}m_i\right\} = \hat{H}_1\\
&\int_{-\Pi_{l_2}}^{0}\left(\frac{\partial\hat{\boldsymbol{p}}_2}{\partial\hat{q}_2}\right)^T\ddot{\hat{\boldsymbol{p}}}_2\Pi_{\rho_2}d\hat{z}_2 - [0\ 0\ \Pi_G]\frac{\partial\bar{\hat{\boldsymbol{p}}}_2}{\partial\hat{q}_2}m_2 = \hat{H}_2\\
&\int_{-\Pi_{l_2}}^{0}\left(\frac{\partial\hat{\boldsymbol{p}}_2}{\partial\hat{\varepsilon}_{12}}\right)^T\ddot{\hat{\boldsymbol{p}}}_2\Pi_{\rho_2}d\hat{z}_2 - [0\ 0\ \Pi_G]\frac{\partial\bar{\hat{\boldsymbol{p}}}_2}{\partial\hat{\varepsilon}_{12}}m_2 = \frac{\partial}{\partial\hat{z}_1}\left(\Pi_{E_1}\Pi_{I_{x_1}}\hat{\mathrm{w}}_1''\right)\Big|_{\hat{z}_1=0}\\
&\int_{-\Pi_{l_2}}^{0}\left(\frac{\partial\hat{\boldsymbol{p}}_2}{\partial\hat{\varepsilon}_{16}}\right)^T\ddot{\hat{\boldsymbol{p}}}_2\Pi_{\rho_2}d\hat{z}_2 - [0\ 0\ \Pi_G]\frac{\partial\bar{\hat{\boldsymbol{p}}}_2}{\partial\hat{\varepsilon}_{16}}m_2 = \Pi_{E_1}\Pi_{I_{x_1}}\hat{\mathrm{w}}_1''\Big|_{\hat{z}_1=0},
\end{aligned}$$

where $\hat{H}_i$ is the nondimensional joint torque.

The nondimensional dynamics describing the link vibrations are

$$\begin{aligned}
&[0\ 1\ 0]T_1^T\ddot{\hat{\boldsymbol{p}}}_1 = \Pi_{E_1}\Pi_{I_{x_1}}\hat{\mathrm{w}}_1(\hat{z}_1,\tau)'''', \quad -1<\hat{z}_1<0\\
&[0\ 1\ 0]T_2^T\ddot{\hat{\boldsymbol{p}}}_2 = \left(\frac{\Pi_{E_2}\Pi_{I_{x_1}}}{\Pi_{\rho_2}}\right)\hat{\mathrm{w}}_2(\hat{z}_2,\tau)'''', \quad -\Pi_{l_2}<\hat{z}_2<0.
\end{aligned}$$

where the following extra terminology was taken from [24]:

T_i homogeneous transformation matrix

$\bar{\tilde{p}}_i$ distance vector to centre of mass of link i

$\hat{\varepsilon}_{12}$ $= \hat{w}_1(0,\tau)$

$\hat{\varepsilon}_{16}$ $= \arctan\left(\hat{w}_1'(0,\tau)\right)$.

For more details, see [24].

The Pi groups predicted by dimensional analysis are clearly present in the nondimensional equations of motion for this manipulator.

3.4 Nondimensionalization Theorems

3.4.1 General Form for Manipulator Pi Group

From the derivation of the Pi groups for rigid and flexible manipulators in the previous sections, a general theorem can be deduced. With this theorem, a nondimensional group corresponding to any manipulator parameter can be found.

Theorem 3.1 (Nondimensional Group for System Parameter)
Let ϕ be any parameter of the manipulator dynamics. Suppose that the fundamental dimensions of ϕ are

$$\phi \equiv [M]^a[L]^b[T]^c, \quad a,b,c \in \mathbb{R}.$$

Then a nondimensional Pi group for ϕ is

1. $\Pi_\phi = \dfrac{\phi}{m_1^a k_1^b \Omega^{-c}}$, *for a rigid manipulator,*

2. $\Pi_\phi = \dfrac{\phi}{m_1^a l_1^b \Omega^{-c}}$, *for a flexible manipulator.*

Proof

The Buckingham Pi method will be used to prove the theorem. Without loss of generality, it is sufficient to prove the result for the rigid link manipulator. The proof for flexible link manipulators is similar.

With the parameter ϕ, the rigid manipulator dynamics are characterized by the following $4n + 2p + 3$ parameters

$$\phi,\ m_i,\ J_i^{xx},\ J_i^{yy},\ J_i^{zz},\ M_j,\ I_j^h,\ g,\ \Omega, \quad i \in [1,n],\ j \in [1,p]$$

According to the Buckingham Pi method, $N_\Pi = 4n + 2p$ Pi groups are expected for this system. From section 3.2.2, the Pi groups are found by solving a system of N_Π equations of the form

$$A = \Lambda X,$$

where A represent the exponents of the base parameters chosen for the Pi groups, and X represents the exponents of the remaining parameters. In addition, it was shown that the number of variables in each Pi group can be minimized by setting X equal to an identity matrix of dimensions $N_\Pi \times N_\Pi$.

Select m_1, J_1, and Ω as base parameters, and set X to the identity matrix. Then, the form of the Pi group corresponding to the parameter ϕ is

$$\Pi_\phi = \phi m_1^\alpha J_1^\beta \Omega^\gamma, \quad \alpha, \beta, \gamma \in \mathbf{R}. \tag{3.34}$$

Solving for the exponents α, β and γ will give the Pi group for ϕ. In terms of fundamental dimensions,

$$\Pi_\phi \equiv ([M]^a[L]^b[T]^c)([M]^\alpha)([ML^2]^\beta)([T]^{-\gamma}) = [M]^0[L]^0[T]^0,$$

which leads to the system of equations:

$$\left\{ \begin{array}{rl} a + \alpha + \beta & = 0 \\ b + 2\beta & = 0 \\ c - \gamma & = 0 \end{array} \right\} \quad \Rightarrow \quad \left\{ \begin{array}{ll} \alpha & = -a + \frac{b}{2} \\ \beta & = -\frac{b}{2} \\ \gamma & = c \end{array} \right\}.$$

Also, recall from (3.4), that the radius of gyration, k_1, is

$$k_1 = \sqrt{\frac{J_1}{m_1}} = \left(J_1 m_1^{-1}\right)^{\frac{1}{2}}$$

Substitution of α, β, γ and k_1 into (3.34) gives the Pi group,

$$\begin{aligned}
\Pi_\phi &= \phi m_1^{(-a+\frac{b}{2})} J_1^{-\frac{b}{2}} \Omega^c \\
&= \phi m_1^{-a} \left(m_1 J_1^{-1}\right)^{\frac{b}{2}} \Omega^c \\
&= \phi m_1^{-a} k_1^{-b} \Omega^c \\
&= \frac{\phi}{m_1^a k_1^b \Omega^{-c}}.
\end{aligned}$$

as required. ■

The parameters m_1, k_1, and Ω, used to nondimensionalize the parameter ϕ, are distinct in their fundamental dimensions. That is, m_1 has dimension of mass only, k_1 has dimension of length only, and Ω has the dimension of time only. Such a set of parameters will be called *fundamentally distinct* parameters.

For the rigid manipulator, m_1, k_1, and Ω form a fundamentally distinct parameter set, whereas for the flexible manipulator, the parameters m_1, l_1, and Ω are fundamentally distinct. Hence, Theorem 3.1 states that an MLT parameter ϕ can be nondimensionalized by a set of parameters fundamentally distinct in mass, length, and time. In Chapter 4, this observation will be used to extend Theorem 3.1 to parameters with more than three fundamental dimensions.

3.4.2 Equivalence of Rigid and Flexible Pi Groups

In this section the Pi groups for the flexible link manipulator (3.28) are reconciled with those for the rigid manipulator (3.19), in the limiting case when the modal frequencies of the flexible links approaches infinity.

Ignoring flexibility, the dynamic behaviour of rigid and flexible manipulators is identical. This has the implication that the *set* of Pi groups for the flexible manipulator (3.28) is equivalent to the set of Pi groups for the rigid manipulator (3.19). The exception is the Pi group for elastic modulus, which does not appear in the set of rigid manipulator Pi groups. In the following development, this equivalence between the two sets of Pi groups will be proved.

Theorem 3.2 (Equivalence)
The set of Pi groups for the flexible manipulators, Π_{flex} are equivalent to the set of Pi groups for the rigid manipulators, Π_{rigid}, where

$$\begin{aligned}\Pi_{flex} &= \left\{\Pi_{\rho_i}, \Pi_{l_i}, \Pi_{E_i}, \Pi_{I_{x_i}}, \Pi_{I_{y_i}}, \Pi_{M_j}, \Pi_{I_j^h}, \Pi_G\right\}, \quad i \in [1,n],\ j \in [1,p],\\ \Pi_{rigid} &= \left\{\Pi_{m_i}, \Pi_{J_i^{xx}}, \Pi_{J_i^{yy}}, \Pi_{J_i^{zz}}, \Pi_{M_j}, \Pi_{I_j^h}, \Pi_G\right\}, \quad i \in [1,n],\ j \in [1,p],\end{aligned}$$

and $\Pi_{E_i} \to \infty$.

Proof
In this proof, each rigid Pi group will be expressed as a combination of Pi groups from the set Π_{flex}. The proof is divided into six parts: Π_{m_i}, $\Pi_{J_i^{zz}}$, $\Pi_{J_i^{xx}}$ and $\Pi_{J_i^{yy}}$, Π_{M_j} and $\Pi_{I_j^h}$, Π_G and Π_{E_i}.

Part 1: Π_{m_i}
For the rigid manipulator,

$$\begin{aligned}\Pi_{m_i} &= \frac{m_i}{m_1}\\ &= \frac{\rho_i l_i}{\rho_1 l_1}\\ &= \Pi_{\rho_i}\Pi_{l_i}.\end{aligned}$$

Part 2: $\Pi_{J_i^{zz}}$
First note that the area of the cross-section of the i^{th} link can be expressed as,

$$A_i = \int\int dx_i dy_i = \int_{A_i} dA_i.$$

Also, by definition,

$$\begin{aligned} J_i^{zz} &\triangleq \int_{m_i} x_i^2 + y_i^2 dm_i \\ I_{x_i} &\triangleq \int_{A_i} y_i^2 dA_i \\ I_{y_i} &\triangleq \int_{A_i} x_i^2 dA_i. \end{aligned}$$

With these definitions, the following can be shown.

$$\begin{aligned} \Pi_{J_i^{zz}} &= \frac{J_i^{zz}}{J_1} \\ &= \frac{1}{m_1 k_1^2} \int_{m_i} (x_i^2 + y_i^2) dm_i \\ &= \frac{1}{\rho_1 l_1 k_1^2} \rho_i \int_{\frac{-l_i}{2}}^{\frac{l_i}{2}} (x_i^2 + y_i^2) dz_i \\ &= \frac{1}{\rho_1 l_1 k_1^2} \frac{\rho_i}{A_i} \int_{\frac{-l_i}{2}}^{\frac{l_i}{2}} \int_{A_i} (x_i^2 + y_i^2) dA_i dz_i \\ &= \Pi_{\rho_i} \frac{1}{l_1 k_1^2 A_i} \int_{\frac{-l_i}{2}}^{\frac{l_i}{2}} (I_{x_i} + I_{y_i}) \, dz_i \\ &= \Pi_{\rho_i} \frac{1}{l_1 k_1^2 A_i} l_i (I_{x_i} + I_{y_i}) \\ &= \Pi_{\rho_i} \Pi_{l_i} \frac{1}{k_1^2 A_i} l_1^4 \left(\frac{I_{x_i}}{l_1^4} + \frac{I_{y_i}}{l_1^4} \right) \\ &= \Pi_{\rho_i} \Pi_{l_i} \left(\frac{l_1}{k_1} \right)^2 \frac{l_1^2}{A_i} \left(\Pi_{I_{x_i}} + \Pi_{I_{y_i}} \right). \end{aligned}$$

But from Lemma 3.2, it is known that l_1 serves as a reference length value for all length variables. Therefore, defining

$$\Pi_{k_1} \triangleq \frac{k_1}{l_1}, \text{ and } \Pi_{A_i} \triangleq \frac{A_i}{l_1^2},$$

gives the following relationship

$$\Pi_{J_i^{zz}} = \Pi_{\rho_i} \Pi_{l_i} \Pi_{k_1}^{-2} \Pi_{A_i}^{-1} \left(\Pi_{I_{x_i}} + \Pi_{I_{y_i}} \right).$$

Note that the Pi groups, Π_{k_1} and Π_{A_i} are *not* new flexible manipulator Pi groups. In fact, from Lemma 3.2, these two Pi groups are *dependent* on the Pi groups Π_{l_i}, $\Pi_{I_{z_i}}$, and $\Pi_{I_{y_i}}$.

Part 3: $\Pi_{J_i^{xx}}$ and $\Pi_{J_i^{yy}}$

Recall that by definition,

$$\begin{aligned} J_i^{xx} &\triangleq \int_{m_i} y_i^2 + z_i^2 dm_i \\ J_i^{yy} &\triangleq \int_{m_i} x_i^2 + z_i^2 dm_i. \end{aligned}$$

Then,

$$\begin{aligned} \Pi_{J_i^{xx}} &= \frac{J_i^{xx}}{J_1} \\ &= \frac{1}{m_1 k_1^2} \int_{m_i} (y_i^2 + z_i^2) dm_i \\ &= \frac{1}{\rho_1 l_1 k_1^2} \rho_i \int_{\frac{-l_i}{2}}^{\frac{l_i}{2}} (y_i^2 + z_i^2) dz_i \\ &= \Pi_{\rho_i} \frac{1}{l_1 k_1^2} \int_{\frac{-l_i}{2}}^{\frac{l_i}{2}} y_i^2 dz_i + \Pi_{\rho_i} \frac{1}{l_1 k_1^2} \frac{l_i^3}{12} \\ &= \Pi_{\rho_i} \frac{1}{l_1 k_1^2 A_i} \int_{\frac{-l_i}{2}}^{\frac{l_i}{2}} \int_{A_i} y_i^2 dA_i dz_i + \frac{1}{12} \Pi_{\rho_i} \Pi_{l_i} \left(\frac{l_i}{k_1} \right)^2 \\ &= \Pi_{\rho_i} \frac{1}{l_1 k_1^2 A_i} \int_{\frac{-l_i}{2}}^{\frac{l_i}{2}} I_{y_i} dz_i + \frac{1}{12} \Pi_{\rho_i} \Pi_{l_i} \left(\frac{l_i}{l_1} \frac{l_1}{k_1} \right)^2 \\ &= \Pi_{\rho_i} \frac{1}{l_1 k_1^2 A_i} l_i I_{y_i} + \frac{1}{12} \Pi_{\rho_i} \Pi_{l_i} \left(\frac{l_i}{l_1} \frac{l_1}{k_1} \right)^2 \\ &= \Pi_{\rho_i} \Pi_{l_i} \frac{l_1^4}{k_1^2 A_i} \Pi_{I_{y_i}} + \frac{1}{12} \Pi_{\rho_i} \Pi_{l_i}^3 \left(\frac{l_1}{k_1} \right)^2 \\ &= \Pi_{\rho_i} \Pi_{l_i} \left(\frac{l_1}{k_1} \right)^2 \left(\frac{l_1^2}{A_i} \Pi_{I_{y_i}} + \frac{1}{12} \Pi_{l_i}^2 \right). \end{aligned}$$

Using the nondimensional length groups, Π_{k_1} and Π_{A_i} defined in Part 2, the expression for $\Pi_{J_i^{xx}}$ becomes

$$\Pi_{J_i^{xx}} = \Pi_{\rho_i} \Pi_{l_i} \Pi_{k_1}^{-2} \left(\Pi_{A_i}^{-1} \Pi_{I_{y_i}} + \frac{1}{12} \Pi_{l_i}^2 \right).$$

Similarly, the expression for $\Pi_{J_i^{yy}}$ evaluates to

$$\Pi_{J_i^{yy}} = \Pi_{\rho_i}\Pi_{l_i}\Pi_{k_1}^{-2}\left(\Pi_{A_i}^{-1}\Pi_{I_{x_i}} + \frac{1}{12}\Pi_{l_i}^2\right).$$

Part 4: Π_{M_j} and $\Pi_{I_j^h}$

From the Pi group definitions, the joint mass Pi group Π_{M_j}, is identical for both rigid and flexible manipulators.

For the joint inertia Pi group for rigid manipulators,

$$\begin{aligned}\Pi_{I_j^h}^{rigid} &= \frac{I_j^h}{J_1} \\ &= \frac{I_j^h}{m_1 k_1^2} \\ &= \frac{I_j^h}{m_1 l_1^2}\frac{l^2}{k_1^2} \\ &= \Pi_{I_j^h}^{flex}\Pi_{k_1}^{-1}.\end{aligned}$$

Part 5: Π_G

For the rigid manipulators

$$\begin{aligned}\Pi_G^{rigid} &= \frac{g}{k_1\Omega^2} \\ &= \frac{g}{l_1\Omega^2}\frac{l_1}{k_1} \\ &= \Pi_G^{flex}\Pi_{k_1}^{-1}.\end{aligned}$$

Part 6: Π_{E_i}

Consider the stress(σ)-strain(ϵ) relationship given by[22],

$$\sigma = E\epsilon \quad \Rightarrow \quad \epsilon = \frac{\sigma}{E},$$

where E is the elastic modulus of the material.

By the assumption of rigid links, the strain ϵ in the material is equal to zero regardless of the applied stress. In effect, this means that the elastic modulus of the material is assumed to be infinite.

So with the assumption of rigid links, the flexible Pi group Π_{E_i} approaches infinity, and has no equivalent to the rigid manipulator Pi groups.

Therefore, all the Pi groups in the set Π_{rigid} can be written as combinations of Pi groups from the set Π_{flex}. Because of the assumption of rigidity for the rigid manipulator links, there is no rigid Pi group which corresponds to the flexible Pi group, Π_{E_i}. ■

3.5 Rigid-Flexible Manipulators

Manipulators composed of both rigid and flexible links can also be scaled using the Pi groups in (3.19) and (3.28). Theorem 3.2 states that the Pi groups for the rigid and flexible manipulators are equivalent, except for Π_{E_i}.

Hence, for a manipulator with both rigid and flexible links, the rigid Pi groups from (3.19) can be used for the rigid links, and the flexible Pi groups from (3.28) can be used for the flexible links. For consistency, it is very important that the same reference variables are used for the entire manipulator. As separate sets, the Pi groups for the rigid and flexible manipulators are referenced to different base parameters: m_1, J_1, Ω for the rigid case, and ρ_1, l_1, Ω for the flexible system.

For a composite link manipulator system, only a single set of base parameters can be chosen. If the rigid manipulator base parameters m_1, J_1, Ω are chosen, the following changes must be made to the *flexible* Pi groups in order for the entire manipulator system to be scaled properly:

- Change reference value for length from l_1 to $k_1 = \sqrt{\frac{J_1}{m}}$.
- Change reference value for density from ρ_1 to $m_1 k_1^{-1}$.
- Change reference value for mass from $m_1 = \rho_1 l_1$ to m_1.

If the flexible manipulator base parameters, ρ_1, l_1, Ω are chosen, then the following changes must be made to the rigid Pi groups:

- Change reference value for mass from m_1 to $\rho_1 l_1$.
- Change reference value for inertia from J_1 to $\rho_1 l_1^3$.
- Change reference value for length from $k_1 = \sqrt{\frac{J_1}{m_1}}$ to l_1.

3.5.1 Example

Five-Bar Manipulator with a Flexible Link

The dynamics of a five-bar manipulator with 3 rigid links and one flexible link are examined by Wang[25]. The configuration of the manipulator is identical to that shown in Figure 3.3, but with the last link flexible in the horizontal direction only. Because of the configuration of the robot, the length of link 4 which is free to vibrate is $L = l_4 - l_2$. The dynamics are a function of the following 23 parameters.

rigid link 1: m_1, J_1^{xx}, J_1^{yy}, J_1^{zz}
rigid link 2: m_2, J_2^{xx}, J_2^{yy}, J_2^{zz}
rigid link 3: m_3, J_3^{xx}, J_3^{yy}, J_3^{zz}
flexible link 4: ρ_4, L, I_4^x, E_4
joint 1: I_1^h
joint 2: M_2, I_2^h
joint 2: M_3, I_3^h
gravitational accel.: g
time scaling: Ω.

The base joint does not translate, so its joint mass M_1 does not affect the dynamics.

Since this is a rigid-flexible manipulator, the results from section 3.5 can be used. Choosing to use the rigid parameters m_1, J_1^{xx}, and Ω as base parameters, the

following 20 Pi groups result.

rigid link 1: $\Pi_{J_1^{yy}} = \dfrac{J_1^{yy}}{J_1}$, $\Pi_{J_1^{zz}} = \dfrac{J_1^{zz}}{J_1}$

rigid link 2: $\Pi_{m_2} = \dfrac{m_2}{m_1}$, $\Pi_{J_2^{xx}} = \dfrac{J_2^{xx}}{J_1}$, $\Pi_{J_2^{yy}} = \dfrac{J_2^{yy}}{J_1}$, $\Pi_{J_2^{zz}} = \dfrac{J_2^{zz}}{J_1}$

rigid link 3: $\Pi_{m_3} = \dfrac{m_3}{m_1}$, $\Pi_{J_3^{xx}} = \dfrac{J_3^{xx}}{J_1}$, $\Pi_{J_3^{yy}} = \dfrac{J_3^{yy}}{J_1}$, $\Pi_{J_3^{zz}} = \dfrac{J_3^{zz}}{J_1}$

flexible link 4: $\Pi_{\rho_4} = \dfrac{\rho_4}{m_1 k_1^{-1}}$, $\Pi_L = \dfrac{L}{k_1}$, $\Pi_{I_4^x} = \dfrac{I_4^x}{k_1^4}$, $\Pi_{E_4} = \dfrac{E_4}{m_1 k_1^{-1} \Omega^2}$

joint 1: $\Pi_{I_1^h} = \dfrac{I_1^h}{J_1}$

joint 2: $\Pi_{M_2} = \dfrac{M_2}{m_1}$, $\Pi_{I_2^h} = \dfrac{I_2^h}{J_1}$

joint 3: $\Pi_{M_3} = \dfrac{M_3}{m_1}$, $\Pi_{I_3^h} = \dfrac{I_3^h}{J_1}$

gravitational accel.: $\Pi_G = \dfrac{g}{k_1 \Omega^2}$.

The equations of motion are presented in [25]. Here, the nondimensional equations with only one mode of vibration will be presented, without loss of generality. Let the mode shape be denoted by $\phi(z)$, and the generalized coordinate for the first mode be denoted by q_4. Define the following modal constants,

$$
\begin{aligned}
a &= \int_0^L \phi(z) dz \equiv [L]^2 \quad \Rightarrow \quad \Pi_a = \frac{a}{k_1^2} \\
b &= \int_0^L \phi(z)''^2 dz \equiv [L]^{-1} \quad \Rightarrow \quad \Pi_b = b k_1 \\
c &= \int_0^L \phi(z)^2 dz \equiv [L]^3 \quad \Rightarrow \quad \Pi_c = \frac{c}{k_1^3} \\
\mu &= \int_0^L z\phi(z) dz \equiv [L]^3 \quad \Rightarrow \quad \Pi_\mu = \frac{c}{k_1^3}.
\end{aligned}
$$

Then, the nondimensional equations of motion are:

$$\left(\hat{M}_{11} + \Pi_{M_2}\Pi_{r_2}^2 + \Pi_{M_3}\Pi_{r_3}^2 + \Pi_{I_1^h}\right)\ddot{\hat{q}}_1 + \frac{\partial \hat{M}_{11}}{\partial \hat{q}_2}\dot{\hat{q}}_1\dot{\hat{q}}_2 + \frac{\partial \hat{M}_{11}}{\partial \hat{q}_3}\dot{\hat{q}}_1\dot{\hat{q}}_3$$
$$+ \left(\Pi_{\rho_4}\Pi_{l_1}\Pi_a \cos(\hat{q}_2) - \Pi_{\rho_4}\Pi_\mu \cos(\hat{q}_3)\right)\ddot{\hat{q}}_4$$
$$-\Pi_{\rho_4}\Pi_{l_1}\Pi_a \sin(\hat{q}_2)\dot{\hat{q}}_2\dot{\hat{q}}_4 + \Pi_{\rho_4}\Pi_\mu \sin(\hat{q}_3)\dot{\hat{q}}_3\dot{\hat{q}}_4 = \hat{H}_1(\tau)$$

$$\left(\hat{M}_{22} + \Pi_{I_2^h}\right)\ddot{\hat{q}}_2 - \frac{1}{2}\frac{\partial \hat{M}_{11}}{\partial \hat{q}_2}\dot{\hat{q}}_1^2 + \Pi_G\left(\Pi_{l_{c1}} + \Pi_{m_3}\Pi_{l_{c3}} - \Pi_{m_4}\Pi_{l_1}\right)\cos(\hat{q}_2)$$
$$+\Pi_{\rho_4}\Pi_{l_1}\Pi_a \sin(\hat{q}_2)\dot{\hat{q}}_1\dot{\hat{q}}_4 = \hat{H}_2(\tau)$$

$$\left(\hat{M}_{33} + \Pi_{I_3^h}\right)\ddot{\hat{q}}_3 - \frac{1}{2}\frac{\partial \hat{M}_{11}}{\partial \hat{q}_3}\dot{\hat{q}}_1^2 + \Pi_G\left(\Pi_{m_2}\Pi_{l_{c2}} + \Pi_{m_3}\Pi_{l_2} - \Pi_{m_4}\Pi_{l_{c4}}\right)\cos(\hat{q}_3)$$
$$+\Pi_{\rho_4}\Pi_\mu \sin(\hat{q}_3)\dot{\hat{q}}_1\dot{\hat{q}}_4 = \hat{H}_3(\tau)$$

$$\left(\Pi_{\rho_4}\Pi_{l_1}\Pi_a \cos(\hat{q}_2) - \Pi_{\rho_4}\Pi_\mu \cos(\hat{q}_3)\right)\ddot{\hat{q}}_1 + \Pi_{\rho_4}\Pi_c\ddot{\hat{q}}_4$$
$$-\Pi_{\rho_4}\Pi_{l_1}\Pi_a \sin(\hat{q}_2)\dot{\hat{q}}_1\dot{\hat{q}}_2 + \Pi_{\rho_4}\Pi_\mu \sin(\hat{q}_3)\dot{\hat{q}}_1\dot{\hat{q}}_3 + \Pi_{E_4}\Pi_{I_4^z}\Pi_b\hat{q}_4 = 0,$$

where

$$\hat{M}_{11} = \left(\Pi_{l_{c1}}^2 + \Pi_{m_3}\Pi_{l_{c3}}^2 + \Pi_{m_4}\Pi_{l_1}^2 + \Pi_{J_1^{yy}} + \Pi_{J_3^{yy}}\right)\cos(\hat{q}_2)^2$$
$$+\left(\Pi_{J_1^{zz}} + \Pi_{J_3^{zz}}\right)\sin(\hat{q}_2)^2$$
$$+\left(\Pi_{m_3}\Pi_{l_2}^2 + \Pi_{m_4}\Pi_{l_{c4}}^2 + \Pi_{m_2}\Pi_{l_{c2}}^2 + \Pi_{J_2^{zz}} + \Pi_{J_4^{zz}}\right)\cos(\hat{q}_3)^2$$
$$+\left(\Pi_{J_2^{yy}} + \Pi_{J_4^{yy}}\right)\sin(\hat{q}_3)^2$$
$$\hat{M}_{22} = \Pi_{l_{c1}}^2 + \Pi_{m_3}\Pi_{l_{c3}}^2 + \Pi_{m_4}\Pi_{l_1}^2 + 1 + \Pi_{J_3^{xx}}$$
$$\hat{M}_{33} = \Pi_{m_3}\Pi_{l_2}^2 + \Pi_{m_4}\Pi_{l_{c4}}^2 + \Pi_{m_2}\Pi_{l_{c2}}^2 + \Pi_{J_2^{xx}} + \Pi_{J_4^{xx}}.$$

Again, it is clear that the Pi groups predicted by the dimensional analysis are indeed present in the nondimensional equations of motion. Simulation results for this system are presented in Chapter 8.

3.6 Pi Group Summary

3.6.1 Rigid Manipulator

A summary of the Pi groups for rigid manipulators (3.19), and a qualitative interpretation of each is presented here.

$$\Pi_{m_i} = \frac{m_i}{m_1}, \ \Pi_{M_j} = \frac{M_j}{m_1}$$

These two mass Pi groups scale the link and joint masses proportional to the mass of the first link. In effect, these Pi groups maintain the relative distribution of mass throughout the manipulator system.

$$\Pi_{J_{ci}} = \frac{1}{J_1} J_{c_i}, \ \Pi_{I_j^h} = \frac{I_j^h}{J_1}$$

The inertial Pi groups scale the link and joint inertia proportional to the inertia of the first link (about one of its principal axes). These Pi groups preserve the inertia distribution throughout the system. Also note, that Π_{m_i} and $\Pi_{J_{ci}}$ together define a length scaling for the system (Lemma 3.1).

$$\Pi_G = \frac{g}{k_1 \Omega^2}$$

This is the effective gravitational acceleration for the nondimensional manipulator. The interpretation of this Pi group can be explained by considering the case of an object falling in a gravitational field. As g increases, the object will fall faster, and correspondingly, as g decreases, the object will fall more slowly. This Pi group is used to moderate the time scaling frequency in response to changes in g. As g decreases, Ω must also decrease to maintain the value of the Pi group. This reduction in Ω corresponds to a slowing down of the system.

3.6.2 Flexible Manipulator

A summary of the Pi groups for flexible manipulators (3.28) is presented here along with an interpretation.

$$\Pi_{\rho_i} = \frac{\rho_i}{\rho_1}$$

This Pi group scales the linear mass density of each link in proportion to the linear mass density of the first link. For a material whose links are all constructed of one type of material ($\Pi_{\rho_i} = 1$), this Pi group indicates that for dynamic equivalence, the same material must always be used for all the links.

$$\Pi_{l_i} = \frac{l_i}{l_1}$$

This Pi group scales the length of each link in proportion to the length of the first link. This group ensures that the relative size of the manipulator remains constant.

$$\Pi_{I_{x_i}} = \frac{I_{x_i}}{l_1^4}, \ \Pi_{I_{y_i}} = \frac{I_{y_i}}{l_1^4}$$

The area moment of inertia of the cross-section is scaled using these Pi groups. These Pi groups ensure that the properties of the cross-section are scaled appropriately. For example, a link with a tall and thin cross-section cannot be scaled to a short and fat cross-section. Along with Π_{l_i}, these Pi groups define a length scaling for the system (Lemma 3.2).

$$\Pi_{E_i} = \frac{E_i}{m_1 l_1^{-1} \Omega^2}$$

This Pi group is a function of the material of which the link is constructed. Because E_i is a material property, selecting the material for

the flexible link has repercussions on the values of m_1, l_1, and Ω in order to maintain dynamic equivalence. For example as E_i increases (a stiffer material), the time scale Ω must also increase, since stiffer materials have higher frequencies of oscillation.

$$\Pi_{M_j} = \frac{M_j}{m_1}$$

The joint mass Pi group scales the joint masses in proportion to the mass of the first link. This Pi groups maintains the relative distribution of joint mass throughout the system.

$$\Pi_{I_j^h} = \frac{I_j^h}{m_1 l_1^2}$$

The joint inertia Pi group scales the joint inertia in proportion to the axial mass-moment of inertia of the first link ($\int z_1^2 dm_1$). This Pi group maintains the relative distribution of joint inertia throughout the system.

$$\Pi_G = \frac{g}{l_1 \Omega^2}$$

The interpretation is the same as for Π_G of the rigid manipulator Pi groups.

3.7 Design Methodology

This section discusses the methodology by which the Pi groups can be used to create dynamically equivalent manipulators. A general procedure is first given, and then several examples are outlined. In all the explanations, the objective is to design a new manipulator (system 2), which is dynamically equivalent to an existing manipulator (system 1). The notation $(\cdot)_1$ and $(\cdot)_2$ will be used to denote parameters of system 1 and system 2 respectively.

3.7.1 General Procedure

Given the physical parameters of a manipulator, the following general procedure is used to determine the physical parameters of another dynamically equivalent manipulator.

1. Identify all the physical parameters of the manipulator (system 1). As this is the original system (system 1), set the time scaling frequency to $\Omega = 1\ \mathrm{s}^{-1}$.

2. Select the base parameters: m_1, J_1, Ω for rigid manipulators, or ρ_1, l_1, Ω for flexible manipulators.

3. Compute values for the appropriate the Pi groups.

4. Select values for three independent parameters of the new manipulator (system 2). For example, gravitational acceleration, mass of one of the links, or the type of material.

5. Using these three parameters, re-arrange the Pi groups to calculate the remaining manipulator parameters for system 2. With this method, the values of the Pi groups for systems 1 and 2 are the same, and therefore, the two manipulators are dynamically equivalent.

3.7.2 Example 1: Rigid Manipulator - Changing Gravity

This example will illustrate how to design dynamically equivalent rigid manipulators in different gravitational fields.

In step 1 of the procedure, values for all the physical parameters of the manipulator (system 1) must be found. All the link and joint masses and inertias must be determined. Let $(g)_1$ denote the gravitational acceleration in the environment of system 1, and set $(\Omega)_1$ to 1 s^{-1}.

Next, choose m_1, J_1, and Ω as base values (step 2), and then compute the Pi values using the rigid Pi groups in (3.19).

In the fourth step, values for three independent parameters of the new manipulator (system 2) must be set. It is in this step that the new manipulator is "designed", since the defining parameters are chosen. For this example, suppose that the new system is to operate in a different gravitational field, of value $(g)_2$. Also, suppose that the desired link 1 mass of the robot is $(m_1)_2$, and the desired inertia for link 1 is $(J_1)_2 = (J_1^{xx})_2$.

In the final step, the values for these three parameters are used to calculate the values for the remaining system parameters. First, the radius of gyration, $(k_1)_2$, can be computed as

$$(k_1)_2 = \sqrt{\frac{(J_1)_2}{(m_1)_2}}.$$

The remaining system parameters can now be computed. With the value for $(g)_2$ and the value for $(k_1)_2$, the value for $(\Omega)_2$ can be found by using the Pi group Π_G. For dynamic equivalence, the parameters $(g)_2$, $(k_1)_2$, and $(\Omega)_2$ must satisfy

$$\Pi_G = \frac{(g)_2}{(k_1)_2(\Omega^2)_2}, \quad \Rightarrow \quad (\Omega)_2 = \sqrt{\frac{(g)_2}{(k_1)_2\Pi_G}}.$$

Finally, since $(m_1)_2$ and $(J_1)_2$ are known, then the remaining link and joint masses and inertias for the system 2 manipulator can be found using

$$\begin{aligned} m_i &= (m_1)_2\Pi_{m_i}, \quad J_{c_i} = (J_1)_2\Pi_{J_{c_i}}, \\ M_j &= (m_1)_2\Pi_{M_j}, \quad I_j^h = (J_1)_2\Pi_{I_j^h}. \end{aligned}$$

Now, all the parameters for the system 2 manipulator have been found. Although, system 1 and system 2 are operating in different gravitational environments, they are dynamically equivalent. This scenario is illustrative of the case where a manipulator to operate on the Moon, can be designed and tested with a dynamically equivalent prototype on the Earth.

3.7.3 Example 2: Rigid Manipulator Changing Link Material

This example illustrates how to incorporate material specifications into the design of a dynamically equivalent rigid manipulator. In this case, the rigid Pi groups incorporating volume mass density (3.20) must be used. The first three steps involve identifying the parameter values, selecting the base parameters (ρ_1^v, J_1, Ω), and computing the Pi values.

In step 4, three parameters of the new manipulator (system 2) are chosen. By selecting a specific material, the value for $(\rho_1^v)_2$ is fixed. The environment of the manipulator automatically fixes the value for gravitational acceleration to a value $(g)_2$. For the final parameter, choose the inertia of link 1 to be $(J_1)_2 = (J_1^{xx})_2$.

In the final step, these three values are used, along with the Pi values, to determine the remaining parameter values for system 2. The time scaling frequency can be found from Π_G,

$$\Pi_G = \left(\frac{(\rho_1^v)_2}{(J_1)_2}\right)^{\frac{1}{5}} \frac{(g)_2}{(\Omega^2)_2} \quad \Rightarrow \quad (\Omega)_2 = \sqrt{\left(\frac{(\rho_1^v)_2}{(J_1)_2}\right)^{\frac{1}{5}} \frac{(g)_2}{\Pi_G}}.$$

The remaining parameter values can be determined as follows:

$$\begin{aligned}
(\rho_i^v)_2 &= (\rho_1^v)_2 \Pi_{\rho_i^v} \\
(J_{c_i})_2 &= (J_1)_2 \Pi_{J_{c_i}} \\
(M_j)_2 &= ((\rho_1^v)^{\frac{2}{5}} J_1^{\frac{3}{5}})_2 \Pi_{M_j} \\
(I_j^h)_2 &= (J_1)_2 \Pi_{I_j^h}.
\end{aligned}$$

Therefore, the links of system 2 have been constructed out of the desired material, and the manipulator is also dynamically equivalent to manipulator system 1.

3.7.4 Example 3: Flexible Manipulator Changing Link Material

In this final example, the way to design a dynamically equivalent flexible manipulator out of a specific material will be discussed. Again, in steps 1 to 3 of the procedure, the parameter values for the flexible manipulator (system 1) are found, the base parameters are identified (ρ_1, l_1, Ω), and the Pi values are computed.

In the next step, three parameters of the new manipulator (system 2) can be specified. The manipulator environment automatically fixes the gravitational acceleration to a value $(g)_2$. Now, by choosing the link material for a flexible manipulator, *two* parameters are fixed: the elastic modulus $(E_1)_2$, and the density $(\rho_1)_2$.

With these three values, the remaining parameters are determined by using the flexible Pi groups from (3.28). The value for $(\Omega)_2$ is found from Π_{E_1},

$$\Pi_{E_1} = \frac{(E_1)_2}{(\rho_1)_2(\Omega^2)_2} \quad \Rightarrow \quad (\Omega)_2 = \sqrt{\frac{(E_1)_2}{(\rho_1)_2\Pi_{E_1}}}.$$

The value of $(l_1)_2$ is found from Π_G,

$$\Pi_G = \frac{(g)_2}{(l_1)_2(\Omega^2)_2} \quad \Rightarrow \quad (l_1)_2 = \frac{(g)_2}{(\Omega^2)_2\Pi_G}.$$

The remaining parameters of manipulator system 2 can now be computed,

$$\begin{aligned}
(\rho_i)_2 &= (\rho_1)_2 \Pi_{\rho_i} \\
(l_i)_2 &= (l_1)_2 \Pi_{l_i} \\
(E_i)_2 &= (\rho_1)_2 (\Omega^2)_2 \Pi_{E_i} \\
(I_{x_i})_2 &= (l_1^4)_2 \Pi_{I_{x_i}} \\
(I_{y_i})_2 &= (l_1^4)_2 \Pi_{I_{y_i}} \\
(M_j)_2 &= (\rho_1)_2 (l_1)_2 \Pi_{M_j} \\
(I_j^h)_2 &= (\rho_1)_2 (l_1^3)_2 \Pi_{I_j^h}.
\end{aligned}$$

Therefore, the two flexible link manipulators, although constructed out of different materials, are dynamically equivalent.

Chapter 4

Actuator Dynamics

In the previous chapter the dynamic equivalence conditions for rigid and flexible manipulators were determined. In the following three chapters, scaling laws for actuator dynamics, control laws, and friction effects will be presented. The overall system is shown in Figure 4.1.

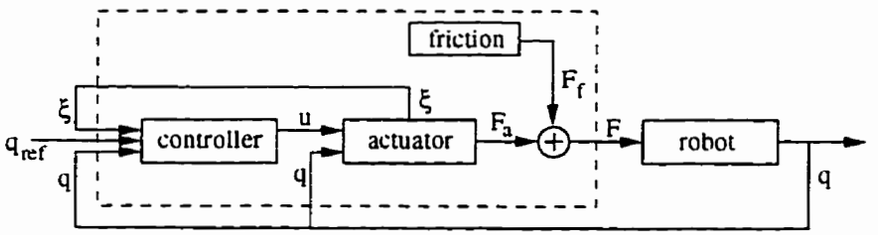

Figure 4.1: Overall Manipulator System

Referring to the figure, the generalized input forces to the manipulator, $\boldsymbol{F}$, can be written in terms of the manipulator generalized coordinates $\boldsymbol{q}$, the controller inputs $\boldsymbol{u}$, the generalized forces applied by the actuators $\boldsymbol{F}_a$, and the friction effects $\boldsymbol{F}_f$, as

$$\boldsymbol{F} = \boldsymbol{F}_a(\boldsymbol{u}, \boldsymbol{q}) + \boldsymbol{F}_f.$$

The manipulator equations can be expressed using the Lagrangian, L.

$$\frac{d}{dt}\left(\frac{\partial L}{\partial \dot{q}}\right) - \frac{\partial L}{\partial q} = F = F_a(u, q) + F_f. \tag{4.1}$$

In this chapter the scaling conditions for actuators will be examined (Figure 4.2). The actuator dynamics generate the generalized forces which are applied to the manipulator through the actuated joints. In order to determine the scaling laws for the actuator dynamics, it is necessary to examine the dynamics behind these generalized forces. A general model for the actuator dynamics will be investigated and scaling laws determined. Joint flexibility will also be discussed in an example.

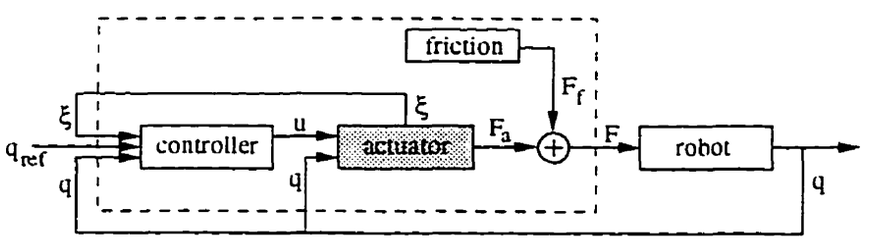

Figure 4.2: Actuator Block

4.1 General Actuators

Before deriving the nondimensional groups characterizing general actuators, the form of a general function to describe the actuator dynamics is required. The dynamics of two actuators will be presented to motivate the notation of the general form.

Example 1: Permanent Magnet DC Motor

The reduced order[1] dynamic equation for a permanent magnet DC motor[20] is

$$I^h\ddot{\xi} + \left(B + \frac{K_b K_m}{R}\right)\dot{\xi} = u(t) - rF(t), \tag{4.2}$$

[1]assumes that the electrical time constant << mechanical time constant, $\frac{I^h}{B}$.

where $\xi(t)$ is the motor angle, $u(t)$ is the control input, $F(t)$ is the load torque (the manipulator), I^h is the gear and armature inertia, B represents motor damping, K_m is the motor torque constant, K_b is the back emf constant, R is the armature resistance, and r is the gear ratio. This equation illustrates the dynamics behind the torque $F(t)$, which the motor applies to the manipulator.

The physical parameters which characterize this actuator can be collected in the set Φ, as

$$\Phi = \left\{ I^h, B, K_b, K_m, R, r \right\}.$$

Scaling the actuator will require the parameters in Φ to be scaled appropriately.

The torque is transferred to the manipulator via the term F. Rewriting (4.2) in terms of F gives

$$F(t) = -\frac{1}{r} I^h \ddot{\xi} - \frac{1}{r} \left(B + \frac{K_b K_m}{R} \right) \dot{\xi} + \frac{1}{r} u(t).$$

In general, this can be written as

$$F(t) = F_a(\dot{\xi}, \ddot{\xi}, u).$$

When the link is rigid and directly attached to the motor shaft, the motor angle ξ is the same as the generalized coordinate for the link, q_i. ■

Example 2: DC Motor and Joint Flexibility

Harmonic drives are often used to actuate robot manipulators because of their minimal backlash. However, these actuators exhibit significant joint flexibility, which is typically modelled as a torsional spring between the motor shaft and the manipulator link. By introducing joint flexibility effects, the manipulator and actuator dynamics become coupled through the stored potential energy in the torsional spring.

Define ξ to be the angular position of the shaft, and q_i the angular position of the link. For this actuator, the torque F applied to the manipulator is the

torsional spring force, which is proportional to the difference between ξ and q_i. The manipulator equations can be written using the Lagrangian L, as in the previous chapter. The coupled equations can be expressed as[20]

$$\begin{aligned} \frac{d}{dt}\left(\frac{\partial L}{\partial \dot{q}_i}\right) - \frac{\partial L}{\partial q_i} &= K_s(\xi - q_i) \\ I^h\ddot{\xi} + B\dot{\xi} &= u(t) - K_s(\xi - q_i), \end{aligned} \tag{4.3}$$

where I^h and B are the motor inertia and damping respectively, u is the control input, and K_s represents the torsional spring constant.

The physical parameters which characterize this actuator are

$$\Phi = \left\{I^h, B, K_s\right\}.$$

Upon examining (4.3), the torque that the actuator applies to the manipulator can be effectively characterized by

$$F = F_a(\xi, \dot{\xi}, \ddot{\xi}, q_i, u).$$

Hence the actuator dynamics are dependent upon the actuator generalized coordinate ξ and its derivatives, the link generalized coordinate q_i, and the control input u. ■

In general, let the set Φ contain the physical parameters of the actuator. Then, if the actuator is defined by m parameters,

$$\Phi = \{\phi_1, \phi_2, \ldots, \phi_m\},$$

where the fundamental dimensions of ϕ_i are,

$$\phi_i \equiv [M]^{a_i}[L]^{b_i}[T]^{c_i}[A]^{d_i}[\Theta]^{e_i}, \quad a_i, b_i, c_i, d_i, e_i \in \mathbf{R}.$$

Although the manipulator is a mechanical system defined solely by the dimensions of mass, length, and time, the actuators themselves may be defined by electrical and thermal dependent quantities. Therefore, the fundamental dimensions of

current $[A]$ and temperature $[\Theta]$, have been included in the possible dimensions of each actuator parameter. Note that the actuator *output* must still be either a force or a torque; namely, a mechanical (MLT) quantity.

In general, it will be assumed that the actuator dynamics are a function of a generalized coordinate, ξ, a link generalized coordinate, q_i, and a control input, u. Furthermore, it will be assumed that ξ has dimensions of length (i.e. measures a translation or rotation). Also, the actuator output is assumed to be a generalized force. Now, with the actuator connected to the i^{th} link, the external force applied by the actuator can be expressed by the function F_a,

$$F_i = F_a\left(\xi, \dot{\xi}, \ldots, \xi^{(n)}, q_i, \dot{q}_i, \ldots, q_i^{(k)}, u\right). \tag{4.4}$$

The actuator dynamics can be nondimensionalized by examining (4.1) for one of the generalized coordinates q_i. The Lagrangian L has dimensions of energy, and the generalized manipulator coordinate q_i has dimensions of length. In terms of fundamental dimensions,

$$t \equiv [T], \quad L \equiv [M][L]^2[T]^{-2}, \quad q_i \equiv [L]^r,$$

where $r = 0$ for a revolute joint and $r = 1$ for a prismatic joint.

By assumption, the actuator generalized coordinate, ξ, has dimensions of length, and the actuator output, F_a, is a force or torque. The dimensions of the control input, u, are not specified. Therefore,

$$\xi \equiv [L]^p, \quad F_a \equiv [M][L]^{2-r}[T]^{-2}, \quad u \equiv [M]^a[L]^b[T]^c[A]^d[\Theta]^e, \quad a, b, c, d, e \in \mathbf{R},$$

where $p = 0$ or $p = 1$ for rotary or translational length respectively.

It is imperative that for a particular manipulator *system* (manipulator, actuator, controller, and friction), the same base variables are always used for the nondimensionalization. In this development, the variables m_1, J_1, and Ω are used as base variables, indicating that the manipulator has rigid links. Without loss of generality, the variables ρ_1, l_1, and Ω could be used as base variables if a flexible manipulator was being scaled.

Because the control input, u, may have dimensions of current and temperature, two new reference values must be defined. Denote the reference value for current by A_0 and for temperature by θ_0.

By Theorem 3.1 (section 3.4), use the manipulator variables m_1, k_1, Ω, and the reference values, A_0, θ_0 to define the nondimensional variables:

$$\tau \triangleq \Omega t, \quad \hat{L}(\tau) \triangleq \frac{L\left(\frac{\tau}{\Omega}\right)}{m_1 k_1^2 \Omega^2}, \quad \hat{\xi}(\tau) \triangleq \frac{\xi\left(\frac{\tau}{\Omega}\right)}{k_1^p}, \quad \hat{q}_i(\tau) \triangleq \frac{q_i\left(\frac{\tau}{\Omega}\right)}{k_1^r},$$
$$\hat{F}_a(\tau) \triangleq \frac{F_a\left(\frac{\tau}{\Omega}\right)}{m_1 k_1^{2-r}\Omega^2}, \hat{u} = \frac{u\left(\frac{\tau}{\Omega}\right)}{m_1^a k_1^b \Omega^{-c} A_0^d \theta_0^e}.$$

Hence, considering only the generalized forces applied by the actuator to the manipulator, F_a, nondimensionalizing (4.1) gives,

$$\begin{aligned}\frac{d}{d\tau}\left(\frac{\partial \hat{L}}{\partial \dot{\hat{q}}_i}\right) - \frac{\partial \hat{L}}{\partial \hat{q}_i} &= m_1 k_1^{2-r}\Omega^2 F_a \\ &= m_1 k_1^{2-r}\Omega^2 F_a\left(\xi, \dot{\xi}, \ldots, \xi^{(n)}, q_i, \ldots, q_i^{(k)}, u\right) \\ &= \hat{F}_a\left(k_1^p\hat{\xi}, k_1^p\Omega\dot{\hat{\xi}}, \ldots, k_1^p\Omega^n\hat{\xi}^{(n)}, k_1^r\hat{q}_i, \ldots, k_1^r\Omega^k\hat{q}_i^{(k)}, m_1^a k_1^b\Omega^{-c}A_0^d\theta_0^e\hat{u}\right).\end{aligned} \tag{4.5}$$

Examining the right-hand side of (4.5), define the nondimensional actuator dynamics by:

$$\begin{aligned}&\hat{F}_a\left(\hat{\xi}, \ldots, \hat{\xi}^{(n)}, \hat{q}_i, \ldots, \hat{q}_i^{(k)}, \hat{u}\right) \\ &\quad\triangleq \frac{1}{m_1 k_1^{2-r}\Omega^2} F_a\left(k_1^p\hat{\xi}, k_1^p\Omega\dot{\hat{\xi}}, \ldots, k_1^p\Omega^n\hat{\xi}^{(n)}, k_1^r\hat{q}_i, \ldots, k_1^r\Omega^k\hat{q}_i^{(k)}, m_1^a k_1^b\Omega^{-c}A_0^d\theta_0^e\hat{u}\right)\end{aligned} \tag{4.6}$$

To determine the scaling law for the actuator dynamics, the parameters in Φ must be examined. Consider the parameter ϕ_i within F_a. In general, the parameter ϕ_i is multiplied by some function γ_i of the variables ξ, q_i and u. Furthermore, ϕ_i may be raised to a real exponent, s_i. Hence, introduce the variable ψ_i to define the product of ϕ_i and γ_i,

$$\psi_i \triangleq \phi_i^{s_i} \times \gamma_i(\xi, \ldots, \xi^{(n)}, q_i, \ldots, q_i^{(k)}, u), \quad s_i \in \mathbf{R}.$$

Within F_a, the parameter ϕ_i may have a multiplicity greater than one. For each occurrence of ϕ_i, there will correspond a different (ψ_i, γ_i) pair. However, from the principle of dimensional homogeneity, the nondimensional group for ϕ_i resulting from each (ψ_i, γ_i) pair will be the same.

Example: Permanent Magnet DC Motor with Nonlinearity

To demonstrate the use of this notation, a modified version of the permanent magnet DC motor equation from (4.2) will be used. In addition, to illustrate how nonlinearities can be handled, a transcendental function (as an example of a nonlinearity) has been added to the actuator dynamics. The resulting actuator dynamic equation is

$$F_a(\xi, \dot{\xi}, \ddot{\xi}, q_i, u) = J_m\ddot{\xi} + \frac{K_b K_m}{R}\dot{\xi} + P_1 q_i^2 \sin(P_2\dot{\xi}) + u(t), \tag{4.7}$$

where F_a and u are torques, and ξ and q_i measure angular position.

The parameter set for (4.7) is

$$\Phi = \{\phi_1, \phi_2, \ldots, \phi_6\} \triangleq \{J_m, K_b, K_m, R, P_1, P_2\},$$

and the parameters have the following fundamental dimensions

$$J_m \equiv [M][L]^2, \quad K_m \equiv [M][L]^2[T]^{-2}[A]^{-1}, \quad K_b \equiv [M][L]^2[T]^{-2}[A]^{-1},$$
$$R \equiv [M][L]^2[T]^{-3}[A]^{-2}, \quad P_1 \equiv [M][L]^2[T]^{-2}, \quad P_2 \equiv [T].$$

Now, for (4.7), using the above notation,

$$\begin{aligned}
\psi_1 &= J_m\ddot{\xi} = J_m \times \ddot{\xi} \quad \Rightarrow \quad \gamma_1 = \ddot{\xi} \\
\psi_2 &= \frac{K_b K_m}{R}\dot{\xi} = K_b \times \frac{K_m}{R}\dot{\xi} \quad \Rightarrow \quad \gamma_2 = \frac{K_m}{R}\dot{\xi} \\
\psi_3 &= \frac{K_b K_m}{R}\dot{\xi} = K_m \times \frac{K_b}{R}\dot{\xi} \quad \Rightarrow \quad \gamma_3 = \frac{K_b}{R}\dot{\xi} \\
\psi_4 &= \frac{K_b K_m}{R}\dot{\xi} = R^{-1} \times K_b K_m\dot{\xi} \quad \Rightarrow \quad \gamma_4 = K_b K_m\dot{\xi}, \quad s_4 = -1 \\
\psi_5 &= P_1 q_i^2 \sin(P_2\dot{\xi}) = P_1 \times q_i^2 \sin(P_2\dot{\xi}) \quad \Rightarrow \quad \gamma_5 = q_i^2 \sin(P_2\dot{\xi}) \\
\psi_6 &= P_2\dot{\xi} = P_2 \times \dot{\xi} \quad \Rightarrow \quad \gamma_6 = \dot{\xi}.
\end{aligned}$$

Returning to the general expression, all the terms in $\hat{F}_a$ are nondimensional by definition. This means that after the nondimensionalization process, the function ψ_i must be transformed into a nondimensional $\hat{\psi}_i$. By definition, the fundamental dimensions of ϕ_i are $[M]^{a_i}[L]^{b_i}[T]^{c_i}[A]^{d_i}[\Theta]^{e_i}$. In terms of fundamental dimensions, express γ_i as,

$$\gamma_i \equiv [M]^{f_i}[L]^{g_i}[T]^{h_i}[A]^{j_i}[\Theta]^{k_i}, \quad f_i, g_i, h_i, j_i, k_i \in \mathbf{R}.$$

Hence, $\psi_i = \phi_i^{s_i}\gamma_i$, has fundamental dimensions,

$$\psi_i \equiv [M]^{(s_i a_i + f_i)}[L]^{(s_i b_i + g_i)}[T]^{(s_i c_i + h_i)}[A]^{(s_i d_i + j_i)}[\Theta]^{(s_i e_i + k_i)}.$$

Since, by assumption, neither the actuator output F_a, nor the generalized coordinates ξ, q_i contain the fundamental dimensions $[A]$ or $[\Theta]$, then every product ψ_i must also be independent of $[A]$ and $[\Theta]$. This implies that for parameters whose dimensions contain $[A]$ and $[\Theta]$, there must be an *internal* cancellation of these dimensions with another parameter. So, $\hat{\psi}_i$ is nondimensional in an MLT sense, which means that the exponents of $[A]$ and $[\Theta]$ in ψ_i must be zero. That is,

$$\begin{aligned} s_i d_i + j_i &= 0 \\ s_i e_i + k_i &= 0. \end{aligned} \tag{4.8}$$

To reiterate, this does *not* mean that the components of ψ_i, namely ϕ_i and γ_i, are independent of $[A]$ and $[\Theta]$. Instead, it implies that for an MLT system, there is an internal cancellation of the "non-MLT" dimensions $[A]$ and $[\Theta]$ between ϕ_i and γ_i.

Since, $\hat{\psi}_i$ is nondimensional, its relationship to ψ_i can be determined by applying Theorem 3.1. Use the reference values A_0 and θ_0 for current and temperature respectively to obtain,

$$\begin{aligned} \hat{\psi}_i &\triangleq \frac{1}{m_1^{(s_i a_i + f_i)} k_1^{(s_i b_i + g_i)} \Omega^{(-s_i c_i - h_i)}} \psi_i \\ &= \frac{1}{m_1^{(s_i a_i + f_i)} k_1^{(s_i b_i + g_i)} \Omega^{(-s_i c_i - h_i)} A_0^{(s_i d_i + j_i)} \theta_0^{(s_i e_i + k_i)}} \phi_i^{s_i}\gamma_i, \quad \text{using (4.8)} \\ &= \left[\frac{1}{m_1^{s_i a_i} k_1^{s_i b_i} \Omega^{-s_i c_i} A_0^{s_i d_i} \theta_0^{s_i e_i}} \phi_i^{s_i}\right]\left[\frac{1}{m_1^{f_i} k_1^{g_i} \Omega^{-h_i} A_0^{j_i} \theta_0^{k_i}} \gamma_i\right] \\ &= \left[\frac{1}{m_1^{a_i} k_1^{b_i} \Omega^{-c_i} A_0^{d_i} \theta_0^{e_i}} \phi_i\right]^{s_i}\left[\frac{1}{m_1^{f_i} k_1^{g_i} \Omega^{-h_i} A_0^{j_i} \theta_0^{k_i}} \gamma_i\right]. \end{aligned}$$

By definition of the fundamental dimensions of ϕ_i and γ_i, the terms in square brackets are both nondimensional. So the nondimensional variables $\hat{\phi}_i$ and $\hat{\gamma}_i$ can be defined as,

$$\hat{\phi}_i \triangleq \frac{1}{m_1^{a_i} k_1^{b_i} \Omega^{-c_i} A_0^{d_i} \theta_0^{e_i}} \phi_i, \quad \hat{\gamma}_i \triangleq \frac{1}{m_1^{f_i} k_1^{g_i} \Omega^{-h_i} A_0^{j_i} \theta_0^{k_i}} \gamma_i.$$

Therefore, the nondimensional group for the actuator parameters can be described by:

$$\Pi_{\phi_i} \triangleq \frac{\phi_i}{m_1^{a_i} k_1^{b_i} \Omega^{-c_i} A_0^{d_i} \theta_0^{e_i}}.$$

This result implies an extension of Theorem 3.1 (section 3.4) to parameters with m fundamental dimensions, and to systems with m fundamentally distinct parameters.

Theorem 4.1 (Pi Group for System Parameter)
Let the m fundamental dimensions be $[u_1], \ldots, [u_m]$, and let ϕ be any parameter of the overall manipulator system. If the dimensions of ϕ are

$$\phi \equiv [u_1]^{p_1} [u_2]^{p_2} \cdots [u_m]^{p_m}, \quad p_i \in \mathbb{R}, \ i \in [1, m],$$

and the manipulator system has m fundamentally distinct parameters: $\{v_1, \ldots, v_m\}$, then a nondimensional group for ϕ is

$$\Pi_\phi = \frac{\phi}{v_1^{p_1} \cdots v_m^{p_m}}.$$

Proof
The structure of this proof is similar to the proof of Theorem 3.1. In this case, after selecting $v_1, \ldots, v_m$ as the base parameters, the Pi group for ϕ will be of the form

$$\Pi_\phi = \phi v_1^{e_1} \cdots v_m^{e_m}, \quad e_i \in \mathbb{R}, \ i \in [1, m],$$

where the e_i are the exponents that have to be solved in order to make the Pi group nondimensional. However, because the base parameters are fundamentally distinct

by assumption, then only one fundamental dimension $[u_i]$ is associated with each parameter v_i. In terms of fundamental dimensions, the Pi group is

$$\Pi_\phi \equiv ([u_1]^{p_1} \cdots [u_m]^{p_m})([u_1])^{c_1} \cdots ([u_m])^{c_m} = [u_1]^0 \cdots [u_m]^0.$$

By inspection, it is obvious, that the values of the exponents c_i must satisfy

$$c_i = -p_i, \quad i \in [1, m].$$

Hence, the nondimensional Pi group for the parameter ϕ is

$$\Pi_\phi = \frac{\phi}{v_1^{p_1} \cdots v_m^{p_m}},$$

as required. ■

Example (cont): Permanent Magnet DC Motor with Nonlinearity

This system is described by the following parameters:

$$\Phi \triangleq \{J_m, K_b, K_m, R, P_1, P_2\}.$$

The fundamental dimensions of each parameter are

$$J_m \equiv [M][L]^2, \quad K_m \equiv [M][L]^2[T]^{-2}[A]^{-1}, \quad K_b \equiv [M][L]^2[T]^{-2}[A]^{-1},$$
$$R \equiv [M][L]^2[T]^{-3}[A]^{-2}, \quad P_1 \equiv [M][L]^2[T]^{-2}, \quad P_2 \equiv [T].$$

Directly applying Theorem 4.1 with the fundamentally distinct parameters m_1, k_1, Ω, and A_0, gives the following nondimensional groups:

$$\hat{\phi}_1 = \frac{J_m}{m_1 k_1^2}, \quad \hat{\phi}_2 = \frac{K_m}{m_1 k_1^2 \Omega^2 A_0^{-1}}, \quad \hat{\phi}_3 = \frac{K_b}{m_1 k_1^2 \Omega^2 A_0^{-1}},$$
$$\hat{\phi}_4 = \frac{R}{m_1 k_1^2 \Omega^3 A_0^{-2}}, \quad \hat{\phi}_5 = \frac{P_1}{m_1 k_1^2 \Omega^2}, \quad \hat{\phi}_6 = P_2 \Omega.$$

This result can also be obtained directly from the nondimensional actuator dynamics,

$$\begin{aligned}\hat{F}_a(\hat{\xi},\dot{\hat{\xi}},\ddot{\hat{\xi}},\hat{q}_i,\hat{u}) &= \frac{1}{m_1k_1^2\Omega^2}F_a(\xi,\Omega\dot{\xi},\Omega^2\ddot{\xi},q_i,m_1k_1^2\Omega^{-2}u)\\ &= \frac{1}{m_1k_1^2\Omega^2}\left(J_m\Omega^2\ddot{\xi}+\frac{K_bK_m}{R}\Omega\dot{\xi}+P_1q_i^2\sin(P_2\Omega\dot{\xi})+m_1k_1^2\Omega^{-2}u\right)\\ &= \frac{J_m}{m_1k_1^2}\ddot{\xi}+\frac{1}{m_1k_1^2\Omega}\frac{K_bK_m}{R}\dot{\xi}+\frac{P_1}{m_1k_1^2\Omega^2}q_i^2\sin(P_2\Omega\dot{\xi})+u.\end{aligned}$$

Since it is known that the parameters K_b, K_m, and R contain the dimension of current $[A]$, the final equation can be expanded further by introducing the reference value for current, A_0.

$$\begin{aligned}\hat{F}_a(\hat{\xi},\dot{\hat{\xi}},\ddot{\hat{\xi}},\hat{q}_i,\hat{u}) &= \frac{J_m}{m_1k_1^2}\ddot{\xi}+\frac{K_b}{m_1k_1^2\Omega^2A_0^{-1}}\frac{K_m}{m_1k_1^2\Omega^2A_0^{-1}}\frac{m_1k_1^2\Omega^3A_0^{-2}}{R}\dot{\xi}\\ &\quad+\frac{P_1}{m_1k_1^2\Omega^2}q_i^2\sin((P_2\Omega)\dot{\xi})+u\\ &= \hat{\phi}_1\ddot{\xi}+\hat{\phi}_2\hat{\phi}_3\hat{\phi}_4^{-1}\dot{\xi}+\hat{\phi}_5q_i^2\sin(\hat{\phi}_6\dot{\xi})+u.\end{aligned}$$

Therefore, the nondimensional groups in the nondimensional actuator equation agree with those obtained directly using Theorem 4.1. ■

4.2 Example

4.2.1 Revolute DC Motor with Joint Flexibility

As described at the beginning of this chapter, the actuator dynamics for a revolute DC motor with joint flexibility can be described by the coupled equations (4.3)

$$\begin{aligned}\frac{d}{dt}\left(\frac{\partial L}{\partial\dot{q}_i}\right)-\frac{\partial L}{\partial q_i} &= K_s(\xi-q_i)\\ I^h\ddot{\xi}+B\dot{\xi} &= u(t)-K_s(\xi-q_i),\end{aligned}$$

where I^h and B are the motor inertia and damping respectively, u is the control input, and K_s represents the torsional spring constant.

The actuator effect can be captured in the function F_a as

$$F_a(\xi, \dot{\xi}, \ddot{\xi}, q_i, u) = K_s(\xi - q_i) = -I^h\ddot{\xi} - B\dot{\xi} + u.$$

The parameters for the actuator are contained in the set

$$\Phi = \{I^h, B, K_s\},$$

and have the following fundamental dimensions

$$I^h \equiv [M][L]^2, \quad B \equiv [M][L]^2[T]^{-1}, \quad K_s \equiv [M][L]^2[T]^{-2}.$$

Applying Theorem 4.1, this actuator can be scaled if the following nondimensional groups are kept constant,

$$\Pi_1 = \frac{I^h}{m_1 k_1^2}, \quad \Pi_2 = \frac{B}{m_1 k_1^2 \Omega}, \quad \Pi_3 = \frac{K_s}{m_1 k_1^2 \Omega^2}.$$

It is straightforward to see that by directly nondimensionalizing the actuator equation, the same nondimensional groups would result. The nondimensional equation is

$$\hat{F}_a(\hat{\xi}, \dot{\hat{\xi}}, \ddot{\hat{\xi}}, \hat{q}_i, \hat{u}) = \Pi_3(\hat{\xi} - \hat{q}_i) = -\Pi_1\ddot{\hat{\xi}} - \Pi_2\dot{\hat{\xi}} + \hat{u}.$$

In particular, the Pi groups indicate that in order to scale joint flexibility effects, the spring constant used to model the flexibility must be scaled appropriately.

Chapter 5

Controller Scaling Laws

In this chapter, a scaling law for a general control strategy will be determined. Again, the controller fits into the overall system as per Figure 5.1. In this setup, the controller provides a control signal, u, to the actuator, based on the manipulator state, the actuator state, previous control signals, and the reference signals. Contrary to the actuator output, the controller output is not restricted to having dimensions of generalized force. For instance, the control output could have dimensions of voltage or current.

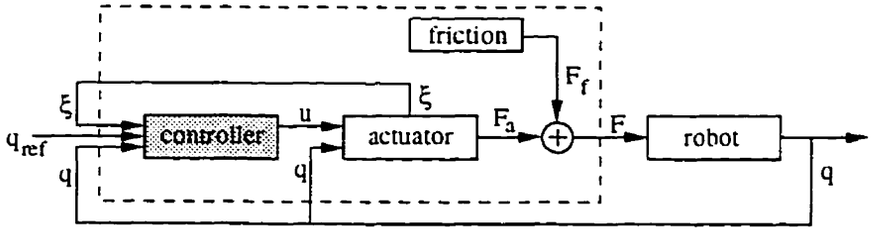

Figure 5.1: Controller Block

The derivation of the controller scaling law is very similar to the derivation of the actuator dynamic equivalence conditions (Chapter 4). In addition to scaling the control law, it is also necessary to scale the *performance specifications* used in the

design of the controller. The scaling conditions for the performance specifications are presented in the final section of the chapter.

5.1 General Control Law

Before developing the scaling conditions for general controllers, some simple examples will be presented.

Example 1: PID Control

A PID controller for the i^{th} manipulator link has the following form

$$u_i(t) = K_p(q_{ref} - q_i) + K_i \int (q_{ref} - q_i)dt + K_d(\dot{q}_{ref} - \dot{q}_i), \tag{5.1}$$

where K_p, K_i, and K_d are the proportional, integral, and derivative gains respectively.

The set of parameters which characterize the PID controller can be collected in the set Φ,

$$\Phi = \{K_p, K_i, K_d\}.$$

Scaling the controller will require that these gains be scaled appropriately.

In general, the PID controller (5.1) can be expressed using a general function, F_c as

$$u_i = F_c(q_{ref}, \dot{q}_{ref}, q_i, \dot{q}_i).$$

■

Example 2: Second-order Transfer Function

An example of a second order transfer function controller is

$$C(s) = \frac{U(s)}{E(s)} = \frac{s + a}{s^2 + bs + c}, \quad a, b, c \in \mathbf{R},$$

where $U(s)$ represents the Laplace transform of the output, and $E(s)$ is the Laplace transform of $q_{ref}(t) - q(t)$. This can be rewritten in terms of $u(t)$ as,

$$u = \frac{1}{c}\left(ac + \dot{c} - b\dot{u} - \ddot{u}\right),$$

where $c = q_{ref} - q$.

The set of controller parameters is

$$\Phi = \{a, b, c\}.$$

In general, the controller could be written using the general function F_c,

$$u = F_c(q_{ref}, \dot{q}_{ref}, q, \dot{q}, \dot{u}, \ddot{u}).$$

■

Every controller is a function of certain parameters whose values define the effect of the control law. Furthermore, these parameters can be *tuned* to adjust the controller performance. Let Φ define the set of the controller parameters for a general controller. Suppose that the controller is defined by m parameters, then,

$$\Phi \triangleq \{\phi_1, \ \phi_2, \ldots, \ \phi_m\},$$

where the fundamental dimensions of ϕ_i are:

$$\phi_i \equiv [M]^{a_i}[L]^{b_i}[T]^{c_i}[A]^{d_i}[\Theta]^{e_i}, \quad a_i, b_i, c_i, d_i, e_i \in \mathbf{R}.$$

In general, the control law will be a function of the link generalized coordinate, q_i and its derivatives, the reference signals q_{ref}, derivatives of the output, u, and also the actuator generalized coordinate, ξ. So, the general control law can be expressed by the function F_c as,

$$u = F_c(q_i, \dot{q}_i, \ldots, q_i^{(n)}, q_{ref}, \ldots, q_{ref}^{(n)}, \xi, \ldots, \xi^{(m)}, \dot{u}, \ldots, u^{(k)}), \tag{5.2}$$

with no restrictions on n, m, or k.

There are no dimensional restrictions on the control signal, u. Therefore, let u have fundamental dimensions:

$$u \equiv [M]^{a_u}[L]^{b_u}[T]^{c_u}[A]^{d_u}[\Theta]^{e_u}, \quad a_u, b_u, c_u, d_u, e_u \in \mathbf{R}.$$

The variables q_i, q_{ref}, and ξ all have dimensions of length,

$$q_i \equiv [L]^r, \quad q_{ref} \equiv [L]^r, \quad \xi \equiv [L]^p,$$

where $r = 0$ if q_i measures angular position, and $r = 1$ if q_i measures translational length. Similarly for p and ξ.

As was stressed in Chapter 4, it is very important that the same base variables are always used throughout the manipulator system (Figure 5.1) for consistency of the nondimensional groups. Using Theorem 4.1 (section 4.1), the manipulator variables m_1, k_1, Ω and the reference values A_0, θ_0 can be used as base variables to nondimensionalize the general control law in (5.2). These five variables form a fundamentally distinct parameter set. Define the following nondimensional variables,

$$\tau \triangleq \Omega t, \quad \hat{q}_i(\tau) \triangleq \frac{q_i\left(\frac{\tau}{\Omega}\right)}{k_1^r} \quad \hat{q}_{ref}(\tau) \triangleq \frac{q_{ref}\left(\frac{\tau}{\Omega}\right)}{k_1^r}, \quad \hat{\xi}(\tau) \triangleq \frac{\xi\left(\frac{\tau}{\Omega}\right)}{k_1^p}, \quad \hat{u} \triangleq \frac{u}{m_1^{a_u} k_1^{b_u} \Omega^{-c_u} A_0^{d_u} \theta_0^{e_u}},$$

where $a_u, b_u, c_u, d_u, e_u \in \mathbf{R}$.

The nondimensionalization of the actuator dynamics in (4.6) introduced a nondimensional variable for the control variable, u, namely,

$$\hat{u} \triangleq \frac{u}{m_1^{a_u} k_1^{b_u} \Omega^{-c_u} A_0^{d_u} \theta_0^{e_u}}, \quad a_u, b_u, c_u, d_u, e_u \in \mathbf{R}.$$

As expected, this definition is identical to the form of $\hat{u}$ defined in this section.

Therefore, nondimensionalizing the general control law from (5.2) and re-arranging gives,

$$\begin{aligned}
\hat{u} &= \frac{1}{m_1^{a_u} k_1^{b_u} \Omega^{-c_u} A_0^{d_u} \theta_0^{e_u}} F_c(q_i, \dot{q}_i, \ldots, q_i^{(n)}, q_{ref}, \ldots, q_{ref}^{(n)}, \xi, \ldots, \xi^{(m)}, \dot{u}, \ldots, u^{(k)}) \\
&= \frac{1}{m_1^{a_u} k_1^{b_u} \Omega^{-c_u} A_0^{d_u} \theta_0^{e_u}} F_c(k_1^r \hat{q}_i, k_1^r \Omega \dot{\hat{q}}_i, \ldots, k_1^r \Omega^n \hat{q}_i^{(n)}, k_1^r \hat{q}_{ref}, \ldots, k_1^r \Omega^n \hat{q}_{ref}^{(n)}, \\
&\qquad k_1^p \hat{\xi}, \ldots, k_1^p \Omega^m \hat{\xi}^{(m)}, \\
&\qquad m_1^{a_u} k_1^{b_u} \Omega^{1-c_u} A_0^{d_u} \theta_0^{e_u} \dot{\hat{u}}, \ldots, m_1^{a_u} k_1^{b_u} \Omega^{k-c_u} A_0^{d_u} \theta_0^{e_u} \hat{u}^{(k)}).
\end{aligned}$$

Examining the right-hand side of the above equation, define the nondimensional control law as

$$\begin{aligned}\hat{F}_c(\hat{q}_i, \dot{\hat{q}}_i, \ldots, \hat{q}_i^{(n)}, \hat{q}_{ref}, \ldots, \hat{q}_{ref}^{(n)}, \hat{\xi}, \ldots, \hat{\xi}^{(m)}, \dot{\hat{u}}, \ldots, \hat{u}^{(k)}) \\ \triangleq \frac{1}{m_1^{a_u} k_1^{b_u} \Omega^{-c_u} A_0^{d_u} \theta_0^{e_u}} F_c(k_1^r \hat{q}_i, k_1^r \Omega \dot{\hat{q}}_i, \ldots, k_1^r \Omega^n \hat{q}_i^{(n)}, k_1^r \hat{q}_{ref}, \ldots, k_1^r \Omega^n \hat{q}_{ref}^{(n)}, \\ k_1^p \hat{\xi}, \ldots, k_1^p \Omega^m \hat{\xi}^{(m)}, \\ m_1^{a_u} k_1^{b_u} \Omega^{1-c_u} A_0^{d_u} \theta_0^{e_u} \dot{\hat{u}}, \ldots, m_1^{a_u} k_1^{b_u} \Omega^{k-c_u} A_0^{d_u} \theta_0^{e_u} \hat{u}^{(k)}).\end{aligned} \tag{5.3}$$

To determine the scaling law for the controller F_c, the parameters in Φ must be examined. As with the actuator dynamics, a parameter ϕ_i within F_c is multiplied by some function γ_i of the variables q_i, q_{ref}, ξ, and derivatives of u. In general, represent the product of ϕ_i and γ_i by the variable ψ_i:

$$\psi_i \triangleq \phi_i^{s_i} \times \gamma_i(q_i, \ldots, q_i^{(n)}, q_{ref}, \ldots, q_{ref}^{(n)}, \xi, \ldots, \xi^{(m)}, \dot{u}, \ldots, u^{(k)}), \quad s_i \in \mathbf{R}.$$

By definition, all the terms in $\hat{F}_c$ (5.3) are nondimensional. Therefore, after the nondimensional process, the function ψ_i must be transformed into a nondimensional $\hat{\psi}_i$. The fundamental dimensions of ϕ_i are defined to be $[M]^{a_i}[L]^{b_i}[T]^{c_i}[A]^{d_i}[\Theta]^{e_i}$. In terms of fundamental dimensions, express γ_i as,

$$\gamma_i \equiv [M]^{f_i}[L]^{g_i}[T]^{h_i}[A]^{j_i}[\Theta]^{k_i}, \quad f_i, g_i, h_i, j_i, k_i \in \mathbf{R}.$$

Hence, ψ_i has fundamental dimensions:

$$\psi_i \equiv [M]^{(s_i a_i + f_i)}[L]^{(s_i b_i + g_i)}[T]^{(s_i c_i + h_i)}[A]^{(s_i d_i + j_i)}[\Theta]^{(s_i e_i + k_i)}.$$

Introducing reference values for current, A_0, and temperature, θ_0, and applying

Theorem 4.1 to $\hat{\psi}_i$ results in:

$$\begin{aligned}
\hat{\psi}_i &\triangleq \frac{1}{m_1^{(s_i a_i + f_i)} k_1^{(s_i b_i + g_i)} \Omega^{(-s_i c_i - h_i)} A_0^{(s_i d_i + j_i)} \theta_0^{(s_i e_i + k_i)}} \psi_i \\
&= \frac{1}{m_1^{(s_i a_i + f_i)} k_1^{(s_i b_i + g_i)} \Omega^{(-s_i c_i - h_i)} A_0^{(s_i d_i + j_i)} \theta_0^{(s_i e_i + k_i)}} \phi_i^{s_i} \gamma_i \\
&= \left[\frac{1}{m_1^{s_i a_i} k_1^{s_i b_i} \Omega^{-s_i c_i} A_0^{s_i d_i} \theta_0^{s_i e_i}} \phi_i^{s_i} \right] \left[\frac{1}{m_1^{f_i} k_1^{g_i} \Omega^{-h_i} A_0^{j_i} \theta_0^{k_i}} \gamma_i \right] \\
&= \left[\frac{1}{m_1^{a_i} l_1^{b_i} \Omega^{-c_i} A_0^{d_i} \theta_0^{e_i}} \phi_i \right]^{s_i} \left[\frac{1}{m_1^{f_i} l_1^{g_i} \Omega^{-h_i} A_0^{j_i} \theta_0^{k_i}} \gamma_i \right] \\
&\triangleq \hat{\phi}_i^{s_i} \hat{\gamma}_i \quad \text{by Theorem 4.1.}
\end{aligned}$$

Therefore, the nondimensional group for the controller parameters can be defined by

$$\Pi_{\phi_i} \triangleq \frac{\phi_i}{m_1^{a_i} k_1^{b_i} \Omega^{-c_i} A_0^{d_i} \theta_0^{e_i}}. \tag{5.4}$$

5.2 Examples

5.2.1 PID Controller

In this example, the above theory is verified for a PID control law. Consider the inputs to be joint angles and the outputs to be motor torque. From (5.1), with $q_{ref} = 0$, the PID control law has the form:

$$u_i(t) = F_c\left(q_i, \dot{q}_i, \int q_i dt\right) = -K_p q_i - K_i \int q_i dt - K_d \dot{q}_i.$$

The PID controller parameters are the proportional, integral, and derivative gains,

$$\Phi = \{\phi_1, \phi_2, \phi_3\} = \{K_p, K_i, K_d\},$$

and have the following fundamental dimensions

$$K_p \equiv [M][L]^2[T]^{-2}, \quad K_i \equiv [M][L]^2[T]^{-3}, \quad K_d \equiv [M][L]^2[T]^{-1}.$$

Applying the result from (5.4), the scaling conditions for the PID gains are

$$\Pi_{K_p} = \frac{K_p}{m_1 k_1^2 \Omega^2}, \quad \Pi_{K_i} = \frac{K_i}{m_1 k_1^2 \Omega^3}, \quad \Pi_{K_d} = \frac{K_d}{m_1 k_1^2 \Omega}.$$

These can be verified directly from the nondimensional form of the controller.

$$\begin{aligned}
\hat{F}_c\left(\hat{q}_i, \dot{\hat{q}}_i, \int \hat{q}_i d\tau\right) &= \frac{1}{m_1 k_1^2 \Omega^2} F_c\left(\hat{q}_i, \Omega \dot{\hat{q}}_i, \Omega^{-1} \int \hat{q}_i d\tau\right) \\
&= \frac{1}{m_1 k_1^2 \Omega^2}\left(-K_p \hat{q}_i - K_i \Omega^{-1} \int \hat{q}_i d\tau - K_d \Omega \dot{\hat{q}}_i\right) \\
&= -\frac{K_p}{m_1 k_1^2 \Omega^2} \hat{q}_i - \frac{K_i}{m_1 k_1^2 \Omega^3} \int \hat{q}_i d\tau - \frac{K_d}{m_1 k_1^2 \Omega} \dot{\hat{q}}_i \\
&= -\Pi_{K_p} \hat{q}_i - \Pi_{K_i} \int \hat{q}_i d\tau - \Pi_{K_d} \dot{\hat{q}}_i,
\end{aligned}$$

which verifies the Pi groups obtained directly using (5.4).

5.2.2 General Linear Controller

All linear lumped-parameter controllers can be expressed as transfer functions of the form,

$$C(s) = K \frac{\prod_{i=1}^{m}(s + z_i)}{\prod_{j=1}^{n}(s + p_j)}, \quad m \leq n \tag{5.5}$$

where K is the gain, z_i are the zeros, and p_j are the poles. Lead-lag, H_2, H_∞ controllers are examples of such linear control laws.

The parameters for this controller are:

$$\Phi = \{K, z_1, \ldots, z_m, p_1, \ldots, p_n\}.$$

The fundamental dimensions of the parameter K depend on the fundamental dimensions of the input and output signals to and from the controller. Let the fundamental dimensions of $C(s)$ be $[M]^a[L]^b[T]^c$, where $a, b, c \in \mathbf{R}$. Then, the fundamental dimensions of the controller parameters are,

$$z_i \equiv [T]^{-1}, \quad p_j \equiv [T]^{-1}, \quad K \equiv [M]^a[L]^b[T]^{(c+m-n)}, \quad i \in [1, m], \; j \in [1, n].$$

Therefore, the Pi groups for the parameters of a general linear controller are,

$$\Pi_{z_i} = \frac{z_i}{\Omega}, \quad \Pi_{p_j} = \frac{p_j}{\Omega}, \quad \Pi_K = \frac{K}{m_1^a l_1^b \Omega^{-(c+m-n)}}, \quad i \in [1, m], \; j \in [1, n]. \tag{5.6}$$

These controller Pi groups can also be verified in a straightforward manner by direct nondimensionalization of the control law. These scaling laws are a generalization of the controller scaling conditions examined by Ghanekar[18], where the linear controller was an H_∞ controller used for position control of a single flexible link manipulator.

5.2.3 Sliding Mode Control

In this example, the scaling conditions for a sliding mode controller are determined. This controller was selected to illustrate the versatility of the scaling theory to nonlinear and switching controllers.

Control Design

In the sliding control technique, the tracking error between the actual and desired system trajectories is represented using a *sliding surface*. Then, two control inputs are designed: the *switching control* input, which drives all trajectories towards the sliding surface, and the *equivalent control* input, which maintains all trajectories on the sliding surface. Both the control inputs are highly nonlinear, and the transition from one control to the other is often discontinuous.

This control strategy is an example of *variable structure control*. The methodology for solving the sliding mode control problem for a given system is described in a tutorial by DeCarlo et al.[26]. In this thesis, the sliding mode control theory will not be covered in detail. For more information see [26].

Let the manipulator dynamics be expressed as a system of first order differential equations

$$\dot{\boldsymbol{x}} = \boldsymbol{f}(\boldsymbol{x}) + \boldsymbol{B}\boldsymbol{u},$$

where $\boldsymbol{x}$ is the $2n \times 1$ state vector, and $\boldsymbol{u}$ is the $n \times 1$ input vector. States x_1 to x_n represent joint positions, whereas states x_{n+1} to x_{2n} represent the corresponding joint velocities.

As described above, the control input is expressed as the sum of the switching control input, $\boldsymbol{u}^{\pm}$, and the equivalent control input, $\hat{\boldsymbol{u}}$. That is:

$$\boldsymbol{u}(t) = \boldsymbol{u}^{\pm}(t) + \hat{\boldsymbol{u}}(t).$$

To determine the equivalent control input $\hat{\boldsymbol{u}}$, the sliding surface itself must be examined. Typically, a sliding surface is selected to be a weighted sum of joint position error and velocity error. Define the tracking error by the vector $\tilde{\boldsymbol{x}} = \boldsymbol{x} - \boldsymbol{x}_{ref}$. Then, in terms of the parameters λ_i, the sliding surfaces, σ_i, are defined, one for each joint, as follows:

$$\sigma_i(\tilde{\boldsymbol{x}}, t) = \lambda_i \tilde{\boldsymbol{x}}_i + \tilde{\boldsymbol{x}}_{n+i}, \quad i \in [1, n].$$

The parameters λ_i determine the rate at which the trajectories approach the desired trajectory on the sliding surface.

Define,

$$\Lambda \equiv \mathrm{diag}\{\lambda_1, \lambda_2, \ldots, \lambda_n\},$$

and then, the sliding surfaces can be equivalently written using the matrix $\boldsymbol{S}$ as,

$$\boldsymbol{S} = [\,\Lambda \quad I_{n \times n}\,]\,\tilde{\boldsymbol{x}} = [\sigma_1, \ldots, \sigma_n]^T.$$

It can be shown[27] that the equivalent control input is:

$$\hat{\boldsymbol{u}} \triangleq (\boldsymbol{SB})^{-1}\,(-\boldsymbol{Sf} - \boldsymbol{S}\dot{\boldsymbol{x}}_{ref}).$$

The switching control input $\boldsymbol{u}^{\pm}$, is used to drive the trajectories toward the sliding surface. For trajectories on the sliding surface, $\sigma_i = 0$. Therefore, this input should intuitively be a function of $\mathrm{sgn}(\sigma_i)$. In terms of the parameters k_i, the switching control input is defined as:

$$\boldsymbol{u}^{\pm} \triangleq -\begin{bmatrix} k_1 \\ \vdots \\ k_n \end{bmatrix} \mathrm{sgn}(\boldsymbol{\sigma}) = -\boldsymbol{k}\,\mathrm{sgn}(\boldsymbol{\sigma}).$$

The sliding control input is given by the formula:

$$\boldsymbol{u}(t) \triangleq -(\boldsymbol{SB})^{-1}(\boldsymbol{Sf}(\boldsymbol{x}) + \boldsymbol{S}\dot{\boldsymbol{x}}_{ref} + \boldsymbol{k}\mathrm{sgn}(\boldsymbol{\sigma})). \tag{5.7}$$

A common artifact of switching controllers is a phenomenon known as chattering. This is caused by the "sgn" operation on the current value of the sliding surface, σ_i. The operator is defined by,

$$\mathrm{sgn}(\sigma_i) \triangleq \begin{cases} 1 & \text{if } \sigma_i > 0 \\ -1 & \text{if } \sigma_i < 0 \end{cases}.$$

The chattering effect can be smoothed out by replacing the sgn operator with a saturation operator of width Δ_i. This operator is defined by,

$$\mathrm{sat}\left(\frac{\sigma_i}{\Delta_i}\right) \triangleq \begin{cases} 1 & \text{if } \dfrac{\sigma_i}{\Delta_i} > 1 \\ \dfrac{\sigma_i}{\Delta_i} & \text{if } -1 \leq \dfrac{\sigma_i}{\Delta_i} \leq 1 \\ -1 & \text{if } \dfrac{\sigma_i}{\Delta_i} < -1 \end{cases}.$$

Scaling Conditions

The value of the sliding surface σ_i has fundamental dimensions of $[T]^{-1}$. Therefore, the width of the saturation operation, Δ_i, must also have dimensions $[T]^{-1}$.

$$\sigma_i \equiv [T]^{-1}, \quad \Delta_i \equiv [T]^{-1}.$$

The parameters defining this controller are:

$$\Phi \triangleq \{\lambda_1, \ldots, \lambda_n, k_1, \ldots, k_n, \Delta_1, \ldots, \Delta_n\},$$

with the following fundamental units:

$$\lambda_i \equiv [T]^{-1}, \quad k_i \equiv [T]^{-2}, \quad \Delta_i \equiv [T]^{-1}.$$

Using the controller scaling laws (5.4), the Pi groups for the controller parameters are,

$$\Pi_{\lambda_i} = \frac{\lambda_i}{\Omega}, \quad \Pi_{k_i} = \frac{k_i}{\Omega^2}, \quad \Pi_{\Delta_i} = \frac{\Delta_i}{\Omega}.$$

Again, these results can be obtained by direct nondimensionalization of the controller equations.

5.3 Performance Specifications

In implementing a controller on a robotic manipulator, the controller parameters are tuned until the system response meets the requirements of the performance specifications. The performance specifications can be divided into three categories: those describing a time criterion (e.g. rise time, settling time), those describing a position criterion (e.g. end-effector position, maximum overshoot), and those giving constraints on the control effort (e.g. maximum torque output). The following notation is used to describe these criteria.

- $\mathcal{T}$ to represent a time specification
- $\mathcal{L}$ to represent a position specification
- $\mathcal{H}$ to represent a control effort specification.

The fundamental dimensions of the specifications are

$$\mathcal{T} \equiv [T], \quad \mathcal{L} \equiv [L]^p, \quad \mathcal{H} \equiv [M][L]^{2-p}[T]^{-2},$$

where $p = 0$ for angular specifications (radians, torque), and $p = 1$ for translational lengths and forces.

Using Theorem 4.1, it is straightforward to find the nondimensional performance specifications for the manipulator system

$$\begin{aligned} \Pi_{\mathcal{T}} &= \Omega \mathcal{T} \\ \Pi_{\mathcal{L}} &= \frac{\mathcal{L}}{l_1^p} \\ \Pi_{\mathcal{H}} &= \frac{1}{m_1 l_1^{2-p} \Omega^2} \mathcal{H}. \end{aligned} \tag{5.8}$$

Equivalently, use k_1 as the reference length value for a rigid manipulator system.

Chapter 6

Friction

Tribology is defined as the science and technology of interacting surfaces in relative motion, and involves the study of friction, wear, and lubrication[28]. Whether it is desired, or is an impediment, friction is present in all engineering applications involving the movement of one solid surface over another. In robot manipulators, friction acts to impede the robot motion. The friction forces are usually present as resistive forces in the actuators driving the manipulator links, and are included in the overall system as per Figure 6.1. From the standpoint of building accurate scale models, it is important to have an idea of the factors that affect the friction forces.

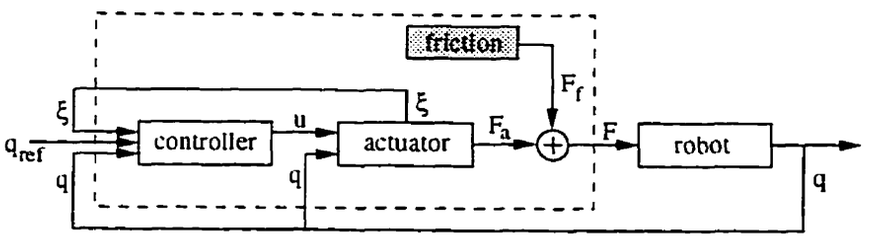

Figure 6.1: Friction Block

6.1 Historical Perspective

The qualitative nature of friction had been known for almost 2000 years before any scientific investigation was begun. In the 15th century, Leonardo da Vinci formulated the two basic laws of friction[29]. These laws, "rediscovered" by Amontons 200 years later in 1699, can be stated as[28]:

1. The friction force is proportional to the normal load.
2. The friction force is independent of the apparent area of contact.

Mathematically, the first law states that if N is the normal load, then the friction force F_f can be expressed as,

$$F_f = \mu N \quad \text{or} \quad \mu = \frac{F_f}{N},$$

where μ is the *coefficient of friction*. The second form of the equation indicates that μ is independent of the normal load. Two friction coefficients are usually considered. The coefficient of static friction μ_s is a measure of the force required to move a body initially at rest. The coefficient of kinetic friction μ_k is a measure of the friction force opposing the inertial force of the body.

There are several theories to explain the presence of the friction force. The model proposed by Coulomb (c.1781) suggests that friction is a result of the surface roughness of two bodies fitting together like a jigsaw puzzle, and the friction *force* results from moving one object against the roughness of the other[29]. It is presently accepted that friction is a result of the interaction between two surfaces at an atomic level. The force arises from an adhesive force at the area of contact, and from a deformation force required to move the harder material through the softer material[28].

To reduce friction, a lubricating fluid can be placed between the two surfaces in contact. The thickness of the fluid layer is greater than the roughness of the surfaces themselves, thereby reducing the friction effect[28].

6.2 Friction Models

There are two classic friction models: Coulomb friction and viscous friction. The scenario used to describe these models is that of a body moving over a fixed surface which has some friction characteristic[30]. In addition, researchers have developed friction models to account for the Dahl effect and Stribeck effect[31].

6.2.1 Coulomb Friction

Coulomb friction describes the situation in which the friction force is constant in magnitude, but opposite to the direction of the motion of the body. The magnitude of the friction force is equal to a friction coefficient, μ, multiplied by the load of the body normal to the surface. This type of friction is also known as *dry friction*, as it occurs in the absence of lubrication. The model used for the Coulomb friction force, F_C, is:

$$F_C = \mu N \text{sgn}(\dot{x}), \tag{6.1}$$

where $\dot{x}$ is the velocity of the body, N is the normal force, and μ is the friction coefficient.

Often, the friction force that must be overcome when moving the body from rest, is greater than the friction force that is present while the body is moving. These two friction forces are known as *static* and *kinetic* friction respectively. Both are proportional to the normal load, but by different friction coefficients; μ_s is the static friction coefficient, and μ_k is the kinetic friction coefficient.

6.2.2 Viscous Friction

Viscous friction describes the situation in which the friction force is proportional to the velocity of the moving body, but opposite to the direction of motion. This model is often used in describing the motion of a body through a fluid. The model

for the viscous friction force, F_V, is:

$$F_V = c_v \dot{x}, \tag{6.2}$$

where $\dot{x}$ is the velocity of the body, and c_v is the viscous friction coefficient.

6.2.3 Dahl and Stribeck Effects

Although the scope of this thesis is not directly with friction, two other friction effects should be mentioned here. The *Dahl effect* describes the observation that for small displacements, the sliding area between two surfaces acts like a linear spring. The *Stribeck effect* describes the low velocity phenomenon when fluid lubrication causes the friction force to *decrease* as velocity increases[31].

A model encompassing all of these friction effects is proposed by Canudas de Wit et al.[31]. The friction mechanism is visualized as two rigid bodies which make contact through elastic bristles. The friction force arises when an applied force (to the body) causes the bristles to deflect like springs. The friction model proposed has two parts. The first part models the average bristle deflection, z, by,

$$\frac{dz}{dt} = v - \frac{|v|}{g(v)} z, \tag{6.3}$$

where v is the relative velocity between the surfaces, and $g(v)$ is a positive function that depends on many factors such as material properties and lubrication.

In the second part, the friction force, F, arising from the deflection of the bristles is modelled by,

$$F = \sigma_0 z + \sigma_1 \frac{dz}{dt} + \sigma_2 v, \tag{6.4}$$

where σ_0, σ_1, and σ_2 are stiffness, damping, and viscous damping coefficients respectively. These coefficients are determined experimentally[31].

Different parameterizations of $g(v)$ are used to describe different friction effects. For the Stribeck effect, the following parameterization is used:

$$\sigma_0 g(v) = F_C + (F_S - F_C) e^{-(\frac{v}{v_s})^2}, \tag{6.5}$$

where F_C is the Coulomb friction level, F_S is the stiction force, and v_s is the Stribeck velocity[31]. The Dahl effect can also be captured by this model, by parametrizing $g(v)$ as,

$$g(v) = \frac{F_C}{\sigma_0}, \quad \sigma_1 = \sigma_2 = 0.$$

6.3 Friction and Manipulators

It will be assumed that, for the robot manipulators considered in this thesis, the friction effects are all confined to the actuator dynamics. In other words, it will be assumed that there is no contact between adjacent robot links, and there is no slippage in the connection attaching the link to the actuator. The actuators used in robotics are typically electrical, hydraulic, or pneumatic actuators. If friction is to be included in the manipulator model, it will be assumed that the the two basic friction models described above are sufficient to characterize the friction effects in the actuators. The extension to more complicated friction models will be straightforward after the results of this section are presented.

6.4 Scaling Friction Effects

Suppose the friction coefficients for a given manipulator are identified. Dimensional analysis can be used to determine the scaling law for the friction coefficients. Theoretically, this will indicate the required values for friction coefficients on a dynamically equivalent manipulator. Whether the specified value can be achieved is a separate issue (section 6.6).

6.4.1 Coulomb Friction

In the Coulomb friction model (6.1), it is clear that the friction coefficient, μ, must be nondimensional by definition. Hence, the nondimensional group for μ is,

$$\Pi_\mu = \mu.$$

For dynamic equivalence, the value of Π_μ has to be the same for both systems. Since μ is a function of the surface material (wood, steel, etc.), the Pi group indicates that the material for the scale model must be such that the friction coefficient is unchanged from the actual manipulator.

6.4.2 Viscous Friction

In the viscous friction model (6.2), the fundamental dimensions of the variables are,

$$F_V \equiv [M][L]^{2-p}[T]^{-2}, \quad \dot{x} \equiv [L]^p[T]^{-1},$$

where $p = 0$ for a rotational system (radians, torque), and $p = 1$ for a translational system (translation, force) system. Hence, the fundamental dimensions of the viscous friction coefficient c_v are

$$c_v \equiv [M][L]^{2-2p}[T]^{-1}.$$

Applying Theorem 3.1, a nondimensional group corresponding to c_v is,

$$\Pi_{c_v} = \frac{c_v}{m_1 l_1^{(2-p)} \Omega}. \tag{6.6}$$

6.4.3 Stribeck Effect

Using the friction model described in (6.3) and (6.4), the Stribeck effect is modelled by (6.5). This description of the friction model is characterized by six parameters: $\sigma_0, \sigma_1, \sigma_2, F_C, F_S$, and v_s. These are the parameters for which nondimensional

groups are required. The parameters have the following fundamental dimensions:

$$\sigma_0 \equiv [M][L][T]^{-2}$$
$$\sigma_1 \equiv [M][L][T]^{-1}$$
$$\sigma_2 \equiv [M][L][T]^{-1}$$
$$F_C \equiv [M][L]^2[T]^{-2}$$
$$F_S \equiv [M][L]^2[T]^{-2}$$
$$v_s \equiv [L][T]^{-1}.$$

Applying Theorem 3.1, the scaling laws for this friction model are:

$$\Pi_{\sigma_0} = \frac{\sigma_0}{m_1 l_1 \Omega^2}$$
$$\Pi_{\sigma_1} = \frac{\sigma_1}{m_1 l_1 \Omega}$$
$$\Pi_{\sigma_2} = \frac{\sigma_2}{m_1 l_1 \Omega}$$
$$\Pi_{F_C} = \frac{F_C}{m_1 l_1^2 \Omega^2}$$
$$\Pi_{F_S} = \frac{F_S}{m_1 l_1^2 \Omega^2}$$
$$\Pi_{v_s} = \frac{v_s}{l_1 \Omega}.$$

Scaling laws for the model describing the Dahl effect can be found similarly.

6.5 Reducing Friction Forces

To construct two dynamically equivalent manipulators, the physical parameters of the robot must be chosen so that the nondimensional Pi groups for both manipulators are the same. It is possible to do this for the tangible quantities, such as link mass and link length, however, it is impossible to construct a material with a given friction coefficient. The friction coefficient is an inherent property of the two materials in contact; it cannot be designed for. One way to rectify this problem is

to attempt to reduce the friction forces in both manipulator systems. This can be done by using ball-bearings in the joints, and with lubrication

A novel approach to minimizing friction is to use a computer to provide active friction compensation. This idea was brought to fruition for a rotating bearing in Smith[32]. This method will be discussed in more detail in Chapter 7.

6.6 Achieving Scaled Values

The nondimensional groups indicate the required friction coefficients for dynamic equivalence. Suppose the required coefficient for dynamic equivalence cannot be achieved. This is a highly likely situation, since friction is usually a system component that is *not* designed for. If the friction on both systems can be minimized through computer friction compensation or high quality bearings and lubrication, then the effect of incorrect friction coefficients can perhaps be overlooked, because of the small magnitudes. However, if the friction on one system is not negligible, then a problem arises. In the next chapter, the sensitivity of the manipulator dynamics to variations in the Pi group values is investigated. For rigid manipulators, a technique exists to compensate for errors in the Pi group values. In this case, the compensation technique also covers errors in the Pi groups for friction.

Chapter 7

Tolerances for Pi Groups

Theoretically, two systems are considered dynamically equivalent *if and only if* the values for their nondimensional groups are *exactly* the same. In practice, because of manufacturing imprecision, it is impossible to achieve the exactness required for dynamic equivalence. The value for a nondimensional group may be close to the value required for dynamic equivalence, but will not be exactly the value required.

Therefore, to allow the scaling theory developed so far to be used practically, the sensitivity of the manipulator dynamics to changes in the nondimensional groups must be determined. Then, provided that the dynamics are relatively insensitive to the deviation of the actual Pi values from those required for dynamic equivalence, the two systems will be considered to be dynamically equivalent. As well, a method will be presented which uses nonlinear feedback to render two systems which are nearly dynamically equivalent to be exactly dynamically equivalent.

7.1 Sensitivity Analysis

When two manipulators are dynamically equivalent, the *nondimensional* dynamics of the two manipulators are identical. Now, if the values of the Pi groups for one of

the manipulators have deviated from the values required for dynamic equivalence, the nondimensional dynamics will no longer be identical. However, the structure of the equation of motion will remain the same. What has to be measured, therefore, is the sensitivity of each nondimensional generalized coordinate, $\hat{q}_i(\tau)$, to changes in each Pi group, Π_j, in the nondimensional dynamic equations.

For a manipulator having unconstrained motion, the nondimensional dynamic equations can be written in matrix form, in terms of the inertia matrix, Coriolis and centripetal acceleration vector, and gravity vector[20]. Define the following nondimensional variables:

- τ - nondimensional time
- $\hat{\boldsymbol{q}}(\tau)$ - $n \times 1$ vector of nondimensional generalized coordinates
- $\hat{\boldsymbol{M}}(\hat{\boldsymbol{q}})$ - nondimensional inertia matrix
- $\hat{\boldsymbol{C}}(\hat{\boldsymbol{q}}, \dot{\hat{\boldsymbol{q}}})$ - nondimensional Coriolis and centripetal acceleration vector
- $\hat{\boldsymbol{G}}(\hat{\boldsymbol{q}})$ - nondimensional gravity vector
- $\hat{\boldsymbol{F}}(\tau)$ - nondimensional external generalized force vector
- $\boldsymbol{\Pi}$ - $m \times 1$ vector of Pi groups for the manipulator.

Then, the nondimensional equations describing the free motion of an unconstrained manipulator can be written as,

$$\hat{\boldsymbol{M}}(\hat{\boldsymbol{q}})\ddot{\hat{\boldsymbol{q}}} + \hat{\boldsymbol{C}}(\hat{\boldsymbol{q}}, \dot{\hat{\boldsymbol{q}}}) + \hat{\boldsymbol{G}}(\hat{\boldsymbol{q}}) = \hat{\boldsymbol{F}}(\tau). \tag{7.1}$$

Also notice that $\hat{\boldsymbol{M}}, \hat{\boldsymbol{C}}$, and $\hat{\boldsymbol{G}}$ are functions of the nondimensional Pi groups, $\boldsymbol{\Pi}$. Therefore, the generalized coordinates, $\hat{\boldsymbol{q}}$, are also functions of $\boldsymbol{\Pi}$. The goal of the sensitivity analysis is to find the change in each $\hat{q}_i$ caused by a change in each Π_j. The sensitivity of the joint velocities $\dot{\hat{q}}_i$, and the joint accelerations $\ddot{\hat{q}}_i$ to parameter changes also provide informative results.

The manipulator dynamic equation (7.1) can be written as a function of one of the nondimensional groups, Π_j,

$$\hat{M}(\hat{q}(\tau;\Pi_j),\Pi_j)\ddot{\hat{q}}(\tau;\Pi_j) + \hat{C}(\hat{q}(\tau;\Pi_j),\dot{\hat{q}}(\tau;\Pi_j),\Pi_j) + \hat{G}(\hat{q}(\tau;\Pi_j),\Pi_j) = \hat{F}(\tau). \tag{7.2}$$

Take the derivative of (7.2) with respect to Π_j,

$$\hat{M}\frac{\partial\ddot{\hat{q}}}{\partial\Pi_j} + \left(\frac{\partial\hat{M}}{\partial\Pi_j} + \sum_{i=1}^{n}\frac{\partial\hat{M}}{\partial\hat{q}_i}\frac{\partial\hat{q}_i}{\partial\Pi_j}\right)\ddot{\hat{q}} + \frac{\partial\hat{C}}{\partial\Pi_j} + \sum_{i=1}^{n}\frac{\partial\hat{C}}{\partial\dot{\hat{q}}_i}\frac{\partial\dot{\hat{q}}_i}{\partial\Pi_j} + \sum_{i=1}^{n}\frac{\partial\hat{C}}{\partial\hat{q}_i}\frac{\partial\hat{q}_i}{\partial\Pi_j} + \frac{\partial\hat{G}}{\partial\Pi_j} + \sum_{i=1}^{n}\frac{\partial\hat{G}}{\partial\hat{q}_i}\frac{\partial\hat{q}_i}{\partial\Pi_j} = 0. \tag{7.3}$$

Because $\hat{M}$ is an inertia matrix, it is always positive definite, and hence it is nonsingular. Therefore, from (7.3), the joint acceleration *sensitivity* can be solved,

$$\frac{\partial\ddot{\hat{q}}}{\partial\Pi_j} = -\hat{M}^{-1}\left[\left(\frac{\partial\hat{M}}{\partial\Pi_j} + \sum_{i=1}^{n}\frac{\partial\hat{M}}{\partial\hat{q}_i}\frac{\partial\hat{q}_i}{\partial\Pi_j}\right)\ddot{\hat{q}} + \frac{\partial(\hat{C}+\hat{G})}{\partial\Pi_j} + \sum_{i=1}^{n}\frac{\partial(\hat{C}+\hat{G})}{\partial\hat{q}_i}\frac{\partial\hat{q}_i}{\partial\Pi_j} + \sum_{i=1}^{n}\frac{\partial\hat{C}}{\partial\dot{\hat{q}}_i}\frac{\partial\dot{\hat{q}}_i}{\partial\Pi_j}\right]. \tag{7.4}$$

Throughout this chapter, the word *sensitivity* will be used to describe the rate of change of one quantity with respect to another. Although not standard, this same terminology is used by Takahashi in applying sensitivity analysis to robotic manipulators[33].

From (7.2), an expression for $\ddot{\hat{q}}$ can be found, and substituted into (7.4) to give the sensitivity expression:

$$\frac{\partial\ddot{\hat{q}}}{\partial\Pi_j} = -\hat{M}^{-1}\left[\left(\frac{\partial\hat{M}}{\partial\Pi_j} + \sum_{i=1}^{n}\frac{\partial\hat{M}}{\partial\hat{q}_i}\frac{\partial\hat{q}_i}{\partial\Pi_j}\right)\hat{M}^{-1}\left(\hat{F}-\hat{C}-\hat{G}\right) + \frac{\partial(\hat{C}+\hat{G})}{\partial\Pi_j} + \sum_{i=1}^{n}\frac{\partial(\hat{C}+\hat{G})}{\partial\hat{q}_i}\frac{\partial\hat{q}_i}{\partial\Pi_j} + \sum_{i=1}^{n}\frac{\partial\hat{C}}{\partial\dot{\hat{q}}_i}\frac{\partial\dot{\hat{q}}_i}{\partial\Pi_j}\right]. \tag{7.5}$$

Although (7.5) is a complicated expression, it is essentially a second order differential equation of the form

$$\frac{d^2\boldsymbol{X}_j}{d\tau^2} = -\sum_{i=1}^{n}(\cdot)\,X_j^i - \sum_{i=1}^{n}(\cdot)\frac{dX_j^i}{d\tau} - (\cdot), \quad X_j^i \triangleq \frac{\partial\hat{q}_i}{\partial\Pi_j}.$$

A solution for $\boldsymbol{X}_j$ can be found by using an iterative algorithm, beginning with initial estimates for $\boldsymbol{X}_j$ and $\dot{\boldsymbol{X}}_j$. With the sensitivity solution X_j^i, the variation in $\hat{q}_i$ caused by a variation in Π_j can be found. In particular,

$$X_j^i = \frac{\partial \hat{q}_i}{\partial \Pi_j} \quad \Rightarrow \quad X_j^i \approx \frac{\Delta \hat{q}_i}{\Delta \Pi_j}.$$

For a given nominal trajectory, the sensitivity $\boldsymbol{X}_j(\tau)$ can be computed off-line. Rearranging the above approximation gives

$$\Delta \hat{q}_i \approx X_j^i(\tau) \Delta \Pi_j.$$

So, for each Pi group Π_j, the above equation can be used to determine by how much the actual manipulator trajectory will vary from the nominal trajectory, for a given change in the value of the Pi group. This information can be used *a priori* to the construction of the manipulator in order to determine which components of the manipulator should be machined more precisely than others.

7.1.1 Computation

A method is required to compute the partial derivatives in (7.5).

$$\frac{\partial \hat{M}}{\partial \Pi_j}, \quad \frac{\partial (\hat{C} + \hat{G})}{\partial \Pi_j}, \quad \frac{\partial \hat{M}}{\partial \hat{q}_i}, \quad \frac{\partial (\hat{C} + \hat{G})}{\partial \hat{q}_i}, \quad \frac{\partial \hat{C}}{\partial \dot{\hat{q}}_i}.$$

For an arbitrary manipulator configuration, the calculation of these derivatives is quite tedious, and computationally intensive. However, for the class of manipulators which are open-chain and have rigid links, Takahashi[33] has presented an *iterative* method of sensitivity analysis which can be implemented efficiently on a computer. In the paper, the sensitivity of the manipulator torques and joint accelerations to parameter changes is examined. The next section will briefly describe how the method in [33] can be used to compute the derivatives in (7.5). Although the method is taken from [33], it has been modified to apply to the nondimensional manipulator dynamic equations of interest in this chapter. In this way, a method of sensitivity analysis is developed for the class of dynamically equivalent open-chain rigid manipulators.

7.1.2 Rigid Open-Chain Manipulators

Because the manipulator is assumed to be an open kinematic chain, the Newton-Euler method can be used to express the dynamics of each link in terms of adjacent links. This method leads to a recursive algorithm by which all of the forces and torques acting on all the links can be found, given the joint positions, velocities, and accelerations.

A recursive scheme was presented by Luh et al.[34] to solve for the generalized forces acting on each link. This scheme was modified by Takahashi[33], so that instead of generating the generalized forces at each link, it generated the sensitivity of the generalized forces at each link to a change in one of the manipulator physical parameters. The method consists of nine equations which are solved recursively[33, 34]. The equations come from the Newton-Euler analysis of the dynamics of one link, and therefore contain all the physical parameters required to characterize the link. In the modified scheme[33], each equation is replaced by the sensitivity equations for each parameter.

For the nondimensional equation of motion, define the function T_1, which measures the sensitivity of $\hat{F}$ to changes in a particular Pi group, Π_j.

$$\frac{\partial \hat{F}}{\partial \Pi_j} = T_1(\hat{q}, \dot{\hat{q}}, \ddot{\hat{q}}) \triangleq \frac{\partial \hat{M}(\hat{q})}{\partial \Pi_j}\ddot{\hat{q}} + \frac{\partial(\hat{C}(\hat{q}, \dot{\hat{q}}) + \hat{G}(\hat{q}))}{\partial \Pi_j}.$$

To compute the sensitivity of the *joint accelerations* (7.5), the function, T_1, can be used with different arguments so that the required partial derivatives (specified above) can be computed. This will be shown below, and will require the definition of the $n \times 1$ unit vector, e_k, where k^{th} element equals 1, and all other elements are zero:

- $\dfrac{\partial(\hat{C} + \hat{G})}{\partial \Pi_j} = T_1(\hat{q}, \dot{\hat{q}}, 0)$
- k^{th} column of $\dfrac{\partial \hat{M}(\hat{q})}{\partial \Pi_j} = T_1(\hat{q}, 0, e_k)$, with $g = 0$ in $\hat{G}$.

The original method [34] was modified to compute the derivative of the joint torque with respect to parameter changes[33]. Define the functions T_2 and T_3:

$$\begin{aligned}\frac{\partial \hat{F}}{\partial \hat{q}_i} &= T_2(\hat{q},\dot{\hat{q}},\ddot{\hat{q}}) \triangleq \frac{\partial \hat{M}(\hat{q})}{\partial \hat{q}_i}\ddot{\hat{q}} + \frac{\partial(\hat{C}(\hat{q},\dot{\hat{q}}) + \hat{G}(\hat{q}))}{\partial \hat{q}_i} \\ \frac{\partial \hat{F}}{\partial \dot{\hat{q}}_i} &= T_3(\hat{q},\dot{\hat{q}}) \triangleq \frac{\partial \hat{M}(\hat{q})}{\partial \dot{\hat{q}}_i}\ddot{\hat{q}} + \frac{\partial(\hat{C}(\hat{q},\dot{\hat{q}}) + \hat{G}(\hat{q}))}{\partial \dot{\hat{q}}_i} = \frac{\partial \hat{C}(\hat{q},\dot{\hat{q}})}{\partial \dot{\hat{q}}_i}.\end{aligned}$$

Varying the arguments of these two functions, the remaining derivatives can be evaluated.

- $\dfrac{\partial(\hat{C}(\hat{q},\dot{\hat{q}}) + \hat{G}(\hat{q}))}{\partial \hat{q}_i} = T_2(\hat{q},\dot{\hat{q}},0)$
- k^{th} column of $\dfrac{\partial \hat{M}(\hat{q})}{\partial \hat{q}_i} = T_2(\hat{q},0,e_k)$, with $g = 0$ in $\hat{G}$
- $\dfrac{\partial(\hat{C}(\hat{q},\dot{\hat{q}}))}{\partial \dot{\hat{q}}_i} = T_3(\hat{q},\dot{\hat{q}})$.

Using this iterative approach with the initial conditions,

$$\frac{\partial \hat{q}}{\partial \Pi_j} = 0, \quad \text{and} \quad \frac{\partial \dot{\hat{q}}}{\partial \Pi_j} = 0,$$

a value for the sensitivity, $\frac{\partial \ddot{\hat{q}}}{\partial \Pi_j}$, as in (7.5) will be approached.

Regardless of the method used, the sensitivity analysis provides a way of measuring the effect of manufacturing errors in different components of the manipulator. The magnitude of these effects for each component can be assessed in simulation, before constructing the robot. For Pi groups causing high sensitivity, the corresponding components must be manufactured with high precision to ensure that the actual value is very close to the value required for dynamic equivalence. This would ensure that the value of the Pi group is close to that required for dynamic equivalence.

7.2 Error Compensation

A computer can be used to compensate for the errors in the Pi groups caused by manufacturing imprecision. This is most useful for friction effects, for which desired values are not easily achieved. In the first section, a method by Smith[32], in which a computer is used to provide active friction compensation for a rotating bearing, is discussed. In the second section, a nonlinear feedback compensation scheme is presented for rigid manipulators. With this compensation, the error between the actual and desired dynamic behaviour is eliminated. Because this error compensation scheme is a special case of the feedback linearization technique, it is not generally applicable to flexible link manipulators. In particular, it will fail for those flexible manipulators which cannot be feedback linearized[35].

7.2.1 Friction Compensation

In Smith[32], the authors constructed a jig to measure and cancel the bearing friction, using a computer to provide torque compensation. Instead of friction cancellation, this method can be used to achieve the required friction forces for dynamic equivalence. The method implemented is essentially a feedback linearization.

In [32], an axle was modelled by the following dynamics,

$$I\frac{d^2\phi}{dt^2} + b\frac{d\phi}{dt} + K\text{sgn}\left(\frac{d\phi}{dt}\right) = 0,$$

where I is the axle moment of inertia, b the velocity damping coefficient, K a damping torque independent of angular velocity, and ϕ is the angular position of the axle.

The electro-magnetic friction compensation introduces two parameters F_1 and F_2, so that with the friction compensation, the axle equation of motion becomes,

$$I\frac{d^2\phi}{dt^2} + (b - F_1)\frac{d\phi}{dt} + (K - F_2)\text{sgn}\left(\frac{d\phi}{dt}\right) = 0.$$

The values of the parameters F_1 and F_2 can be adjusted to achieve friction cancellation by setting $F_1 = b$ and $F_2 = K$. The resulting equation of motion is then simply:

$$I\frac{d^2\phi}{dt^2} = 0.$$

Now, suppose that for dynamic equivalence, specific non-zero values for the velocity damping coefficient and damping torque were required. Denote these values by $\bar{b}$ and $\bar{K}$ respectively. With the friction compensation apparatus, the parameters F_1 and F_2 could be tuned so that,

$$F_1 = b - \bar{b}, \quad F_2 = K - \bar{K},$$

and the desired friction coefficients for dynamic equivalence would be obtained.

7.2.2 Nonlinear Compensation for Rigid Manipulators

Manufacturing imprecision may cause errors in the values of the system parameters, thereby causing the Pi group values to be different from those required for dynamic equivalence. In this method, a nonlinear state feedback is implemented on rigid manipulator systems to eliminate the error between the actual and desired dynamic behaviour.

With this approach it may appear that *any* deviation from the required Pi values for dynamic equivalence can be tolerated. This is true theoretically, however, practically, the method is only feasible for small deviations in the Pi groups. The reason stems from the way in which the error compensation is provided, namely through compensation torques from the actuators. The greater the deviation of the actual Pi values from the required values, the greater the magnitude of the compensation torques. Since the actuators are probably designed to operate within the torque range of the dynamically equivalent system, they may not be able to provide the large compensation torques required to correct for large deviations of the Pi values from those required for dynamic equivalence.

For unconstrained rigid manipulators, let the desired dynamic equations be

$$M(q)\ddot{q} + C(q,\dot{q}) + G(q) = F, \tag{7.6}$$

where M, C, G, and F are the inertia matrix, the coriolis and centripetal acceleration vector, the gravity vector, and the external generalized force vector respectively.

Defining

$$h(q,\dot{q}) \triangleq C(q,\dot{q}) + G(q),$$

allows (7.6) to be rewritten compactly as,

$$M(q)\ddot{q} + h(q,\dot{q}) = F(t). \tag{7.7}$$

For this manipulator, let Π denote the Pi values required for dynamic equivalence. Suppose, however, that because of manufacturing imprecision, some of the manipulator parameters are not machined to the exact specifications required for dynamic equivalence. For this manipulator, then, let $\bar{\Pi}$ denote the values of the Pi groups, where

$$\bar{\Pi} \neq \Pi.$$

Let (7.7) denote the equations of motion of the desired (dynamically equivalent) system. For the manipulator with Pi values $\bar{\Pi}$, denote the "actual" equations of motion by

$$\bar{M}(q)\ddot{q} + \bar{h}(q,\dot{q}) = F. \tag{7.8}$$

The objective is to use nonlinear state feedback to make the input-output dynamics between the control signal and the manipulator generalized coordinate appear as (7.7). In Figure 7.1, the actual manipulator dynamics are represented by the block with input F and output q. In addition, two nonlinear function blocks are shown in the Figure. Let $f(q,\dot{q},v)$ be called the *inner* nonlinear compensation, and let $g(q,\dot{q},w)$ be the *outer* nonlinear compensation. The controller signal is denoted by w.

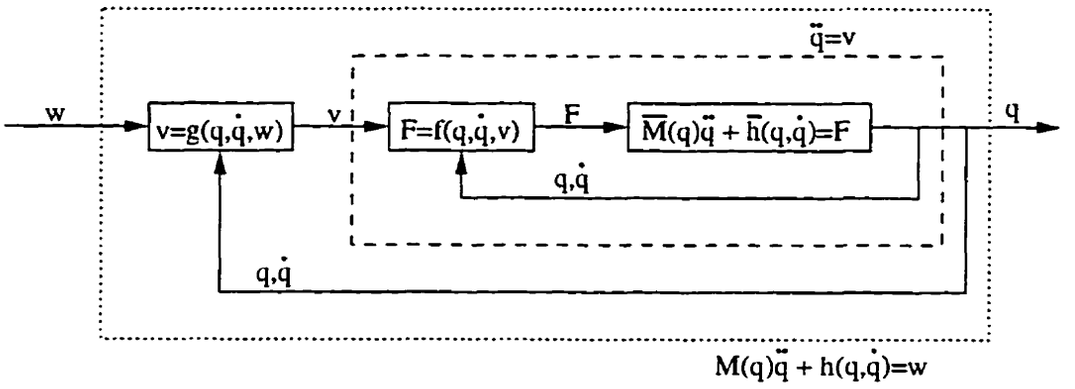

Figure 7.1: Error Compensation Scheme using Nonlinear Feedback

The inner nonlinear block is an inverse dynamics block which makes the system from the input v to the output q appear as a double integrator[20]. Now, the outer nonlinear block is another inverse dynamics block which makes the system from w to q exhibit the desired dynamics according to (7.7). The definitions of f and g to achieve this will now be described.

Define the inner nonlinear function, $f(q, \dot{q}, v)$, to be

$$F(t) = f(q, \dot{q}, v) \triangleq \bar{M}(q)v(t) + \bar{h}(q, \dot{q}). \tag{7.9}$$

Because $\bar{M}(q)$ is an inertia matrix, it is invertible, and hence, substituting into (7.8) results in the double integrator equation,

$$\ddot{q} = v(t). \tag{7.10}$$

Now, define the outer block, $g(q, \dot{q}, w)$, to be

$$v(t) = g(q, \dot{q}, w) \triangleq M(q)^{-1}\left(-h(q, \dot{q}) + w(t)\right). \tag{7.11}$$

Substitution into (7.10) and simplification reveals the dynamic equation,

$$M(q)\ddot{q} + h(q, \dot{q}) = w(t),$$

which represents the desired dynamics (7.7), with w as the input signal. This is the system from w to q in Figure 7.1.

So, the overall inverse dynamics controller is given by combining (7.9) and (7.11) to give,

$$\boldsymbol{F}(t) = -\bar{\boldsymbol{M}}(\boldsymbol{q})\boldsymbol{M}(\boldsymbol{q})^{-1}\boldsymbol{h}(\boldsymbol{q},\dot{\boldsymbol{q}}) + \bar{\boldsymbol{h}}(\boldsymbol{q},\dot{\boldsymbol{q}}) + \bar{\boldsymbol{M}}(\boldsymbol{q})\boldsymbol{M}(\boldsymbol{q})^{-1}w(t). \tag{7.12}$$

The values for $\bar{\boldsymbol{M}}$ and $\bar{\boldsymbol{h}}$ are known, since these represent the actual manipulator that has been constructed. The values for $\boldsymbol{M}$ and $\boldsymbol{h}$ are also known, since these represent the desired dynamic behaviour. Therefore, given a control input $w(t)$, all the quantities in (7.12) are known, and the control loop can be implemented. Hence, placing an inner control loop around the actual manipulator, can make the manipulator exhibit the desired dynamic behaviour.

The extra control effort required to achieve the desired dynamic behaviour can also be calculated. Without the compensation provided by (7.12), $w(t)$ is the control signal to the manipulator. Hence, the additional control effort provided by (7.12) can be computed by,

$$\begin{aligned} F_{extra}(t) &= \boldsymbol{F}(t) - w(t) \\ &= \left(-\bar{\boldsymbol{M}}(\boldsymbol{q})\boldsymbol{M}(\boldsymbol{q})^{-1}\boldsymbol{h}(\boldsymbol{q},\dot{\boldsymbol{q}}) + \bar{\boldsymbol{h}}(\boldsymbol{q},\dot{\boldsymbol{q}}) + \bar{\boldsymbol{M}}(\boldsymbol{q})\boldsymbol{M}(\boldsymbol{q})^{-1}w\right) - w \\ &= -\bar{\boldsymbol{M}}(\boldsymbol{q})\boldsymbol{M}(\boldsymbol{q})^{-1}\boldsymbol{h}(\boldsymbol{q},\dot{\boldsymbol{q}}) + \bar{\boldsymbol{h}}(\boldsymbol{q},\dot{\boldsymbol{q}}) + \left(\bar{\boldsymbol{M}}(\boldsymbol{q})\boldsymbol{M}(\boldsymbol{q})^{-1} - I\right) w(t). \end{aligned} \tag{7.13}$$

In the limit, as the difference between the actual and desired dynamics approaches zero, the extra control effort required goes to zero, as would be expected.

$$\begin{aligned} \lim_{\substack{\bar{\boldsymbol{M}}\to\boldsymbol{M} \\ \bar{\boldsymbol{h}}\to\boldsymbol{h}}} F_{extra}(t) &= -\boldsymbol{M}\boldsymbol{M}^{-1}\boldsymbol{h} + \boldsymbol{h} + \left(\boldsymbol{M}\boldsymbol{M}^{-1} - I\right) w(t) \\ &= -\boldsymbol{h} + \boldsymbol{h} + (I - I)w \\ &= 0. \end{aligned}$$

This nonlinear feedback technique is illustrated via simulation in Chapter 8.

Chapter 8

Application to Sample Systems

In this chapter, the theory developed thus far will be applied to several sample manipulator-control systems. In all the examples, the feedback configuration shown in Figure 8.1 is employed.

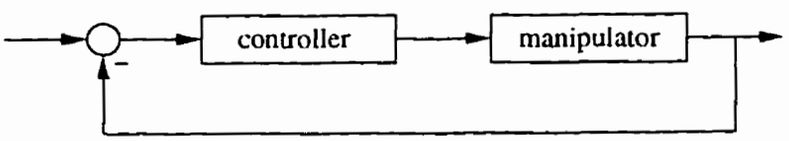

Figure 8.1: Standard Feedback Configuration

Using the appropriate Pi groups, the parameters for two dynamically equivalent manipulators will be determined. Next, a controller will be designed for one of the manipulators. Using the controller Pi groups, the controller will be scaled so that it can be applied to the other dynamically equivalent robot. Using computer simulation, the responses of each manipulator to the designed controller will be observed. It will be found that because the manipulators *and* controllers are dynamically equivalent, all the responses are exactly scalable.

In the sample systems, rigid and flexible manipulators, and linear and nonlinear controllers will be examined. In order to encompass many manipulator and controller scenarios, the following systems will be investigated:

1. two-link rigid elbow manipulator with PID control
2. two-link rigid elbow manipulator with sliding-mode control
3. two-link rigid elbow manipulator with friction and error compensation
4. single flexible link with two degrees of vibration and PD control
5. five-bar linkage manipulator with a flexible link, and PD control

In the third example, a manipulator will be designed whose parameter values do not exactly meet the Pi group specifications. For this system, the error compensation technique of section 7.2 will be illustrated. The pre and post-compensation control will be done using a PID controller.

In this chapter, all system responses are simulated and generated using the software package MATLAB™.

8.1 Sample System 1: Rigid Two-Link Elbow with PID Control

8.1.1 Scenario

Suppose a two-link elbow manipulator is required for operation on the Moon. Using the rigid manipulator Pi groups(3.19), a dynamically equivalent manipulator can be constructed on Earth for testing and control design. Furthermore, using the controller Pi groups(5.4), the controller designed on Earth can be scaled to apply to the Moon-based manipulator, with predictable results. The equations of motion for the two-link elbow manipulator were presented in section 3.2.4.

8.1.2 Manipulator Design

Denote the parameters for the Moon-based manipulator by the subscript 'm'. Let the time scaling factor be $(\Omega)_m = 1\ \mathrm{s}^{-1}$, since this is the original system. Each link is a solid cylinder (length 5.0 m, radius 0.039 m). The parameters for the manipulator are defined in Table 8.1.

Link Parameters	Variable	Link 1	Link 2
mass (kg)	$(m_i)_m$	60.0	60.0
mass moment	$(J_i^{xx})_m$	0.044	0.044
of inertia	$(J_i^{yy})_m$	125.02	125.02
($\mathrm{kg\,m^2}$)	$(J_i^{zz})_m$	125.02	125.02
Joint Parameters		Joint 1	Joint 2
mass (kg)	$(M_j)_m$	12.0	6.0
inertia ($\mathrm{kg\,m^2}$)	$(I_j^h)_m$	3.0	3.0
General Parameters		Value	
gravitational accel. ($\mathrm{m\,s^{-2}}$)	$(g)_m$	1.64	
time scaling ($\mathrm{s^{-1}}$)	$(\Omega)_m$	1.0	

Table 8.1: Parameters for Moon-based Manipulator (System 1)

Let the base variables for the nondimensionalization be $(m_1)_m$, $(J_1)_m = (J_1^{xx})_m$, and $(\Omega)_m$. Calculate the radius of gyration, k_1, using

$$k_1 = \sqrt{\left(\frac{(J_1)_m}{(m_1)_m}\right)} = 0.027 \text{ m}.$$

The Pi groups for rigid manipulators are defined in (3.19). Using these definitions, the values for the 12 Pi groups for this manipulator are given in Table 8.2.

Pi - links	Form	Link 1	Link 2
Π_{m_i}	$\frac{m_i}{m_1}$	n/a	1.0
$\Pi_{J_i^{xx}}$	$\frac{J_i^{xx}}{J_1}$	n/a	1.0
$\Pi_{J_i^{yy}}$	$\frac{J_i^{yy}}{J_1}$	2813.0	2813.0
$\Pi_{J_i^{zz}}$	$\frac{J_i^{zz}}{J_1}$	2813.0	2813.0
Pi - joints		Joint 1	Joint 2
Π_{M_j}	$\frac{M_j}{m_1}$	0.2	0.1
$\Pi_{I_j^h}$	$\frac{I_j^h}{J_1}$	67.5	67.5
Pi - gravity		Value	
Π_G	$\frac{g}{k_1\Omega^2}$	60.0737	

Table 8.2: Pi groups for Two-Link Elbow Manipulator

With these Pi groups, the dynamically equivalent Earth-based manipulator can be constructed. The values of three base parameters must be chosen. Since the manipulator is on Earth, $g = 9.81\ \mathrm{m\,s^{-2}}$. Also, choose the mass of the first link to be $m_1 = 1.27$ kg. Finally, with the local x-axis running along the length of link 1, choose $J_1 = J_1^{xx} = 7.2 \times 10^{-5}\ \mathrm{kg\,m^2}$. Calculating $(k_1)_e = \sqrt{(J_1)_e(m_1^{-1})_e}$, and using the Pi values in Table 8.2, the remaining parameter values for the Earth-based manipulator can be calculated to satisfy the dynamic equivalence condition. For example,

$$\begin{aligned}(m_2)_e &= (m_1)_e\Pi_{m_i} = (1.27\ \mathrm{kg})(1.0) = 1.27\ \mathrm{kg},\\ (\Omega)_e &= \sqrt{\frac{(g)_e}{(k_1)_e\Pi_G}} = \sqrt{\frac{9.81\ \mathrm{m\,s^{-2}}}{(0.0075\ \mathrm{m})(60.0737)}} = 4.66\ \mathrm{s^{-1}},\end{aligned}$$

where $(k_1)_e = \sqrt{\frac{(J_1)_e}{(m_1)_e}}$. In this manner all the parameter values for the Earth-based manipulator are calculated. These values are given in Table 8.3.

Notice that the Pi groups do *not* require that the *link shape* be scaled; only

Link Parameters	Variable	Link 1	Link 2
mass (kg)	$(m_i)_e$	1.27	1.27
mass moment	$(J_i^{xx})_e$	7.2×10^{-5}	7.2×10^{-5}
of inertia	$(J_i^{yy})_e$	0.20	0.20
($\mathrm{kg\,m^2}$)	$(J_i^{zz})_e$	0.20	0.20
Joint Parameters		Joint 1	Joint 2
mass (kg)	$(M_j)_e$	0.25	0.13
inertia ($\mathrm{kg\,m^2}$)	$(I_j^h)_e$	0.0049	0.0049
General Parameters		Value	
gravitational accel. ($\mathrm{m\,s^{-2}}$)	$(g)_e$	9.81	
time scaling ($\mathrm{s^{-1}}$)	$(\Omega)_e$	4.66	
radius of gyration (m)	$(k_1)_e$	0.0075	

Table 8.3: Parameters for Earth-based Manipulator (System 2)

the inertia must be scaled. Therefore, although the Moon-based manipulator has cylindrical links, the Earth-based manipulator can be designed such that its links are solid rectangular bars. In fact, with the i^{th} link a solid rectangular bar of length l_i and cross-section $b_i \times h_i$, its inertial properties are given by[19],

$$\begin{aligned} J_i^{xx} &\triangleq \frac{m_i}{12}\left(b_i^2 + h_i^2\right) = 7.2 \times 10^{-5}\ \mathrm{kg\,m^2} \\ J_i^{yy} &\triangleq \frac{m_i}{12}\left(l_i^2 + b_i^2\right) = 0.20\ \mathrm{kg\,m^2} \\ J_i^{zz} &\triangleq \frac{m_i}{12}\left(l_i^2 + h_i^2\right) = 0.20\ \mathrm{kg\,m^2}. \end{aligned}$$

Solving for the physical dimensions of links 1 and 2 gives,

$$\begin{aligned} l_1 &= 1.38\ \mathrm{m}, \quad b_1 = 0.018\ \mathrm{m}, \quad h_1 = 0.018\ \mathrm{m} \\ l_2 &= 1.38\ \mathrm{m}, \quad b_2 = 0.018\ \mathrm{m}, \quad h_2 = 0.018\ \mathrm{m}. \end{aligned}$$

Assuming cylindrical links for the Earth-based manipulator, the length l_i, and the cross-sectional link radius r_i, required to satisfy the computed inertial values, are,

$$l_i = 1.38 \text{ m}, \quad r_i = 0.011 \text{ m}, \quad i \in [1, 2].$$

It can be shown that by scaling the mass and inertia according to Π_{m_i} and $\Pi_{J_{ci}}$, the length parameters of the links have also automatically been scaled. From Lemma 3.1, the lengths are scaled by k_1, and hence

$$\begin{aligned} \Pi_{(l_i)_m} &= \frac{(l_i)_m}{(k_1)_m} = \frac{5.0 \text{ m}}{0.027 \text{ m}} = 183.71 \\ \Pi_{(l_i)_e} &= \frac{(l_i)_e}{(k_1)_e} = \frac{1.38 \text{ m}}{0.0075 \text{ m}} = 183.71. \end{aligned}$$

Since the Pi groups for link length are equal, then the lengths have scaled between the two manipulator systems. This can also be shown for the link cross-sectional radius, r_i.

Notice that for this Earth-based system, the value of the time scaling parameter is $\Omega = 4.66 \text{ s}^{-1}$. The implication of this is that the motion of the Earth-based manipulator is approximately 4.7 times *faster* than the dynamically equivalent Moon-based counterpart.

8.1.3 Control Design

Suppose that a PID controller is required to move the Moon manipulator from an initial position of $(q_1, q_2) = (0, 0)$ to a final position of $(q_1, q_2) = (\frac{\pi}{2}, -\frac{\pi}{2})$. In addition, there are performance specifications indicating acceptable system behaviour.

Now that the dynamically equivalent Earth manipulator has been determined, a PID controller is designed to meet the *scaled* performance specifications. The performance criteria are not stated here, but are scaled according to (5.8). Let the

following gains provide the desired performance.

$$\text{Joint } 1 : K_{P_1} = 200, \quad K_{I_1} = 50, \quad K_{D_1} = 50$$
$$\text{Joint } 2 : K_{P_2} = 100, \quad K_{I_2} = 100, \quad K_{D_2} = 50.$$

The proportional gains have units of $\mathrm{kg\,m^2\,s^{-2}}$, the integral gains have units of $\mathrm{kg\,m^2\,s^{-3}}$, and the derivative gain units are $\mathrm{kg\,m^2\,s^{-1}}$.

For the Earth-based manipulator, $m_1 = 1.27$ kg, $k_1 = 0.0075$ m, and $\Omega = 4.66\ \mathrm{s^{-1}}$. Hence, using the controller Pi groups defined in (5.4), the values for the Pi groups for these joint controllers can be found:

$$\text{Joint } 1 : \Pi_{K_{P_1}} = 1.28 \times 10^5. \quad \Pi_{K_{I_1}} = 6.87 \times 10^3. \quad \Pi_{K_{D_1}} = 1.49 \times 10^5$$
$$\text{Joint } 2 : \Pi_{K_{P_2}} = 6.40 \times 10^4. \quad \Pi_{K_{I_2}} = 1.38 \times 10^4 \quad \Pi_{K_{D_2}} = 1.49 \times 10^5.$$

Now, for the Moon-based manipulator, $m_1 = 60$ kg, $k_1 = 0.027$ m, and $\Omega = 1\ \mathrm{s^{-1}}$. Using the given Pi values, the gains for the scaled PID controller are computed to be:

$$\text{Joint } 1 : K_{P_1} = 5692.0, \quad K_{I_1} = 305.6, \quad K_{D_1} = 6627.2$$
$$\text{Joint } 2 : K_{P_2} = 2846.0, \quad K_{I_2} = 611.1, \quad K_{D_2} = 6627.2.$$

The entire procedure of finding a dynamically equivalent prototype, designing a controller for the prototype, and scaling the controller to the original system, is depicted in Figure 8.2.

8.1.4 Responses

In Figures 8.3 to 8.6, the responses for both the Earth-based and the Moon-based manipulators with $q_{ref} = (\frac{\pi}{2}, -\frac{\pi}{2})$ are given. Figures 8.3 and 8.5 show the joint angle histories, and Figures 8.4 and 8.6 show the torque histories for each system.

For each pair of plots (one from the Earth-based system and one from the Moon-based system), it is clear that although the axes sizes are different, the response

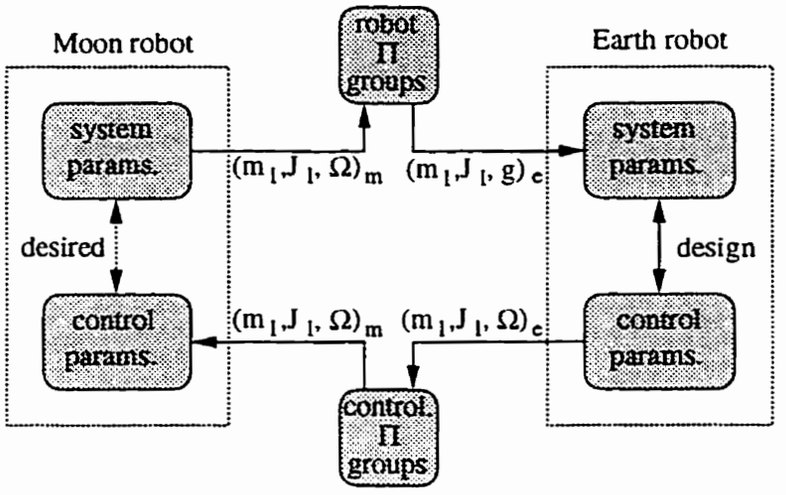

Figure 8.2: Design Process

of the Moon-based manipulator is an *exact scaled version* of the Earth-based manipulator response. This can be easily explained by considering the scaling factors involved. Let the subscripts e and m denote the Earth-based and Moon-based systems respectively. Then,

$$\text{time:} \quad \tau = (\Omega)_m t_m = (\Omega)_e t_e \quad \Rightarrow \quad t_m = 4.66 t_e$$

$$\text{torque:} \quad \hat{H} = \frac{H_m}{(m_1 k_1^2 \Omega^2)_m} = \frac{H_e}{(m_1 k_1^2 \Omega^2)_e} \quad \Rightarrow \quad H_m = 28.46 H_e,$$

where the actual scaling values are obtained from the system parameters for this example. Therefore, stretching the time axis of the Earth-based system responses by a factor of 4.66 will give the time axis for the Moon-based system responses. Similarly, the torques are scaled by a factor of 28.46.

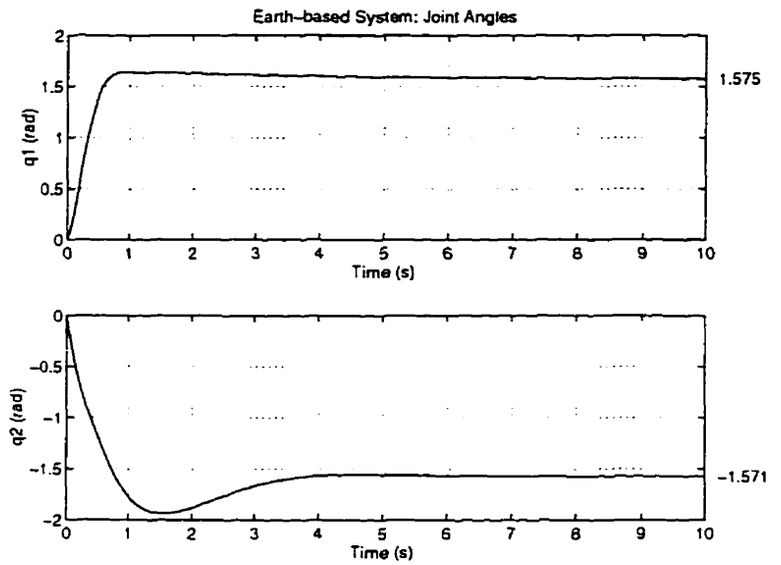

Figure 8.3: Earth-based: Joint Angles

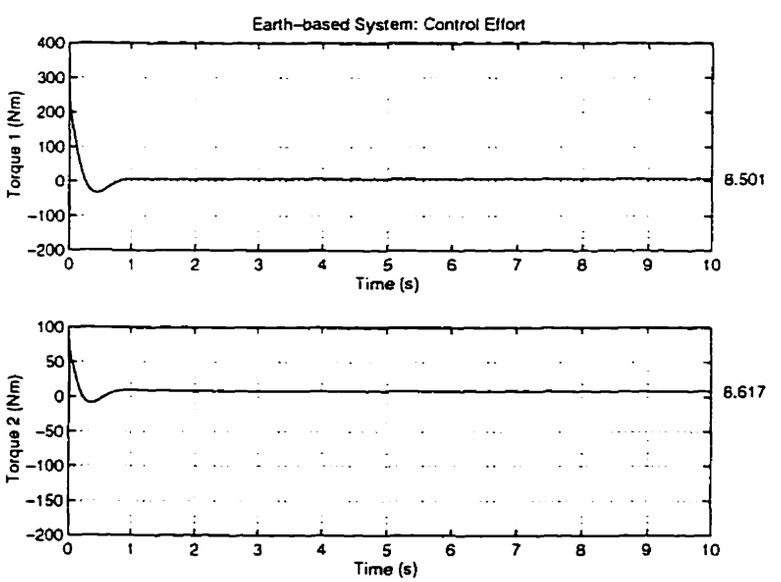

Figure 8.4: Earth-based: Control Effort

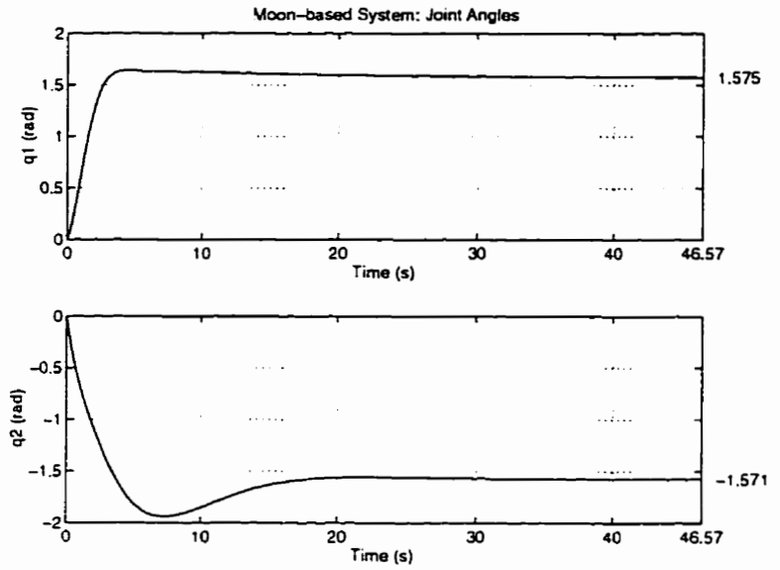

Figure 8.5: Moon-based: Joint Angles

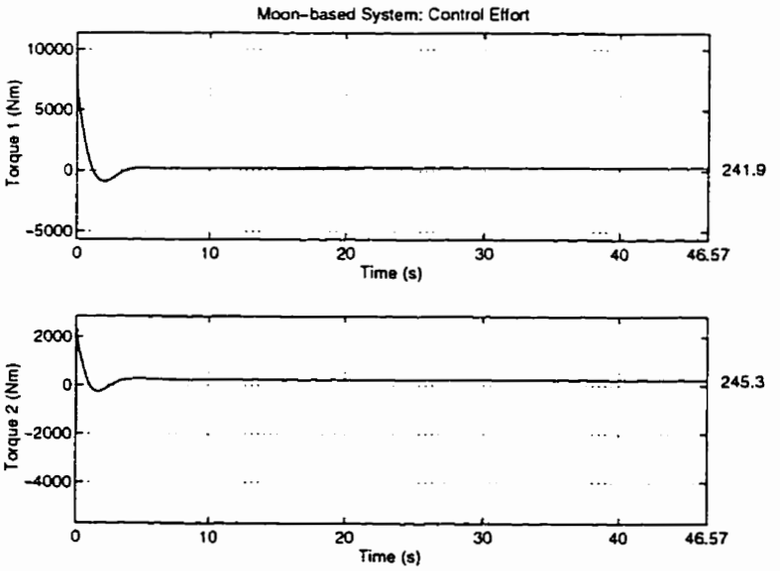

Figure 8.6: Moon-based: Control Effort

Note:

By assumption, the manipulator links are rigid. However, examination of the physical dimensions of the links reveals that they are long and slender, and hence, quite flexible. Suppose the links on both manipulators are made of aluminum ($E = 6.9 \times 10^{10}\ \mathrm{kg\,m^{-1}\,s^{-2}}$, $\rho^v = 2700\ \mathrm{kg\,m^{-3}}$), the first modal frequency can be estimated by approximating each link as a clamped-free link,

$$\omega_1 = \sqrt{\frac{EI}{\rho^v A L^4}}\beta_1^2,$$

where L is the link length, I is the area moment of inertia of the cross-section, and $\beta_1 = 1.875$ is the first solution of the clamped-free transcendental equation $1 + \cos(\beta_i)\cosh(\beta_i) = 0$[12].

For the cylindrical links of the Moon manipulator,

$$L = 5.0\ \mathrm{m},\quad A = 0.0047\ \mathrm{m^2},\quad I = 1.73 \times 10^{-6}\ \mathrm{m^4} \quad \Rightarrow \quad \omega_1 = 13.69\ \mathrm{s^{-1}},$$

and for the rectangular links of the Earth manipulator,

$$L = 1.38\ \mathrm{m},\quad A = 0.00034\ \mathrm{m^2},\quad I = 9.64 \times 10^{-9}\ \mathrm{m^4} \quad \Rightarrow \quad \omega_1 = 49.68\ \mathrm{s^{-1}}.$$

Now, by Theorem 3.1, a nondimensional group for the frequency of vibration is

$$\Pi_{\omega_1} = \frac{\omega_1}{\Omega}.$$

Computing this quantity for both manipulators gives,

$$(\Pi_{\omega_1})_m = 13.69,\quad (\Pi_{\omega_1})_e = 10.67.$$

Because the values for the two Pi groups are not equal, this indicates that the first mode of vibration is *not* scaled between the Earth and Moon manipulators. This illustrates the importance of correctly modelling the system. In this example, the actual manipulator will clearly exhibit oscillatory dynamics, even though it is modelled as having rigid links. Since the Earth prototype and the Moon manipulator are not dynamically equivalent from a flexibility standpoint, the results

obtained on the prototype will *not* accurately predict the actual behaviour of the Moon manipulator.

In the extreme case, by not including flexibility effects, the actual manipulator on Earth may be significantly stiffer than the Moon robot, although the two manipulators would still be dynamically equivalent according to the *rigid* Pi groups. In this situation, the controller for the Earth robot would not provide vibration suppression by design, and hence, the scaled version of this controller would not provide the required vibration suppression on the flexible Moon robot. For this sample system, it would have been more appropriate to use the flexible manipulator Pi groups. Examples of flexible manipulator Pi groups will be examined in the final two sample systems in this chapter.

8.2 Sample System 2: Rigid Elbow with Sliding Mode Control

8.2.1 Scenario

This example is the same as the previous example, but instead of PID control, a sliding mode controller is used to control the manipulator motion. The same two manipulators will be used in this example.

8.2.2 Control Design

In this example, a sliding mode controller is designed for the two-link rigid elbow manipulator. The sliding mode controller is nonlinear and discontinuous, and illustrates the versatility of the scaling theory to complicated control strategies. This control methodology was described in Chapter 5. For more information on sliding mode control see [26].

As described in section 5.2.3, the parameters that characterize the sliding mode controller for a two-link elbow manipulator are,

$$\Phi \triangleq \{\lambda_1, \lambda_2, k_1, k_2, \Delta_1, \Delta_2\},$$

with the following fundamental dimensions,

$$\lambda_i \equiv [T]^{-1}, \quad k_i \equiv [T]^{-2}, \quad \Delta_i \equiv [T]^{-1}, \quad i \in [1, 2].$$

As with the previous example, a sliding mode controller is designed for the Earth-based manipulator in order to meet the *scaled* performance specifications. The following parameter values meet the criteria,

$$\begin{aligned} \lambda_1 &= 10\ \mathrm{s}^{-1}, \quad k_1 = 10\ \mathrm{s}^{-2}, \quad \Delta_1 = 0.17\ \mathrm{s}^{-1}, \\ \lambda_2 &= 10\ \mathrm{s}^{-1}, \quad k_2 = 10\ \mathrm{s}^{-2}, \quad \Delta_2 = 0.17\ \mathrm{s}^{-1}. \end{aligned}$$

Using Theorem 4.1, the Pi groups for the controller parameters are,

$$\Pi_{\lambda_i} = \frac{\lambda_i}{(\Omega)_e} = 1.76, \quad \Pi_{k_i} = \frac{k_i}{(\Omega^2)_e} = 0.31, \quad \Pi_{\Delta_i} = \frac{\Delta_i}{(\Omega)_e} = 0.03, \quad i \in [1,2].$$

Since $(\Omega)_m = 1\ \mathrm{s}^{-1}$, then the values of the controller parameters for the scaled Moon-based controller are,

$$\begin{aligned} \lambda_1 &= 1.76\ \mathrm{s}^{-1}, \quad k_1 = 0.31\ \mathrm{s}^{-2}, \quad \Delta_1 = 0.03\ \mathrm{s}^{-1}. \\ \lambda_2 &= 1.76\ \mathrm{s}^{-1}, \quad k_2 = 0.31\ \mathrm{s}^{-2}, \quad \Delta_2 = 0.03\ \mathrm{s}^{-1}. \end{aligned}$$

8.2.3 Responses

The joint angle histories and torque histories for both systems are given in Figures 8.7 to 8.10. Even for this nonlinear, discontinuous control strategy, the corresponding pairs of plots scale exactly. The scaling factors for time and torque are,

$$\begin{aligned} \text{time:} \quad & \tau = (\Omega)_m t_m = (\Omega)_e t_e \quad \Rightarrow \quad t_m = 4.66 t_e \\ \text{torque:} \quad & \hat{H} = \frac{H_m}{(m_1 k_1^2 \Omega^2)_m} = \frac{H_e}{(m_1 k_1^2 \Omega^2)_e} \quad \Rightarrow \quad H_m = 28.46 H_e. \end{aligned}$$

Notice that the scaling factors are *identical* to the scaling factors obtained in the previous example. This highlights the point that the scaling factors for time, length, and control effort are determined by the *manipulator* dynamic equivalence conditions, and are independent of the specific control strategy implemented.

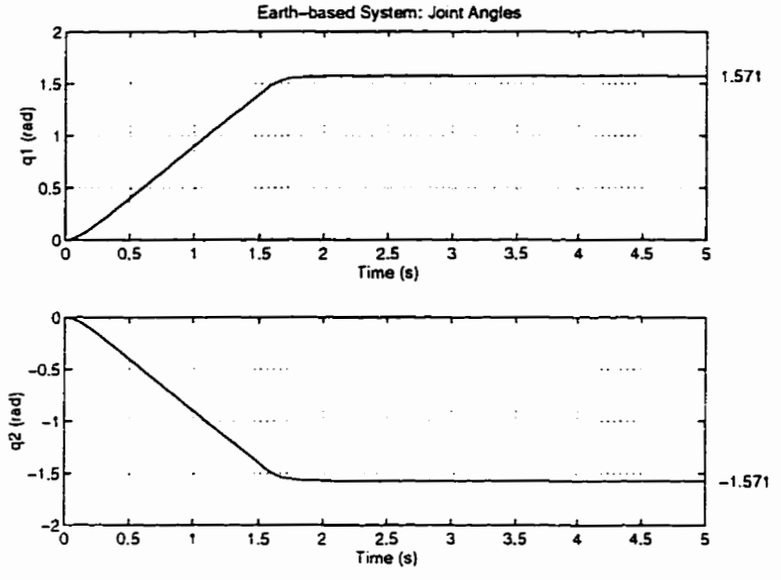

Figure 8.7: Earth-based: Joint Angles

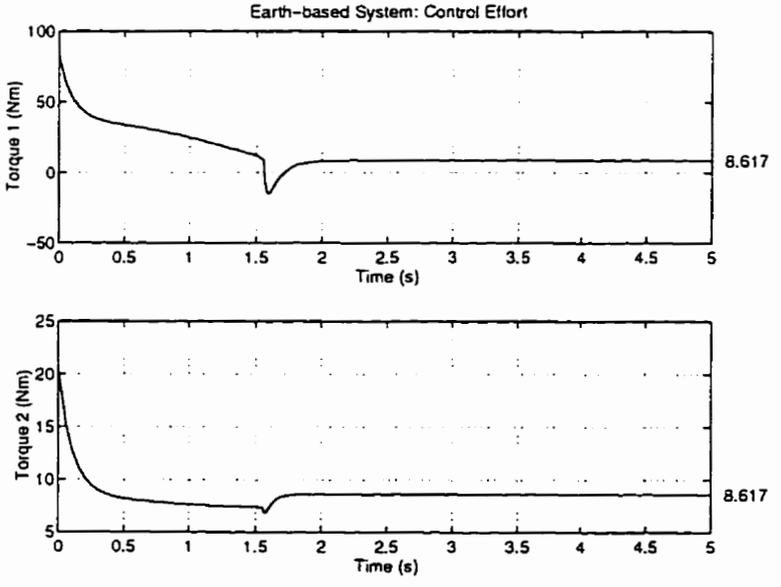

Figure 8.8: Earth-based: Control Effort

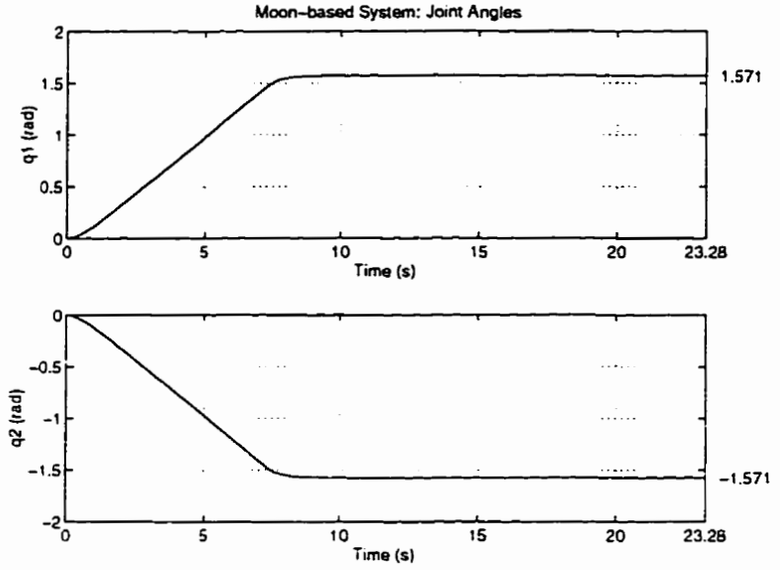

Figure 8.9: Moon-based: Joint Angles

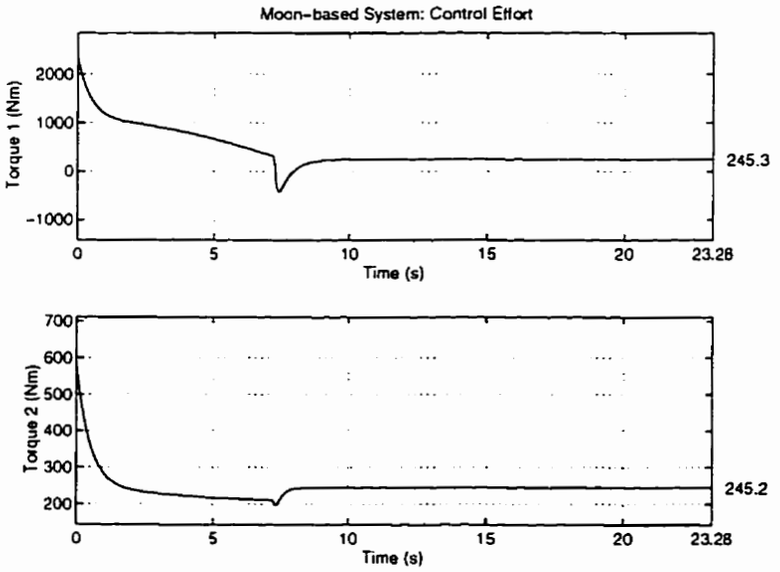

Figure 8.10: Moon-based: Control Effort

8.3 Sample System 3: Error Compensation

Because of manufacturing imprecision, it is impossible to construct a manipulator such that the Pi values required for dynamic equivalence are *exactly* attained. In Chapter 7, it was shown that for rigid link manipulators, a nonlinear feedback loop can be implemented around the manipulator, such that the manipulator and nonlinear feedback *together* provide the required dynamic behaviour.

In this example, the same Earth-based and Moon-based elbow manipulators are examined, and viscous friction is added to each joint(6.2.2). For the Earth-based manipulator, suppose that the friction coefficient, c_v, has the value,

$$(c_v)_e = 50 \text{ kg m}^2 \text{ s}^{-1},$$

for both joints.

The scaling condition for viscous friction is computed using (6.6)

$$\Pi_{c_v} = \frac{(c_v)_e}{(m_1)_e (k_1)_e^2 (\Omega)_e} = 1.49 \times 10^5.$$

The values required for dynamic equivalence are given in Tables 8.1 and 8.3. Table 8.1 provides the desired parameters for the Moon-based manipulator. For the Moon-based manipulator, the friction coefficient required for dynamic equivalence can be found using Π_{c_v} to be

$$(c_v)_m = (m_1)_m (k_1)_m^2 (\Omega)_m \Pi_{c_v} = 6630 \text{ kg m}^2 \text{ s}^{-1}.$$

Notice that the magnitude of the friction coefficient has changed by a significant factor (from 50 to 6630 $\text{kg m}^2 \text{ s}^{-1}$).

A dynamically equivalent Earth-based manipulator was constructed, and a PID controller designed to provide the desired performance. Now, the Moon-based manipulator must be constructed so that it can be sent to the Moon. Suppose that after the manipulator has been assembled, it is found that there is an error between the actual and desired values for some of the the manipulator parameters.

Because of this, the Pi values are not equal to those required for dynamic equivalence, and hence, the constructed manipulator is dynamically "unequivalent" to the Earth-based prototype. For this example, the following arbitrary errors were introduced:

- m_2 - 50% error
- J_1^{yy}, J_2^{yy} - 100% error
- M_1 - 50% error
- I_2^h - 75% error
- c_v - 4900% error.

The errors were purposefully made large in order to be able to illustrate the effect of having Pi values other than those required for dynamic equivalence (Figures 8.11 and 8.12). The error for the friction coefficient is the largest, since the friction coefficient was not changed to the required value (6630 $\mathrm{kg\,m^2\,s^{-1}}$), but was kept at $c_v = 50\ \mathrm{kg\,m^2\,s^{-1}}$ for both systems. Note however, that such a large error for the friction coefficient is not necessarily unrealistic. Suppose the prototype had a direct drive motor, and the larger manipulator had a 50:1 gear ratio. Assuming that the friction increases by a factor of 50, then this would be a 5000% error.

Using the scaled PID controller, the manipulator is moved from $(q_1, q_2) = (0, 0)$ to $(\frac{\pi}{2}, -\frac{\pi}{2})$. The responses are given in Figures 8.11 and 8.12. It is clear that the responses are *not* those desired for dynamic equivalence (dashed line).

To remedy the situation, the error compensation technique of section 7.2 is implemented. From the values for the Pi groups, the parameter values for the dynamically equivalent Moon manipulator are known. Substitution of these parameters into the dynamic equations for the two-link elbow manipulator give the desired inertia matrix, $\boldsymbol{M}$, and the desired Coriolis, centripetal, and gravity effects vector, $\boldsymbol{h}$. With the errant values for the parameters m_2, J_1^{yy}, J_2^{yy}, M_1, I_2^h and c_v, specified above, the "actual" inertia matrix, $\bar{\boldsymbol{M}}$, and "actual" Coriolis, centripetal, and gravity effects vector, $\bar{\boldsymbol{h}}$, is also calculated. With these four matrices

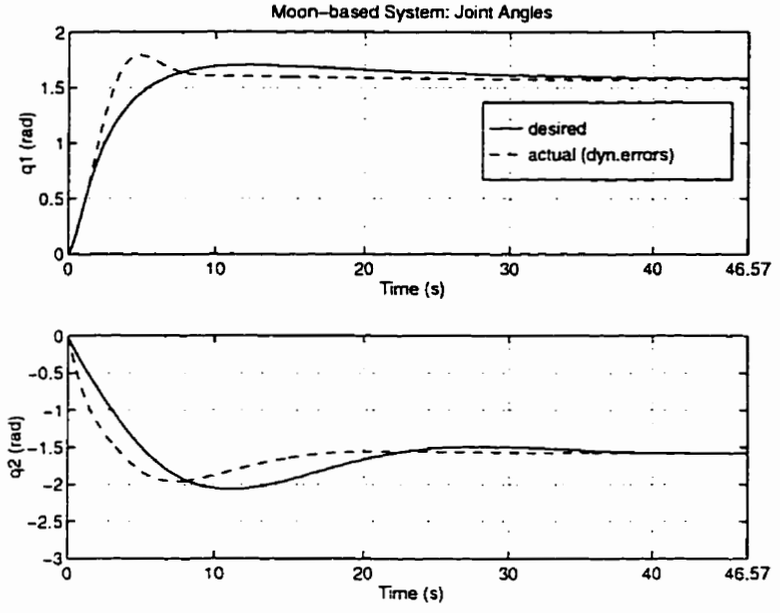

Figure 8.11: Moon-based with Errors: Joint Angles

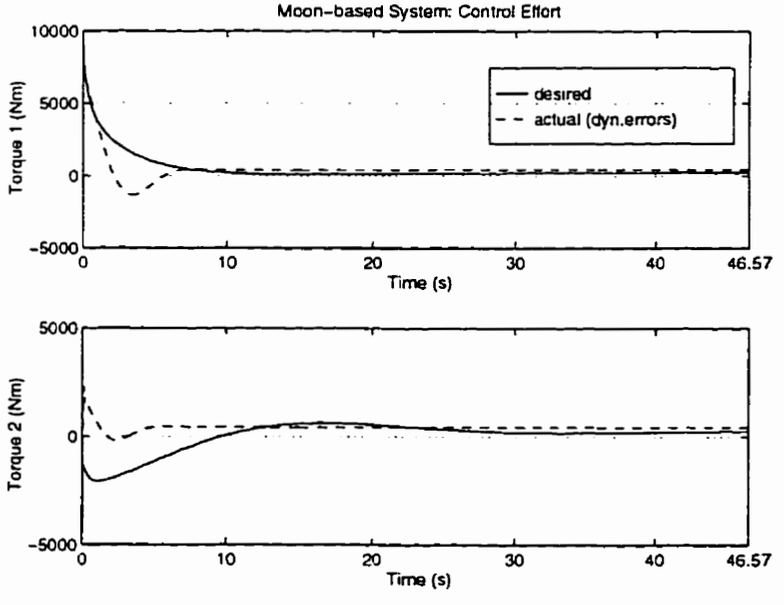

Figure 8.12: Moon-based with Errors: Control Effort

and the PID controller signal, the error compensation torque from (7.12) is implemented. Because manipulators cannot be built to have certain friction coefficients, the friction effects are the best candidates for the torque compensation techniques of section 7.2.

The same motion is now performed with the scaled PID controller *and* the error compensation. The desired scaled performance is achieved (Figures 8.13 and 8.14). The extra compensation torques provided by the inner compensation loop are shown in Figure 8.15.

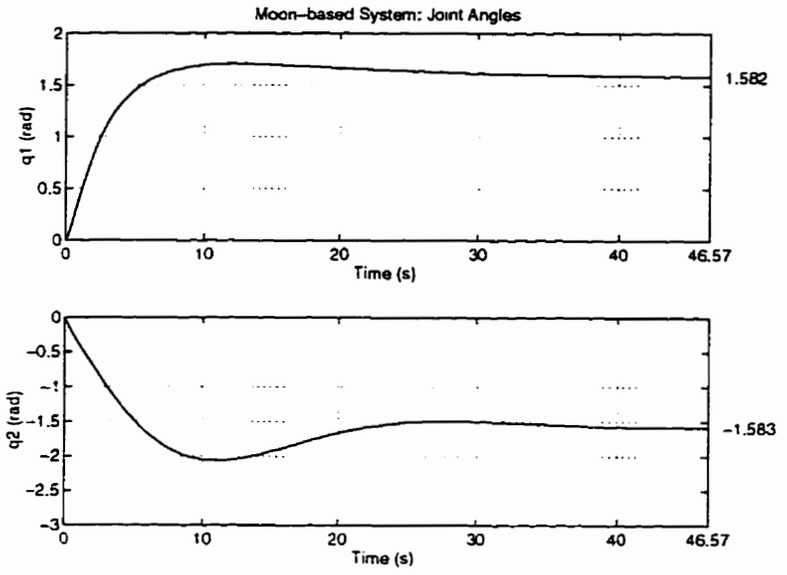

Figure 8.13: Moon-based with Compensation: Joint Angles

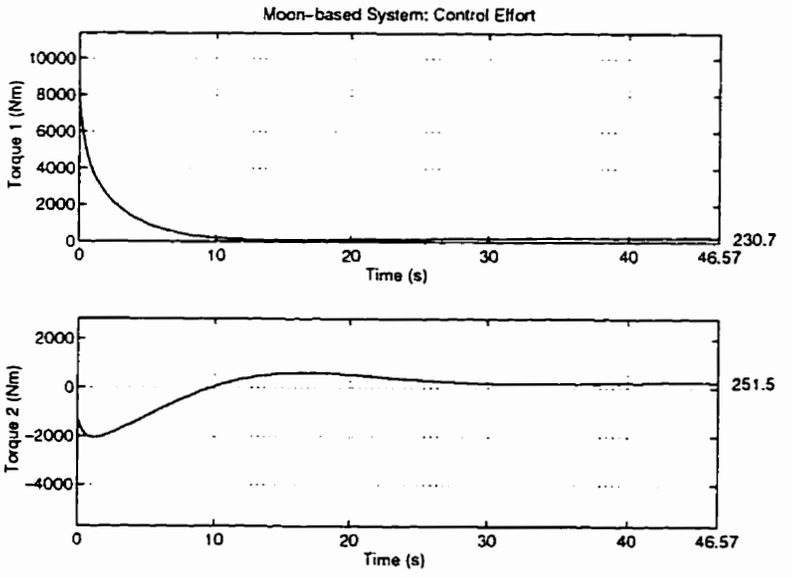

Figure 8.14: Moon-based with Compensation: Control Effort

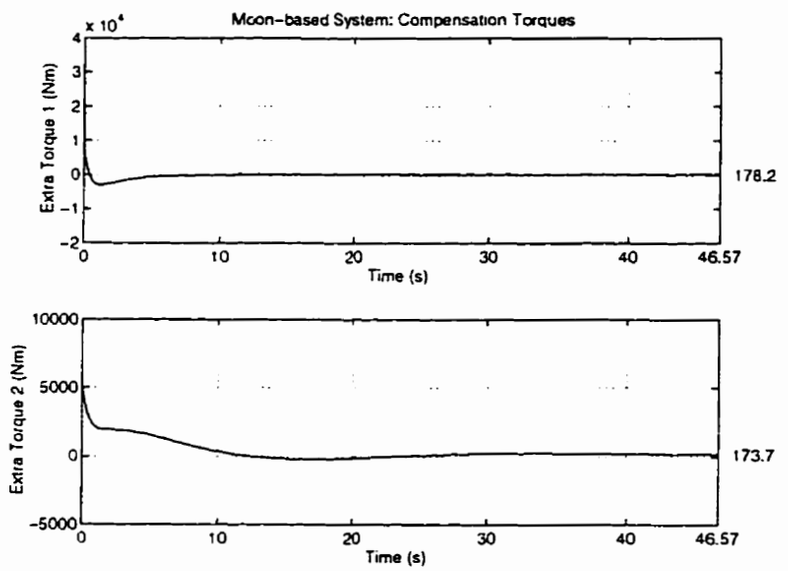

Figure 8.15: Moon-based with Compensation: Compensation Torques

8.4 Sample System 4: Flexible Link with Two Degrees of Vibration

8.4.1 Scenario

In this example, a single flexible link with two degrees of vibrational freedom is controlled using PID control. The manipulator has two actuators at the base of the link, providing excitation for the horizontal and vertical vibrations. The equations of motion were presented in section 3.3.5. Two dynamically equivalent manipulators are designed, one made of aluminum for use on the Earth, and the second made of coastal Douglas fir for use on the Moon.

8.4.2 Manipulator Design

The link is constructed of aluminum ($E_1 = 6.9 \times 10^{10}$ kg m^{-1} s^{-2}, $\rho_1^v = 2700$ kg m^{-3}), has a length of $l_1 = 1$ m and a square cross-section of 1 cm $\times$ 1 cm. The hub inertias of the actuators are each $I^h = 0.5$ kg m^2. Because the cross-section is square and the link is uniform, the mode shapes and modal frequencies for the horizontal and vertical vibrations will be the same. The gravitational acceleration is $g = 9.81$ m s^{-2}, and the time scaling frequency is selected to be unity: $\Omega = 1$ s^{-1}.

With the given information about the physical dimensions of the link, the following quantities can be computed,

$$\begin{aligned} m_1 &= 0.27 \text{ kg} \\ I_{x_1} &= \frac{(0.01 \text{ m})^4}{12} = 8.3 \times 10^{-10} \text{ m}^4 \\ I_{y_1} &= \frac{(0.01 \text{ m})^4}{12} = 8.3 \times 10^{-10} \text{ m}^4. \end{aligned}$$

The base parameters are ρ_1^v, l_1, and Ω. Since the volume mass density ρ_1^v is specified instead of linear mass density, then, the modified flexible Pi groups from (3.32) are

used. Therefore, the values of the Pi groups are

$$\begin{aligned}
\Pi_{E_1} &= \frac{E_1}{\rho_1^v l_1^2 \Omega^2} = 2.56 \times 10^{11} \\
\Pi_{I_{x_1}} &= \frac{I_{x_1}}{l_1^4} = 8.3 \times 10^{-10} \\
\Pi_{I_{y_1}} &= \frac{I_{y_1}}{l_1^4} = 8.3 \times 10^{-10} \\
\Pi_{I_1^h} &= \frac{I_1^h}{\rho_1^v l_1^5} = 1.85 \times 10^{-4} \\
\Pi_{I_2^h} &= \frac{I_2^h}{\rho_1^v l_1^5} = 1.85 \times 10^{-4} \\
\Pi_G &= \frac{g}{l_1 \Omega^2} = 9.81.
\end{aligned}$$

The frequency of the first mode of vibration is

$$\omega_1 = \sqrt{\frac{E_1 I_{x_1}}{\rho_1 l_1^4}} \beta_1 = 55.59 \text{ s}^{-1},$$

where $\beta_1 = 1.952$ is the first solution of the exact transcendental equation[36]

$$(1 + \cos(\beta_k)\cosh(\beta_k)) + \frac{\rho_1 l_1^3}{I_1^h \beta_k^3} (\cosh(\beta_k)\sin(\beta_k) - \sinh(\beta_k)\cos(\beta_k)) = 0.$$

Suppose a dynamically equivalent manipulator is to be constructed out of a different material, and on the Moon. The values of the Pi groups above can be used to determine the dimensions of the corresponding manipulator. Three parameters must be fixed. Choosing the material fixes two parameters (E and ρ^v). Choosing the gravitational acceleration g fixes the third parameter.

Set $g = 1.62 \text{ m s}^{-2}$ (for the Moon), and construct the link out of coastal Douglas fir ($E_1 = 1.21 \times 10^{10} \text{ kg m}^{-1} \text{s}^{-2}$, $\rho_1^v = 498.2 \text{ kg m}^{-3}$)[22]. The Pi groups Π_{E_1} and Π_G both contain Ω,

$$\Pi_{E_1} = \frac{E_1}{\rho_1^v l_1^2 \Omega^2}, \quad \Pi_G = \frac{g}{l_1 \Omega^2}.$$

Since E_1, ρ_1^v, and g are specified, solving for Ω gives

$$\Omega^2 = \frac{E_1}{\rho_1^v l_1^2 \Pi_{E_1}} = \frac{g}{l_1 \Pi_G} \quad \Rightarrow \quad l_1 = \frac{E_1}{\rho_1^v g} \frac{\Pi_{E_1}}{\Pi_G}.$$

Substituting the values for the Pi groups computed for the aluminum system gives,

$$l_1 = 5.70 \text{ m}, \quad \Omega = 0.17 \text{ s}^{-1}.$$

With the values for l_1 and Ω determined, the Pi groups can be used to compute the parameter values for I_{x_1}, I_{y_1}, I_1^h and I_2^h:

$$\begin{aligned} I_{x_1} &= 8.81 \times 10^{-7} \text{ m}^4 \\ I_{y_1} &= 8.81 \times 10^{-7} \text{ m}^4 \\ I_1^h &= 556.2 \text{ kg m}^2 \\ I_2^h &= 556.2 \text{ kg m}^2. \end{aligned}$$

The physical dimensions of the square cross-section corresponding to I_{x_1} and I_{y_1} are 5.7 cm $\times$ 5.7 cm.

The frequency of the first mode of oscillation can be computed to be

$$\omega_1 = \sqrt{\frac{E_1 I_{x_1}}{\rho_1 l_1^4}} \beta_1 = 9.50 \text{ s}^{-1}.$$

This frequency can be verified by examining the value of the *nondimensional* first mode frequency for both systems

$$\hat{\omega}_1 = \frac{\omega_1}{\Omega} = \underbrace{\frac{55.59 \text{ s}^{-1}}{1.0 \text{ s}^{-1}}}_{\text{system 1}} = \underbrace{\frac{9.50 \text{ s}^{-1}}{0.17 \text{ s}^{-1}}}_{\text{system 2}} = 55.59,$$

which are identical, meaning that the frequency is scaled correctly.

8.4.3 Control Design

Both systems were controlled using a PD control law. For the aluminum link, the PD gains for both actuators are,

$$K_p = 5 \text{ kg m}^2 \text{ s}^{-2}, \quad K_d = 1 \text{ kg m}^2 \text{ s}^{-1}.$$

The Pi groups for the controller gains are,

$$\Pi_{K_p} = \frac{K_p}{m_1 l_1^2 \Omega^2} = 18.519, \quad \Pi_{K_d} = \frac{K_d}{m_1 l_1^2 \Omega} = 3.704.$$

Using these Pi groups, the PD gains for the wooden link are found to be

$$\begin{aligned} K_p &= m_1 l_1^2 \Omega^2 \Pi_{K_p} = 162.57 \text{ kg m}^2 \text{ s}^{-2}, \\ K_d &= m_1 l_1^2 \Omega \Pi_{K_d} = 190.19 \text{ kg m}^2 \text{ s}^{-1}. \end{aligned}$$

8.4.4 Responses

Both joints were moved through a step of one radian. This was sufficient to induce both horizontal and vertical oscillations in the link. For each system, figures showing tip deflection, tip position, and control effort are given (Figures 8.16 to 8.21). The corresponding figures from each system are shown together on a page to allow them to be compared easily.

As expected, each pair of figures are scaled versions of each other. Using subscripts 1 and 2, to denote each system, the scaling factors for time t, lengths $\mathcal{L}$, and torques H are:

$$\begin{aligned} &\text{time: } t_2 = t_1 \frac{\Omega_1}{\Omega_2} = 5.85 t_1 \\ &\text{length: } \mathcal{L}_2 = \mathcal{L}_1 \frac{(l_1)_2}{(l_1)_1} = 5.70 \mathcal{L}_1 \\ &\text{torque: } H_2 = H_1 \frac{(m_1 l_1^2 \Omega^2)_2}{(m_1 l_1^2 \Omega^2)_1} = 32.51 H_1. \end{aligned}$$

In particular, the time scaling factor indicates that a motion on the Moon (system 2), will take approximately six times longer to execute than the corresponding motion on the Earth (system 1).

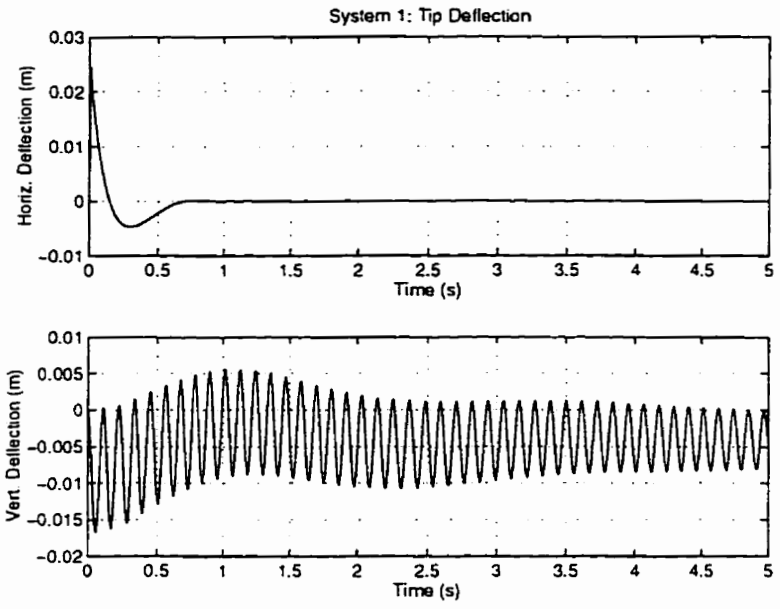

Figure 8.16: System 1: Tip Deflection

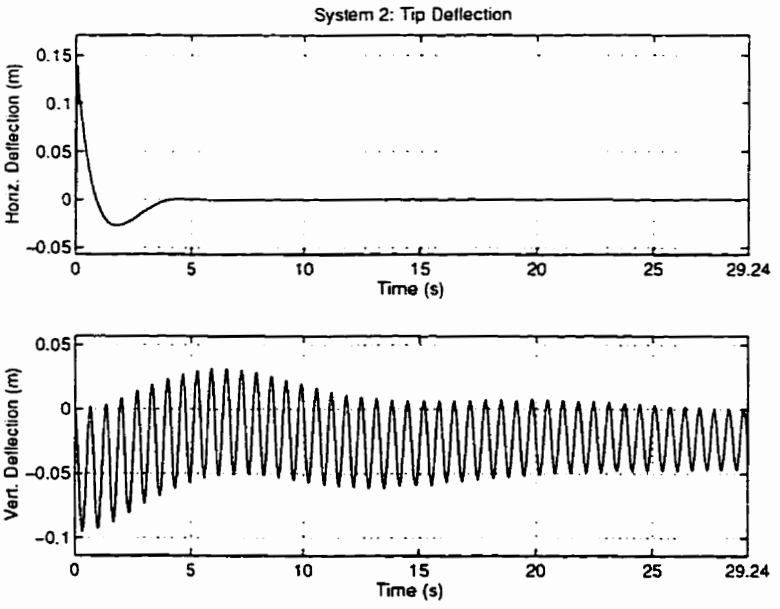

Figure 8.17: System 2: Tip Deflection

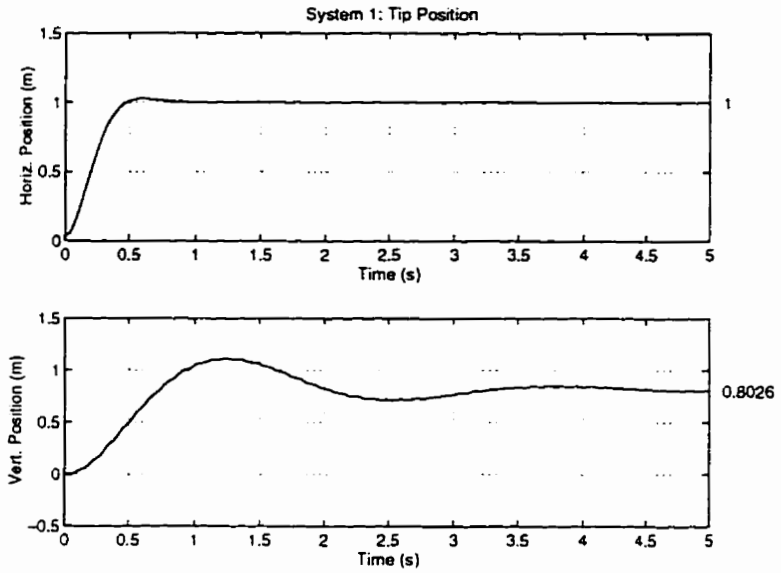

Figure 8.18: System 1: Tip Position

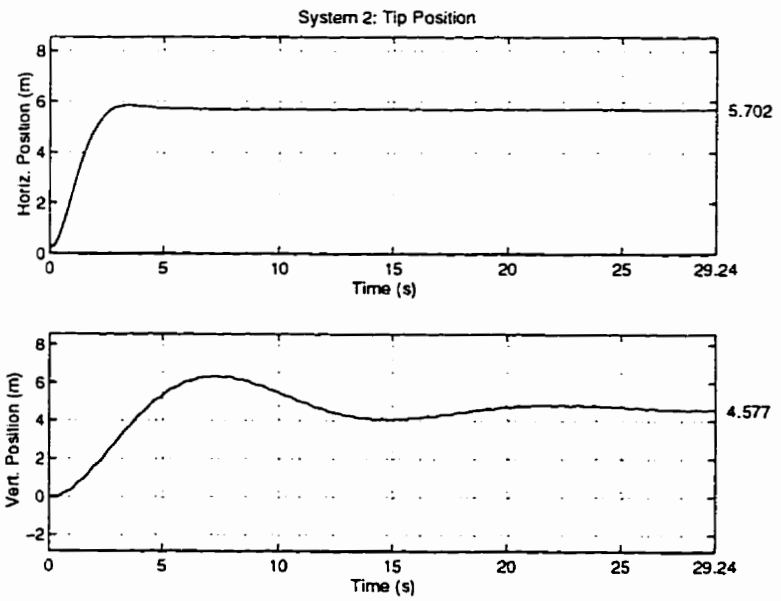

Figure 8.19: System 2: Tip Position

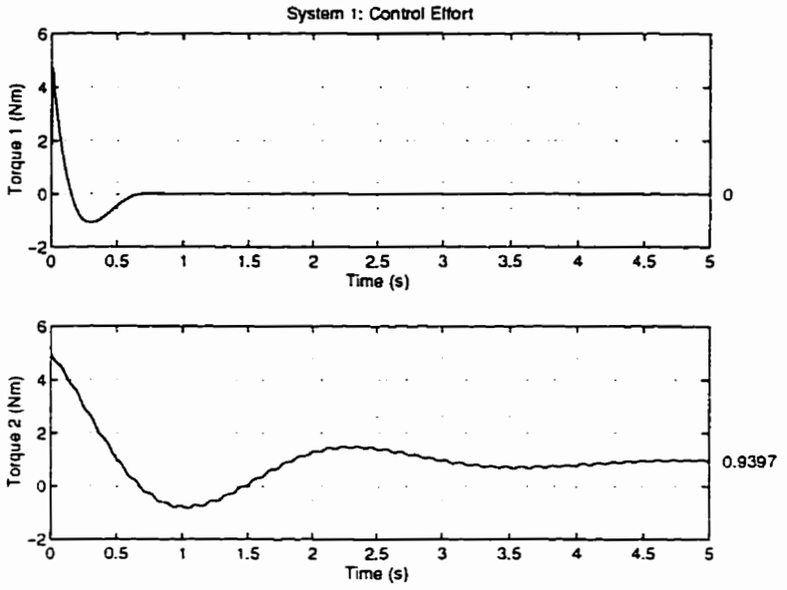

Figure 8.20: System 1: Control Effort

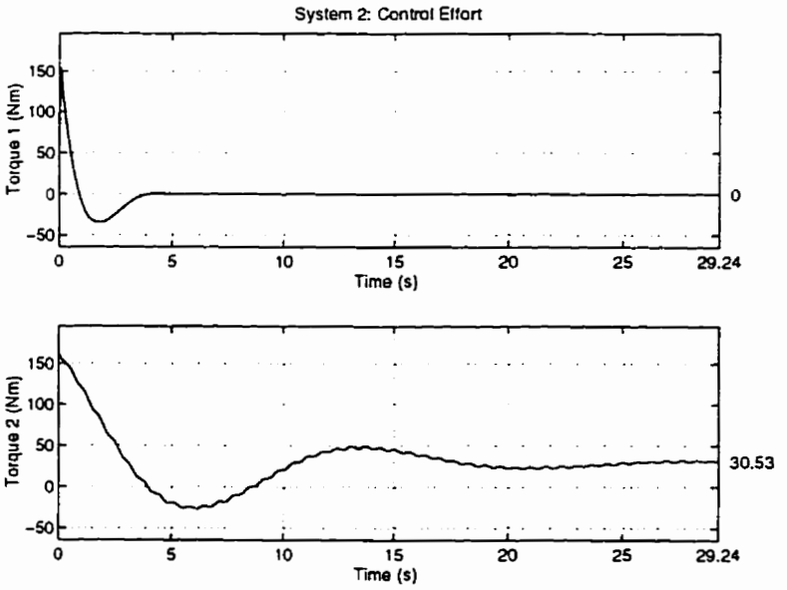

Figure 8.21: System 2: Control Effort

8.5 Sample System 5: Five-Bar Linkage with a Flexible Link

8.5.1 Scenario

This sample system is an example of a manipulator composed of both rigid and flexible links. This issue was addressed in section 3.5. This manipulator has three rigid links and one flexible link. The flexible link has a rectangular cross-section with the height ten times greater than the base, and hence, can vibrate horizontally only. The parallelogram structure of the manipulator simplifies the dynamic equations of the rigid body motion. The equations of motion were presented in section 3.5.1. In this example, two dynamically equivalent manipulators are designed, one out of aluminum, and the other out of steel.

8.5.2 Manipulator Design

All the manipulator links are rectangular, and are composed of aluminum. The link lengths are $l_1 = 30$ cm, $l_2 = 6.25$ cm, $l_3 = 30$ cm, and $l_4 = 50$ cm. Because of the configuration of the manipulator (similar to Figure 3.3, but with link 4 flexible), the length of the flexible link allowed to vibrate is $L = l_4 - l_2 = 43.75$ cm. The cross-sections of the three rigid links are 3 cm $\times$ 3 cm, whereas the flexible link cross-section is 0.3 cm $\times$ 3 cm. The system parameters are given in Table 8.4.

Choose the base parameters to be the rigid manipulator variables m_1, $J_1 = J_1^{xx}$, and Ω. Then, with

$$k_1 = \sqrt{\frac{J_1}{m_1}} = 0.087 \text{ m},$$

the nondimensional Pi groups can be calculated. For the three rigid links, the rigid Pi groups will be used, while for the flexible link, the flexible link Pi groups will be used. Because this manipulator has both rigid and flexible links, and the base parameters are chosen to be the rigid link parameters, then the flexible link Pi

groups will be modified according to section 3.5. The values of the Pi groups are given in Table 8.5.

A dynamically equivalent manipulator is designed but with all the links constructed out of steel instead of aluminum. Fix $g = 9.81\ \mathrm{m\,s^{-2}}$, and the material properties of steel $E = 20.7 \times 10^{10}\ \mathrm{kg\,m^{-1}\,s^{-2}}$, $\rho^v = 7833\ \mathrm{kg\,m^{-3}}$. Then, using the Pi groups in the table, the properties for the dynamically equivalent manipulator can be determined (Table 8.6).

Rigid Links	Variable	Link 1	Link 2	Link 3
mass (kg)	m_i	0.73	0.15	0.73
mass moment	J_i^{xx}	5.52×10^{-3}	6.08×10^{-5}	5.52×10^{-3}
of inertia	J_i^{yy}	5.52×10^{-3}	2.28×10^{-5}	5.52×10^{-3}
($\mathrm{kg\,m^2}$)	J_i^{zz}	1.09×10^{-4}	6.08×10^{-5}	1.09×10^{-4}
Flexible Link		Link 4		
length (m)	L	0.4375		
area moment	I_x	6.75×10^{-11}		
of inertia ($\mathrm{m^4}$)	I_y	6.75×10^{-9}		
elastic mod. ($\mathrm{kg\,m^{-1}\,s^{-2}}$)	E	6.9×10^{10}		
mass density ($\mathrm{kg\,m^{-3}}$)	ρ^v	2700		
1^{st} mode freq. ($\mathrm{s^{-1}}$)	ω	80.42		
Joint Parameters		Joint 1	Joint 2	Joint 3
inertia ($\mathrm{kg\,m^2}$)	I_j^h	0.05	0.05	0.05
General Parameters		Value		
grav.accel. ($\mathrm{m\,s^{-2}}$)	g	9.81		
time scaling ($\mathrm{s^{-1}}$)	Ω	1.0		

Table 8.4: Parameters for Aluminum Five-bar Linkage Manipulator

Pi - Rigid	Form	Link 1	Link 2	Link 3
Π_{m_i}	$\frac{m_i}{m_1}$	n/a	0.208	1.0
$\Pi_{J_i^{xx}}$	$\frac{J_i^{xx}}{J_1}$	n/a	0.011	1.0
$\Pi_{J_i^{yy}}$	$\frac{J_i^{yy}}{J_1}$	1.0	0.0041	1.0
$\Pi_{J_i^{zz}}$	$\frac{J_i^{zz}}{J_1}$	0.0198	0.011	0.0198
Pi - Flexible	Form	Link 4		
Π_{ρ^v}	$\frac{\rho^v}{m_1 k_1^{-3}}$	2.442		
Π_l	$\frac{L}{k_1}$	5.027		
Π_{I_x}	$\frac{I_x}{k_1^4}$	1.18×10^{-6}		
Π_{I_y}	$\frac{I_y}{k_1^4}$	1.18×10^{-4}		
Π_E	$\frac{E}{m_1 k_1^{-1} \Omega^2}$	8.24×10^9		
Pi - Joints		Joint 1	Joint 2	Joint 3
$\Pi_{I_j^h}$	$\frac{I_j^h}{J_1}$	9.05	9.05	9.05
General Parameters		Value		
Π_G	$\frac{g}{k_1 \Omega^2}$	112.71		

Table 8.5: Pi groups for Five-bar Linkage Manipulator

Rigid Links	Variable	Link 1	Link 2	Link 3
mass (kg)	m_i	2.34	0.49	2.3386
mass moment	J_i^{xx}	1.89×10^{-2}	2.09×10^{-4}	1.89×10^{-2}
of inertia	J_i^{yy}	1.89×10^{-2}	7.81×10^{-5}	1.89×10^{-2}
($\mathrm{kg\,m^2}$)	J_i^{zz}	3.75×10^{-4}	2.09×10^{-4}	3.75×10^{-4}
Flexible Link		Value		
length (m)	L	0.4524		
area moment	I_x	7.72×10^{-11}		
of inertia ($\mathrm{m^4}$)	I_y	7.74×10^{-9}		
elastic mod. ($\mathrm{kg\,m^{-1}\,s^{-2}}$)	E	20.7×10^{10}		
mass density ($\mathrm{kg\,m^{-3}}$)	ρ^v	7833		
1^{st} mode freq. ($\mathrm{s^{-1}}$)	ω	79.08		
Joint Parameters		Joint 1	Joint 2	Joint 3
inertia ($\mathrm{kg\,m^2}$)	I_j^h	0.17	0.17	0.17
General Parameters		Value		
grav.accel. ($m_1\,\mathrm{s^{-2}}$)	g	9.81		
time scaling ($\mathrm{s^{-1}}$)	Ω	0.98		

Table 8.6: Parameters for Steel Five-bar Linkage Manipulator

For the steel manipulator, assuming rectangular links, the physical dimensions of each link can be found. The link lengths are $l_1 = 31$ cm, $l_2 = 6.5$ cm, $l_3 = 31$ cm, $l_4 = 52$ cm. The rigid links have a cross-section of 3.1 cm $\times$ 3.1 cm. The cross-section of the flexible link is 0.31 cm $\times$ 3.1 cm.

Notice that the physical dimensions of the steel manipulator are almost identical to the dimensions of the aluminum manipulator. Also, from Table 8.6, the values for Ω and ω are very close to the corresponding values of the aluminum robot. Therefore, although the two manipulators are constructed out of significantly different materials, their length and time properties are almost equal. This coincidence arises from the material properties of aluminum and steel, and can easily be explained.

For the second system, values for E, ρ^v, and g were specified. The values for m_1, k_1, and Ω are found from the three Pi groups:

$$\Pi_E = \frac{E}{m_1 k_1^{-1} \Omega^2}, \quad \Pi_{\rho^v} = \frac{\rho^v}{m_1 k_1^{-3}}, \quad \Pi_G = \frac{g}{k_1 \Omega^2}.$$

Solving these simultaneously for m_1, k_1, and Ω gives

$$k_1 = \frac{E}{\rho^v g} \frac{\Pi_{\rho^v} \Pi_G}{\Pi_E}, \quad m_1 = \frac{\rho^v}{\Pi_{\rho^v} k_1^{-3}}, \quad \Omega = \sqrt{\frac{g}{k_1 \Pi_G}}. \tag{8.1}$$

Now, coincidentally, the ratios of elastic modulus E to volume mass density ρ^v for aluminum and steel are approximately equal,

$$\left(\frac{E}{\rho^v}\right)_{\text{alum.}} = 2.56 \times 10^7 \text{ m}^2 \text{s}^{-2}, \quad \left(\frac{E}{\rho^v}\right)_{\text{steel}} = 2.64 \times 10^7 \text{ m}^2 \text{s}^{-2}.$$

With this information, the similarity of the two systems can be explained by referring to the calculation of k_1 and Ω in (8.1). Because the value of g is constant for both systems, and the Pi groups Π_{ρ^v}, Π_G and Π_E are also constant, then by keeping the value of the ratio $E : \rho^v$ almost the same, the value of k_1 becomes almost the same for both systems. Consequently, with k_1 the same, the calculation of Ω in (8.1), means that Ω will also have a similar value for both systems.

Because k_1 is used as a length scaling parameter, since the value of k_1 is similar for both systems, then both systems will have similar physical dimensions. Also,

because Ω has a similar value for both systems, then both systems will operate at approximately the same speed. Consequently, frequencies of vibration will be close in value for both systems.

8.5.3 Control Design

Both systems were controlled using a PD control law. For the aluminum system, the PD gains for all three actuators are,

$$K_p = 10 \text{ kg m}^2 \text{ s}^{-2}, \quad K_d = 1 \text{ kg m}^2 \text{ s}^{-1}.$$

The Pi groups for the controller gains are,

$$\Pi_{K_p} = \frac{K_p}{m_1 k_1^2 \Omega^2} = 1810.9, \quad \Pi_{K_d} = \frac{K_d}{m_1 k_1^2 \Omega} = 181.1.$$

Using these Pi groups, the PD gains for the steel manipulator are found to be

$$\begin{aligned} K_p &= m_1 l_1^2 \Omega^2 \Pi_{K_p} = 33.17 \text{ kg m}^2 \text{ s}^{-2}. \\ K_d &= m_1 l_1^2 \Omega \Pi_{K_d} = 3.37 \text{ kg m}^2 \text{ s}^{-1}. \end{aligned}$$

8.5.4 Responses

The initial joint positions are $(q_1, q_2, q_3) = (0, \frac{\pi}{2}, \pi)$. The responses of each system to a step of one radian on each joint are given in Figures 8.22 to 8.27. For each system, the responses for base angle and tip deflection, planar joint angles, and control efforts are presented. The corresponding plots from each system are shown together to ease comparison.

Each pair of plots is a scaled version of the other. The scaling factors for time,

length, and control effort are:

$$\text{time: } t_2 = t_1 \frac{\Omega_1}{\Omega_2} = 1.02 t_1$$

$$\text{length: } \mathcal{L}_2 = \mathcal{L}_1 \frac{(k_1)_2}{(k_1)_1} = 1.03 \mathcal{L}_1$$

$$\text{torque: } H_2 = H_1 \frac{(m_1 k_1^2 \Omega^2)_2}{(m_1 k_1^2 \Omega^2)_1} = 3.32 H_1.$$

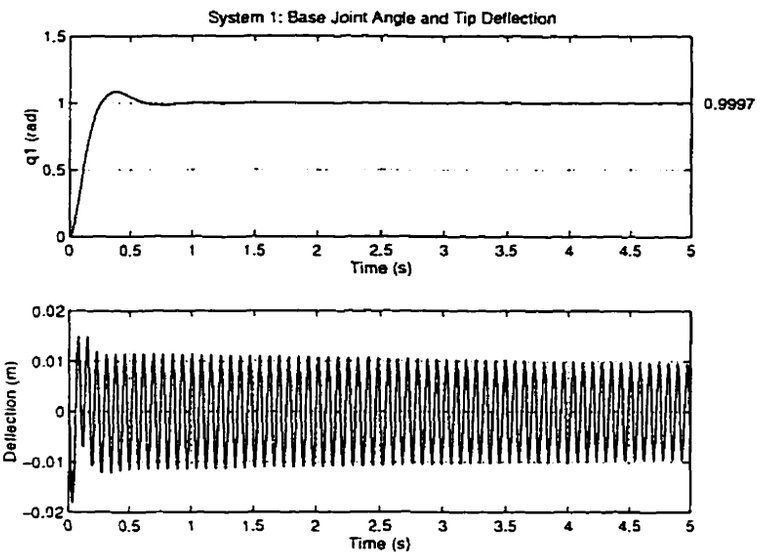

Figure 8.22: System 1: Base Angle and Tip Deflection

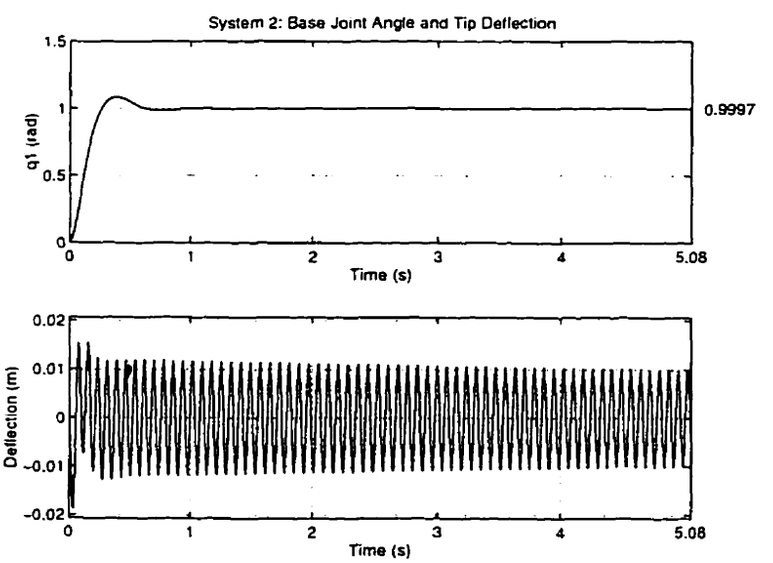

Figure 8.23: System 2: Base Angle and Tip Deflection

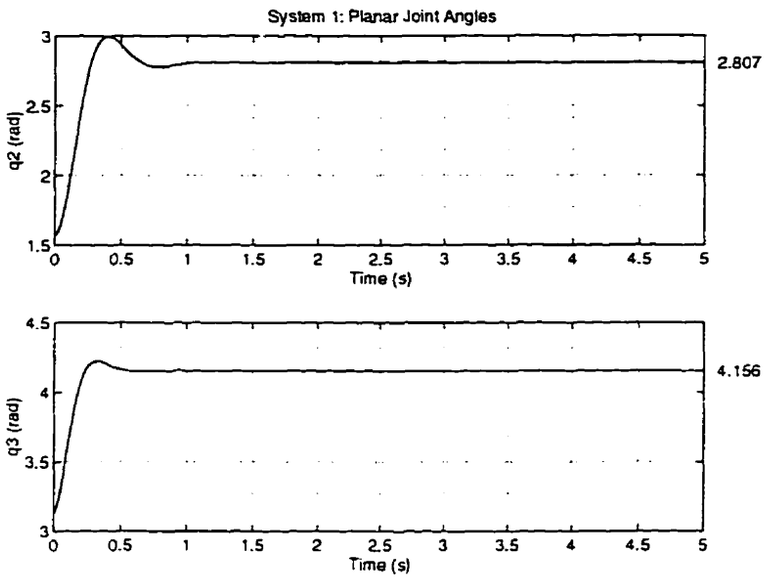

Figure 8.24: System 1: Planar Joint Angles

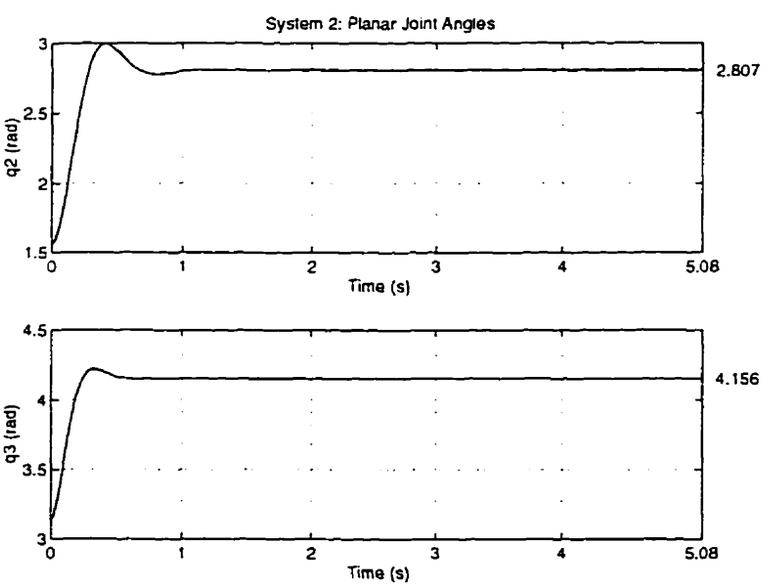

Figure 8.25: System 2: Planar Joint Angles

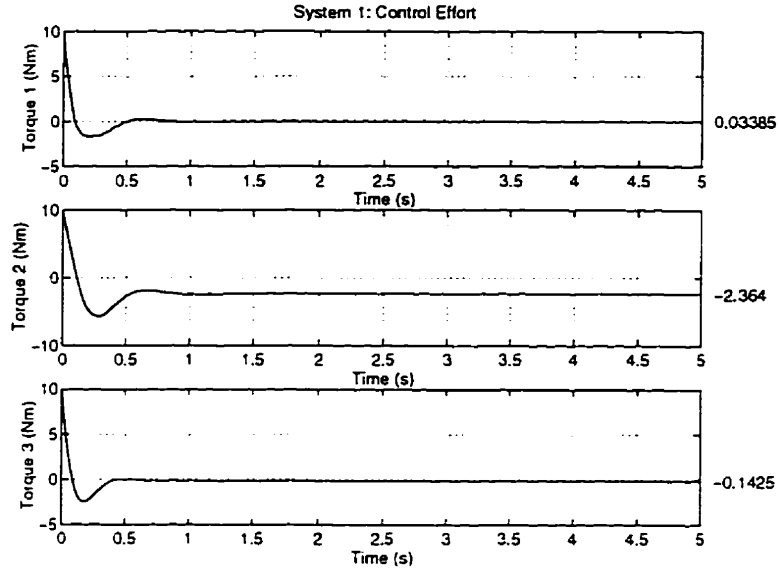

Figure 8.26: System 1: Control Effort

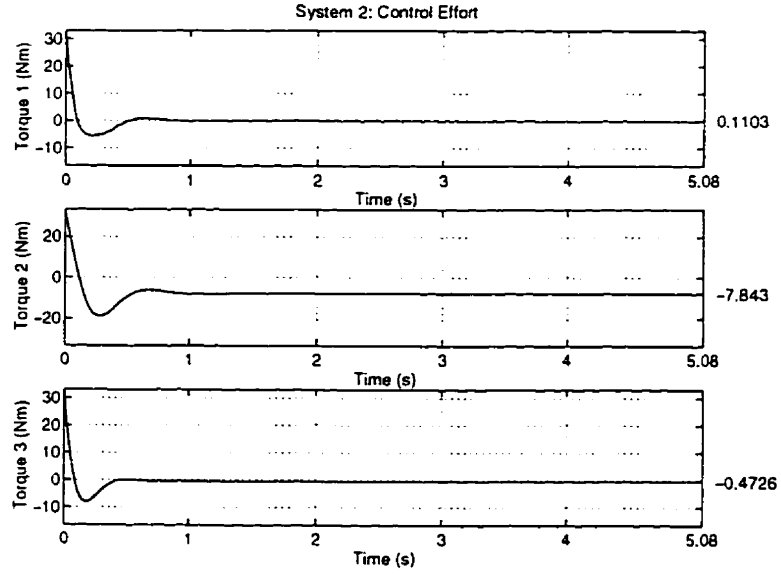

Figure 8.27: System 2: Control Effort

Chapter 9

Conclusions

In this thesis, the dynamic equivalence conditions, and controller scaling laws, for robotic manipulators were developed. In this chapter, the process by which the scaling conditions were determined is summarized. In addition, the novel contributions of the research are presented, and several possible avenues for future research are proposed.

9.1 Summary

In this thesis, dimensional analysis is applied to a general robotic manipulator system. The nondimensional Pi groups for rigid link and flexible link manipulators were found by directly examining the nondimensional energy expressions, and these Pi groups were verified by applying the Buckingham Pi theorem. Although the parameters used to characterize the dynamics of rigid and flexible manipulators are different, it was proved that the nondimensional Pi groups for the rigid system can be obtained through combinations of the flexible Pi groups. In addition, a theorem regarding the form of the nondimensional group for *any* parameter of the manipulator system was presented and proved.

Using the same reference values as used for the manipulator Pi groups, nondimensional groups for the actuator dynamics, control law, and friction effects were found. With the actuator and controllers, the set of fundamental dimensions was extended to include the dimensions of current $[A]$ and temperature $[\Theta]$. This allowed the general form to capture effects such as voltage or temperature signals within the system.

Practically it is impossible to build a manipulator so that the actual Pi group values *identically* match the desired values. Because of this manufacturing imprecision, a measure of the magnitude of the error is required. Therefore, a method of obtaining the sensitivity of the manipulator dynamics to changes in the Pi groups was presented. Also, for rigid link manipulators, a nonlinear feedback technique was presented to compensate for errors in the Pi groups. Using this compensation technique, the actual manipulator dynamics can be made to appear as the desired dynamics.

Finally, simulation results for rigid and flexible manipulators using different control strategies were presented. The simulation results validated the theoretical scaling conditions developed in the thesis.

In conclusion, this dissertation derived and presented the dynamic equivalence conditions which characterize rigid and flexible manipulators, actuator dynamics, control laws, and friction effects. With these scaling laws, control design can be carried out on a small prototype robot, and the results obtained can be scaled directly and quantitatively to predict the dynamic behaviour of a dynamically equivalent large manipulator.

9.2 Contributions

The contributions of this thesis are briefly summarized here:

- application of dimensional analysis to robotic manipulator systems
- determined dynamic equivalence conditions for rigid and flexible link manipulators
- proposed a general form for the actuator dynamics, and presented the scaling conditions for the actuator parameters
- presented a general form for an arbitrary control law, and developed the scaling conditions for the controller characteristic parameters
- examined various friction models, and presented the nondimensional Pi groups for the friction parameters
- proposed a novel nonlinear feedback technique to compensate for errors between the actual and desired Pi group values
- verified the theoretical results in simulation on various manipulator-controller combinations.

9.3 Future Research

9.3.1 Experimental Verification

In order to validate the theoretical results developed in this thesis, it is necessary to perform some experimental verification. In [18], scaling laws for *linear* controllers of dynamically equivalent single flexible link manipulators were presented. These theoretical results were successfully validated experimentally. Based on the success of these linear system experiments, it is expected that the general scaling laws developed in this research will also be successfully validated through experiments.

9.3.2 Non-Uniform Flexible Links

In the situation where the links of the flexible manipulator are not uniform, the link no longer has a constant cross-sectional area. In particular, this means that the area moments of inertia, I_{x_i} and I_{y_i}, are no longer constant, and are in fact functions of the axial coordinate, z_i. This would seem to suggest that the nondimensional Pi groups for I_{x_i} and I_{y_i} are also functions of the axial coordinate. The Pi groups for these terms should be determined using the Buckingham Pi method, and verified by direct nondimensionalization of the system equations of motion.

9.3.3 Micro-manipulators

The scaling conditions could potentially be used to make a *large* prototype of a micro-manipulator. Because of different dynamic effects at the microscopic level (e.g. high friction), the parameters used to characterize the manipulator dynamics would have to be different. However, the methodology developed in this thesis could be used to construct a "magnified" version of a micro-manipulator, thereby facilitating design and analysis.

References

[1] R.C. Weast. *CRC Handbook of Chemistry and Physics, A Ready-Reference Book of Chemical and Physical Data, 66th edition.* CRC Press Inc., Boca Raton, 1985.

[2] R.C. Pankhurst. *Dimensional Analysis and Scale Factors.* Reinhold Publishing Corporation, New York, 1964.

[3] Frank M. White. *Fluid Mechanics*, chapter 5. McGraw-Hill Book Company, New York, 1986.

[4] H.E. Huntley. *Dimensional Analysis.* Rinehart & Company Inc., New York, 1951.

[5] E. Buckingham. On Physically Similar Systems; Illustrations of the Use of Dimensional Equations. *Physical Review*, **IV**(4):345–376, 1914.

[6] P.W. Bridgman. *Dimensional Analysis.* Yale University Press, New Haven, 1931.

[7] D.C. Ipsen. *Units, Dimensions, and Dimensionless Numbers.* McGraw-Hill Book Company, Inc., New York, 1960.

[8] Murphy G. *Similitude in Engineering.* The Ronald Press Company, New York, 1950.

[9] H.L. Langhaar. *Dimensional Analysis and Theory of Models.* Robert E. Krieger Publishing Company, Huntington, 1980.

[10] Canadian Standards Association. *The International System of Units (SI).* Canadian Standards Association. Rexdale, Ontario, Canada. 1973.

[11] N.D. Fowkes and J.J. Mahoney. *An Introduction to Mathematical Modelling.* John Wiley & Sons, Brisbane. 1994.

[12] L. Meirovitch. *Analytical Methods in Vibrations.* The MacMillan Company, Toronto, 1969.

[13] A.M. Reinhorn, T.T. Soong, and M.A. Riley. Full-Scale Implementation of Active Control in Structures. In *Innovative Large Span Structures*, pages 452-463. 1992.

[14] F.J. Jong. *Dimensional Analysis for Economists.* North Holland. Amsterdam. 1967.

[15] R. Kurth. *Dimensional Analysis and Group Theory in Astrophysics.* Pergammon. New York. 1972.

[16] H. Zhang, Y. Liu. and M. Xu. Nondimensionalized Method for Modeling and Simplification of Robot Manipulator Dynamics. *2nd National Applied Mechanisms and Robotics Conference*, **IIB.1**:1-7, 1991.

[17] Milind Ghanekar. Scaling Laws for Linear Controllers of Dynamically Equivalent Single Flexible Link Manipulators. Master's thesis, University of Waterloo. 1994.

[18] M. Ghanekar, D.W.L. Wang, and G.R. Heppler. Scaling Laws for Linear Controllers of Flexible Link Manipulators Characterized by Nondimensional Groups. *IEEE Transactions on Robotics and Automation*, **13**(1):117-127, February 1997.

[19] Donald T. Greenwood. *Principles of Dynamics.* Prentice-Hall, Inc., Englewood Cliffs, 1988.

[20] M.W. Spong and M. Vidyasagar. *Robot Dynamics and Control.* John Wiley & Sons, New York. 1989.

[21] J.P. Huissoon and D. Wang. On the Design of a Direct Drive 5-Bar-Linkage Manipulator. *Robotica*, **9**:441–446, 1991.

[22] E.P. Popov. *Mechanics of Materials*. Prentice-Hall, Inc., New Jersey, 1976.

[23] J.L. Humar. *Dynamics of Structures*. Prentice-Hall, Englewood Cliffs, 1990.

[24] X. Ding, T. Tarn, and A.K. Bejczy. A Novel Approach to the Modelling and Control of Flexible Robot Arms. *Proceedings of the 27th IEEE Conference on Decision and Control*, **1**:52–57, 1988.

[25] D. Wang and M. Vidyasagar. Modeling a Class of Multilink Manipulators with the Last Link Flexible. *IEEE Transactions on Robotics and Automation*, **8**(1):33–41, 1992.

[26] R.H. DeCarlo, S.H. Zak, and G.P. Matthews. Variable Structure Control of Nonlinear Multivariable Systems. *Proceedings of the IEEE*, **76**(3):212–232, March 1988.

[27] J. Slotine and W Li. *Applied Nonlinear Control*. Prentice-Hall, Inc., New Jersey, 1991.

[28] I.M. Hutchings. *Tribology: Friction and Wear of Engineering Materials*. CRC Press Inc., Boca Raton, 1992.

[29] F.P. Bowden and D. Tabor. *Friction: An Introduction to Tribology*. Heinemann, London, 1974.

[30] Singiresu S. Rao. *Mechanical Vibrations, 2nd ed.* Addison-Wesley Publishing Company, New York, 1990.

[31] C. Canudas de Wit, H. Olsson, and K.J. Åström. A New Model for Control of Systems with Friction. *IEEE Transactions on Automatic Control*, **40**(3):419–425, March 1995.

[32] H.J.T. Smith and M.D Smith. A Method of Compensating for the Friction of a Rotating Bearing. *The Review of Scientific Instruments*, **65**(7):2402–2405, July 1994.

[33] T. Takahashi. A Method of Sensitivity Analysis and its Applications to Robot Manipulators. *Control-Theory and Advanced Technology*, **3**(1):73–84, March 1987.

[34] J.Y.S. Luh, M.W. Walker, and R.P.C. Paul. On-Line Computational Scheme for Mechanical Manipulators. *Journal of Dynamic Systems, Measurement, and Control*, **102**:69–76, June 1980.

[35] D. Wang and M. Vidyasagar. Control of a Class of Manipulators with the Last Link Flexible - Part I: Feedback Linearization. *ASME Journal of Dynamic Systems, Measurement, and Control*, **113**(4):655–661, December 1991.

[36] F. Bellezza, L. Lanari, and G. Ulivi. Exact Modelling of the Flexible Slewing Link. *Proceedings of the 1990 IEEE International Conference on Robotics and Automation*, **3**:734–739, 1990.

Appendix A

Table of Nomenclature

In this appendix, the nomenclature used throughout the thesis is presented. The nomenclature is organized into six categories:

- Table of Standard SI Units
- Dimensional Analysis
- Manipulator Dynamics
- Manipulator Pi Groups
- System Components
- Mathematical Notation.

Standard Système Internationale (SI) Units		
kg	kilogram	(unit of mass)
m	metre	(unit of length)
s	second	(unit of time)
A	ampere	(unit of current)
K	kelvin	(unit of temperature)
cd	candela	(unit of luminous intensity)
mol	mole	(unit of amount of substance)

Dimensional Analysis	
$[M]$	fundamental dimension of mass
$[L]$	fundamental dimension of length
$[T]$	fundamental dimension of time
$[A]$	fundamental dimension of current
$[\Theta]$	fundamental dimension of temperature
mol	fundamental dimension of the amount of substance
cd	fundamental dimension of luminous intensity
$\equiv$	indicates the dimensions of a variable
Π	nondimensional Pi group
$\mathbf{\Pi}$	vector of Pi groups for dynamic equivalence
$\bar{\mathbf{\Pi}}$	vector of Pi groups with errant values
N_Π	total number of Pi groups
$\hat{(\cdot)}$	nondimensional variable for $(\cdot)$
τ	nondimensional time variable
Ω	time scaling frequency

Manipulator Dynamics	
T	kinetic energy
V	potential energy
L	Lagrangian: $L = T - V$
$\boldsymbol{q}$	vector of generalized manipulator coordinates
q_i	i^{th} generalized manipulator coordinate
Q_i	i^{th} generalized external force
$\mathcal{F}_0$	inertial frame of reference
$\mathcal{F}_{ci}$	principal body fixed frame at centre of mass of rigid link i
$\mathcal{F}_i$	frame attached to one end of link i
t	time variable
m_i	mass of link i
J_i^{xx}	mass moment of inertia of link i about principal x-axis
J_i^{yy}	mass moment of inertia of link i about principal y-axis
J_i^{zz}	mass moment of inertia of link i about principal z-axis
$\boldsymbol{J}_{c_i}$	$diag\{J_i^{xx}, J_i^{yy}, J_i^{zz}\}$
J_1	one of $\{J_1^{xx}, J_1^{yy}$, or $J_1^{zz}\}$
k_1	radius of gyration of m_1 about the axis defined by J_1 $\left(\sqrt{\frac{J_1}{m_1}}\right)$
M_j	mass of joint j
I_j^h	rotational inertia of joint j
g	gravitational acceleration
$\boldsymbol{s}$	unit gravity vector

Manipulator Dynamics	
l_i	length of i^{th} flexible link
I_{x_i}	area moment of inertia of cross-section about local x_i axis
I_{y_i}	area moment of inertia of cross-section about local y_i axis
ρ_i	linear mass density of the material of i^{th} flexible link
ρ_i^v	volume mass density of a material
E_i	elastic modulus of the material of i^{th} flexible link
$\phi_i(z)$	i^{th} mode shape
$\hat{q}$	nondimensional generalized manipulator coordinates
$\hat{M}$	nondimensional inertia matrix for a manipulator
$\hat{C}$	nondimensional Coriolis and centripetal acceleration vector
$\hat{G}$	nondimensional gravity vector
$\hat{F}$	nondimensional external force vector
$\hat{h}$	Coriolis, centripetal, and gravity vector
$\mathcal{T}$	generalized time parameter
$\mathcal{L}$	generalized length parameter
$\mathcal{H}$	generalized control effort parameter

Manipulator Pi Groups	
Π_{m_i}	Pi group for the i^{th} link mass (m_i)
$\Pi_{J_i^{xx}}$	Pi group for the inertia of the i^{th} rigid link (J_i^{xx})
$\Pi_{J_i^{yy}}$	Pi group for the inertia of the i^{th} rigid link (J_i^{yy})
$\Pi_{J_i^{zz}}$	Pi group for the inertia of the i^{th} rigid link (J_i^{zz})
Π_{M_j}	Pi group for mass of the j^{th} joint (M_j)
$\Pi_{I_j^h}$	Pi group for the inertia of the j^{th} joint (I_j^h)
Π_G	Pi group for gravitational acceleration
Π_{ρ_i}	Pi group for linear mass density of the i^{th} flexible link (ρ_i)
Π_{l_i}	Pi group for the length of the i^{th} flexible link (l_i)
$\Pi_{I_{x_i}}$	Pi group for area moment of cross-section in x direction
$\Pi_{I_{y_i}}$	Pi group for area moment of cross-section in y direction
Π_{E_i}	Pi group for elastic modulus of the i^{th} flexible link

System Components	
F_f	external friction force
F_a	input force from actuator
u	controller output
ξ	actuator generalized coordinate
Φ	set of actuator or controller characteristic parameters
ϕ_i	an actuator or controller characteristic parameter
K_p	proportional gain (PID)
K_i	integral gain (PID)
K_d	derivative gain (PID)
σ_i	sliding surface (sliding mode)
λ_i	convergence rate parameter (sliding mode)
k_i	switching control gain (sliding mode)
Δ_i	width of saturation operator (sliding mode)
c_v	viscous friction coefficient

Mathematical Notation	
$\mathbf{R}$	set of real numbers
$\sum_{i=1}^{n}(\cdot)_i$	summation of the argument as i ranges from 1 to n
$\prod_{i=1}^{n}(\cdot)_i$	product of the argument as i ranges from 1 to n
$[1, n]$	the integers $\{1, 2, \ldots, n\}$
$\in$	"is a member of"
$\dot{(\cdot)}$	the first derivative of $(\cdot)$ with respect to time
$\ddot{(\cdot)}$	the second derivative of $(\cdot)$ with respect to time
$(\cdot)^{(n)}$	the n^{th} derivative of $(\cdot)$ with respect to time
$(\cdot)'$	the second derivative of $(\cdot)$ with respect to space
$(\cdot)''$	the second derivative of $(\cdot)$ with respect to space
$(\cdot)^T$	transpose of a vector or matrix
$\Gamma_{a\to b}$	$\{\Gamma_a, \Gamma_{a+1}, \ldots, \Gamma_b\}$
$diag\{A_1, A_2, \ldots, A_n\}$	the diagonal matrix with elements $A_1, \ldots, A_n$
sgn	signum function
sat	saturation function